Institute of Physical Chemistry, Polish Academy of Sciences

Kasprzaka 44/52, 01-224 Warsaw

Jędrzej Solarski

Quenching of the excited ^{3}MLCT (metal-to-ligand-charge transfer) states in energy transfer processes

Ph.D. dissertation prepared under the supervision of
prof. dr hab. Andrzej Kapturkiewicz

This dissertation has been completed in the framework of the International Ph.D. Studies at the Institute of Physical Chemistry of the Polish Academy of Sciences

Warsaw 2015

Dla Mamy

Abstract

The general aim of presented dissertation is to contribute to understanding of factors that govern kinetics of the Dexter-type energy transfer in the liquid media between excited triplet ^{3}*MLCT *metal-to-ligand-charge-transfer* states (acting as energy donor) and organic molecules (acting as energy acceptors). We have decided to investigate this topic since so far published data indicated that the commonly known kinetic models (Sandros and Balzani) cannot correctly interpret experimentally obtained kinetic for this kind of processes.

The main object of investigation were luminescent Ir(III) complexes. Due to their unique properties (long life-times in μs range and high quantum yields up to 90%) the time resolved emission spectroscopy technique could be utilized to obtain energy transfer rate constants. Also the use of time resolved emission spectroscopy allowed to develop a more accurate method for obtaining energy transfer rate constants than extracted from commonly used transient absorption technique studies. The analysis of obtained luminescence decays profiles allowed examination of energy transfer processes in both izo-energetic and exothermic regions. Research conducted in room temperature for selected model systems (iridium (III) complex – aromatic hydrocarbon) in different protic and aprotic solvents. Additionally for two selected systems ($Ir(ppy)_3$ – chrysene and $Ru(bpy)_3^{2+}$ – pyrene) the studies of energy transfer kinetics in different temperatures were performed.

On the basis of obtained results a new kinetic model (which includes quantum magnetic conservation rule) was proposed. The outcome of the performed research could not be explained in the terms of two models proposed by Sandros and Balzani. A general conclusion is that proposed model with quantum magnetic number conservation leads to the proper prediction of the solvent viscosity effects as well as temperature dependence.

Streszczenie

Celem przygotowywanej rozprawy doktorskiej pracy było zbadanie kinetyki procesów przeniesienia energii zachodzących pomiędzy trypletowymi stanami wzbudzonymi typu ^{3}*MLCT *metal-to-ligand-charge-transfer* (będącymi donorami energii) a aromatycznymi węglowodorami (będącymi akceptorami energii). Powyższa tematyka została podjęta albowiem dostępne w literaturze przedmiotu dane wskazywały, że dotychczas przyjęte modele kinetyczne (Sandros oraz Balzani) nie potrafią poprawnie zinterpretować doświadczalnie otrzymywanych stałych szybkości tego typu procesów.

Głównymi obiektami wykonanych badań były metaloorganiczne kompleksy irydu(III), które dzięki specyficznym właściwościom (czasy życia luminescencji w granicach 1-30 μs oraz duże wydajności kwantowe luminescencji) pozwalają na wykorzystanie technik czasowo rozdzielczej luminescencji w pomiarach stałych szybkości procesów przeniesienia energii zachodzących z ich udziałem. Zastosowanie technik luminescencyjnych pozwoliło na opracowanie znacznie dokładniejszej metody pomiaru szybkości przeniesienia energii niż stosowane dotychczas techniki absorpcji przejściowej, a opracowana metodyka analizy profili zaniku emisji ^{3}*MLCT na badanie zarówno procesów izo-energetycznego jak i egzotermicznego przeniesienia energii. Badania wykonano w temperaturze pokojowej dla szeregu wybranych układów modelowych (kompleks irydu(III) – węglowodór aromatyczny) w szeregu różnych, aprotycznych i protycznych rozpuszczalników organicznych. Dodatkowo, dla dwóch układów modelowych ($Ir(ppy)_3$ – chryzen oraz izo-elektronowy $Ru(bpy)_3^{2+}$ – pyren) wykonano w kilku rozpuszczalnikach badania wpływu temperatury na kinetykę zachodzących w tych układach procesów przeniesienia energii.

Na podstawie otrzymanych wyników zaproponowano nowy (biorący pod uwagę zasadę zachowania magnetycznej liczby kwantowej) model kinetyczny opisujący, poprawniej niż dotychczasowe rozwiązania, kinetykę procesów przeniesienia energii w roztworach. Zaproponowany model opisuje zarówno wpływ temperatury jak i lepkości medium reakcji na zachodzące w nim procesy przeniesienia energii.

Publications

List of papers

1. J. Solarski, G. Angulo, A. Kapturkiewicz,
   Time-resolved luminescence investigations of the reversible energy transfer from the excited ^{3}*MLCT states to organic acceptors – An alternative method for the determination of triplet state energies and lifetimes.
   J. Photochem. Photobiol. A: Chemistry. **218**, 2011, 58-63.

2. J. Solarski, G. Angulo, A. Kapturkiewicz,
   Energy transfer from the excited ^{3}*MLCT states to organic acceptors – Solvent effect studies.
   J. Photochem. Photobiol. A: Chemistry, **274**, 2014, 73-82

3. J. Solarski, A. Kapturkiewicz,
   Energy transfer from the excited ^{3}*MLCT states to organic acceptors – Temperature effect studies.
   J. Photochem. Photobiol. A: Chemistry, **292**, 2014, 10-15

List of conference presentations

1. J. Solarski, A. Kapturkiewicz,
   Procesy wygaszania stanu wzbudzonego cząsteczki $Ir(ppy)_3$.
   Polish Photoscience Seminar
   Lipnik, June, 1 - 2, 2007 (Poland)

2. J. Solarski, G. Angulo, A. Kapturkiewicz,
   Reversible energy transfer in liquid solutions in terms of Kramers theory.
   International Conference on Photochemistry.
   Beijing, August 7 - 12, 2011 (China)

3. J. Solarski, G. Angulo, A. Kapturkiewicz,
   Investigation of the bimolecular energy transfer processes in liquid solutions.
   Molecules and Light 2011. Autumn Meeting of the Polish Photochemistry Group.
   Zakopane, September 19 - 23, 2011 (Poland)

4. J. Solarski, G. Angulo, A. Kapturkiewicz,
   Viscosity dependence of bimolecular energy transfer rates. An easy way to improve light up-conversion efficiency.
   Reaction Kinetics in Condensed Media – merging experiments and theory (RKCM meeting)
   Łochów, September, 11 - 16, 2012 (Poland)

5. J. Solarski, G. Angulo, A. Kapturkiewicz,
   Dexter-type energy transfer in liquid solution. A new approach to kinetic description.
   Molecules and Light 2013. Autumn Meeting of the Polish Photochemistry Group.
   Zakopane, September 23 - 27, 2013 (Poland)

6. J. Solarski, A. Kapturkiewicz,
   Dexter-type energy transfer in solutions. A new approach to kinetic description.
   Central European Conference on Photochemistry
   Bad Hofgastein, February 08 - 14, 2014 (Austria)

Table of contents

1. Introduction

Photoinduced energy transfer constitutes one of the most basic and fundamental photochemical reactions [1-5]. Excitation energy transfer itself, can occur according to the Forster [6] or the Dexter [7] mechanisms. Interestingly, the same outcome may be achieved in two completely different manners. Forster type energy transfer does not require for molecules to be in contact and can still be effective at large distances (up to 100 Å) [8]. On contrary Dexter type is a close contact interaction requiring intermolecular orbital overlap that operates at distances up to 10 Å. Different selection rules for both types as well as presence of allowed or forbidden transitions in the energy donor and the energy acceptor molecules cause that those two mechanisms rarely come together [9]. For allowed transitions the Coulombic interaction is predominant, even at short distances while for triplet-triplet energy transfer the Coulombic interaction are negligible and the exchange mechanism is dominant. From theoretical point of view the Forster type of mechanism is well established and described. Theoretical and experimental efforts were mainly focused on the Forster type energy transfer and resulted in a quite good understanding of this phenomenon [10]. As an outcome, it may serve as a tool for investigating the structure and dynamics of matter or living systems at a molecular or supramolecular level [11, 12]. In case of the Dexter type of electronic energy transfer, however, there are still some doubts especially concerning kinetics of the process [13]. Those may stem from the fact that quantitative use of the Dexter model is nearly exclusive for crystals (systems with fixed distances between species involved in the energy transfer process). In liquid phase, which is one of the most complicated and difficult for theoretical description state of matter, the processes of translational and rotational diffusion of the reactants, as well as an interaction with the solvent are components of the puzzle of the diffusion influenced Dexter-type energy transfer reactions. Theories present in the literature encounter serious difficulties to properly explain experimental results [14]. The general aim of this thesis is to contribute to understanding of factors that govern efficiency of the Dexter-type energy transfer in liquid state, to a deeper and better knowledge of interplay between diffusion and elementary energy transfer reaction step. To accomplish that a photo-induced energy transfer reactions have been used as they

allow for an easy triggering of the reaction and, in the case of luminescent reactants, for a straightforward monitoring of the evolution of concentration of the excited species of the donor and/or acceptor.

Absorption of a visible light photons by a molecule provides what is called electronically excited state, which is a starting point for subsequent reactions steps. Excited states can be deactivated either via intramolecular processes (internal conversion, intersystem crossing or luminescence) or via interactions with other molecules. De-excitation processes involving interaction of an excited molecule *D with another molecule, Q, is called quenching and it is quantitatively described by quenching rate constant k_q. The rate k_q may be a composition of rates of different processes [15] but the observable quantity *i.e*. fluorescence characteristic decay time and/or fluorescence quantum yield, will reflect change of concentration of the excited state of molecules involved in the process. Due to its significance quenching phenomenon received a special attention because analysis can provide information on the process itself, about involved molecules or even on the medium surrounding quenched fluorophore [16]. Most of the experimental data obtained during the course of this thesis were extracted from quenching experiments as it was the main experimental tool.

To test prediction of any model describing the energy transfer processes one can principally use any combination of acceptor (A) and donor (D) molecules if all additional possible reactions between A and D (*e.g*., electron transfer) are ruled out. In our opinion, however, the best systems to study such energy transfer processes are luminescent transition metal complexes acting as energy donors together with appropriate organic quenchers as an energy acceptors. In such systems, due to unique luminescence properties of some transition metal chelates [17] (long life-times in μs range and high quantum yields up to 90%) time-resolved emission measurements can be straightforwardly applied instead of commonly used transient absorption technique. Considering that signals coming from luminescence are orders of magnitude stronger than those available from transient absorption measurements, necessary kinetic data can be extracted with distinctly higher precision, what is especially important in the case of iso-energetic rate constant determination when back energy transfer ^{3}*A +D → A + ^{3}*D cannot be neglected [18]. Putting it all together, use of luminescent transition metal complexes in quenching

experiments provided enough data to propose a new approach in the kinetic description of the bimolecular Dexter-type energy transfer processes [19]. An important part of proposed model is implementation of the magnetic number conservation rule [20] (known also as the Winans selection rule) to the kinetic scheme of energy transfer processes. In comparison with models already available in the literature [21, 22] the proposed approach provides better agreement between theory and experiment.

2. Reactions involving excited state – bimolecular processes in solutions

2.1 Kinetic models – basic concepts

The pre-equilibrium approximation (PEA) is one of several useful methods that allow one to go from complex systems of differential equations (the kinetic rate equations [23]) to simple explicit solutions. The mechanism of a reaction may involve two or more consecutive reactions, first fast reversible reaction and sequences of slower product forming reaction. The mechanism will illustrate kinetic scheme in a form

$$\mathrm{A} \underset{k_2}{\overset{k_1}{\rightleftarrows}} \mathrm{B} \xrightarrow{k_3} \mathrm{C} \qquad 2.1.1$$

The PEA means that $(k_1 + k_2) >> k_3$. The A ↔ B equilibrium is maintained during the course of the reaction therefore we could write equilibrium constant K = [B]/[A] = k_1 / k_2. Now the overall rate constant for this system is given by

$$\frac{d[\mathrm{C}]}{dt} = k_3[\mathrm{B}] = k_3 K[\mathrm{A}] \qquad 2.1.2$$

This method is valid for the cases when slow irreversible reaction precede fast reversible one. Using this model one can describe monomer-excimer kinetics, enzyme-substrate reaction (Michelis-Menten) or even a case with bimolecular outgoing steps. More general view is presented [24].

The next method is called steady-state approximation and is based on the assumption that an intermediate in the reaction mechanism is consumed as quickly as it is generated. Its concentration remains constant during the reaction. If we assume N consecutive reactions which eventually lead to product as presented in the kinetic scheme

$$\mathrm{A} \xrightarrow{k_0} \mathrm{N_1} \xrightarrow{k_1} \mathrm{N_n} .... \xrightarrow{k_n} \mathrm{C} \qquad 2.1.3$$

Mathematical complexity of analytical solution for this problem considerably increases if the reaction mechanism has more than a few steps. Reaction scheme involving many steps some of which may be reversible are nearly always unsolvable analytically and an

alternative method of solution is necessary. Steady-state approximation assumes that, after an initial induction period, the concentrations of intermediates rise from zero to some value and changes of concentrations of all reaction intermediates are negligibly small during the major part of the reaction

$$\frac{d[\mathrm{N}]_n}{dt} = 0 \qquad 2.1.4$$

This approximation greatly simplifies the discussion of reaction schemes. A big advantage of this method is it versatility and that it allows obtaining approximate solutions even for very complicated schemes. If we now try to solve kinetic scheme of the previous example

$$\mathrm{A} \underset{k_2}{\overset{k_1}{\rightleftharpoons}} \mathrm{B} \xrightarrow{k_3} \mathrm{C} \qquad 2.1.5$$

the result can be applied beyond condition $(k_1 + k_2) >> k_3$ and takes form

$$\frac{d[\mathrm{C}]}{dt} = \frac{k_3 k_1}{k_2 + k_3}[\mathrm{A}] \qquad 2.1.6$$

The pre-equilibrium approximation can only be used if the first step of a reaction is much faster than the second step, whereas the steady state method is more universal. If we now give the rate constant k_1, k_2, k_3 a particular meaning, that is if k_1, k_2 are the rate constants of transport of the reactants through the reaction medium (forward and backward diffusion rate constants) and k_3 is the rate constant of the primary process (like electron transfer, energy transfer or ordinary chemical reaction) then we can distinguish two limiting cases. In the first case, if the diffusion is much faster than reaction rate (k_1, $k_2 >> k_3$) then, assuming that diffusion rates in both directions are comparable, the rate constant k_3 is a rate determining step as overall reaction rate depend only on k_3. In such case reaction is called kinetic-controlled. On the other hand if the first steps of a reaction are much slower than the second step (k_1, $k_2 << k_3$) then overall speed of the reaction is controlled solely by the k_1 rate constant and such reactions are termed diffusion-controlled. Interestingly, in photophysical kinetics, even the very sophisticated reaction mechanisms usually possess this two limiting cases [25] of kinetic and diffusion control. It is important to note that observed rate constant k_{obs} in both regimes depend on different

factors. In case of diffusion control the rate is influenced by factors controlling diffusion like viscosity of the medium or the diffusion coefficient. In case of kinetic control observable rate is solely influenced by factors controlling k_3 rate.

2.2 Diffusional limitations

Marian Ritter von Smoluchowski derived an equation for the rate constant of colloids aggregation in liquid suspensions [26]. His way of reasoning helps to understand what a diffusion rate constant is. Starting point for his consideration is an irreversible reaction between two freely diffusing species in solution

$$\mathrm{A} + \mathrm{B} \xrightarrow{k} \mathrm{C} \qquad 2.2.1$$

A convenient assumption is also that one of the reactants, *B*, is in great excess and therefore the reaction is of pseudo-first order (then $[\mathrm{B}] = [\mathrm{B}]_0$ = constants). The kinetic equation for this process is given by

$$-\frac{d[\mathrm{A}]}{dt} = k(t)[\mathrm{A}][\mathrm{B}]_0 \qquad 2.2.2$$

The next assumption is that a single A molecule is stationary and the B molecules are diffusing in solution. The molecule A has an effective radius, σ, which is the sum of the radius of A and B, and that B molecules are geometrical points. This is so called Smoluchowski target problem.

Whenever a B molecule comes into contact with A, reaction occurs and B disappears. The critical distance between A and B necessary for reaction to occur is σ. The important assumption is that local concentration of B in the vicinity of A is not uniform. Concentration of B at distance σ is zero ([B] = 0 at $r = \sigma$) and increases to the bulk concentration $[\mathrm{B}]_0$ at $r = \infty$ where r is the distance between A and B. One can calculate the rate at which B flows toward A using the Fick's law of diffusion. The flow of B is given by the Fick's first law of diffusion which states that the flux in any direction (flow of molecules per unit area per unit time) is proportional to the concentration gradient in that direction.

$$\Phi_{\mathrm{B}} = -D_{\mathrm{B}} \nabla C_{\mathrm{B}} \qquad 2.2.3$$

where Φ_B and ∇C_B are the flux and the concentration gradient respectively (both are vectors) and D_B is the translational diffusion coefficient for molecule with radius σ. The gradient ∇C_B is equal to

$$\nabla C_B = -\frac{d[B(t,r)]}{dr} \qquad 2.2.4$$

where $B(t,r)$ is a function dependent both on the distance and time. For convenience we define the density distribution function which is function $B(t,r)$ divided by initial concentration of B.

$$\rho(t,r) = \frac{B(t,r)}{[B]_0} \qquad 2.2.5$$

with the boundary conditions for the new function

$$\rho(\sigma,r) = 0 \ , \ \rho(\infty,r) = 1 \qquad 2.2.6$$

Putting all together, the number of B molecules crossing the spherical surface of radius σ can be described by equation

$$I(\sigma,t) = 4\pi\sigma^2\Phi_B = 4\pi\sigma^2 D[B]_0 \left.\frac{d\rho(t,r)}{dr}\right|_\sigma \qquad 2.2.7$$

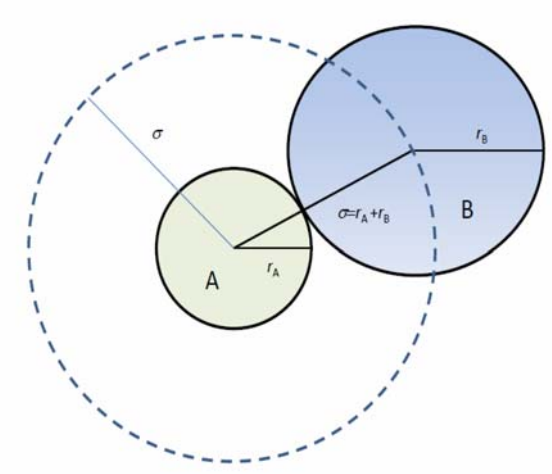

Figure 2.2.1. Illustration of the Smoluchowski target problem. Two spherical molecules are reduced to a single sphere and a point molecule where r_A and r_B are the radius of each molecule, and σ the sum of both [27].

The expression for the density distribution function is can be obtained by solving the second Fick's law with the above presented boundary conditions.

$$\rho(t,r) = 1 - \frac{\sigma}{r}\,\mathrm{erfc}\left[\frac{r-\sigma}{\sqrt{4Dt}}\right] \qquad 2.2.8$$

where $\mathrm{erfc}(x)$ is a complementary gauss error function. The derivative of $d\rho(t,r)/dr$ is given by a quite complicated expression

$$\frac{d\rho(t,r)}{dr} = \frac{\sigma}{r}\left[\frac{1}{r}\mathrm{erfc}\left(\frac{r-\sigma}{\sqrt{4Dt}}\right) + \frac{1}{\sqrt{\pi Dt}}\exp\left[-\left[\frac{r-\sigma}{\sqrt{4Dt}}\right]^2\right]\right] \qquad 2.2.9$$

that fortunately (at distance $r = \sigma$) simplifies to

$$\left.\frac{d\rho(t,\mathrm{r})}{dr}\right|_{r=\sigma} = \frac{1}{\sigma}\left(1 + \frac{\sigma}{\sqrt{\pi Dt}}\right) \qquad 2.2.10$$

Substituting derived $d\rho(t,r)/dr$ term into equation 2.2.7 one obtains

$$I(\sigma,t) = 4\pi\sigma^2\Phi_{\mathrm{B}} = 4\pi\sigma D[\mathrm{B}]_0\left[1 + \frac{\sigma}{\sqrt{\pi Dt}}\right] \qquad 2.2.11$$

If we now notice that the above expression describes the number of molecules at the encounter distance equal to σ , diffusing towards A molecule per second which is also the reaction rate of A + B → C. Multiplying this expression by number of reactant A per unit volume (namely the concentration of A molecules) one obtains the right hand side of the kinetic equation 2.2.2. So comparing equation 2.2.2 with equation 2.2.11 we identify the Smoluchowski rate coefficient as

$$k(t) = 4\pi\sigma D\left[1 + \frac{\sigma}{\sqrt{\pi Dt}}\right] \qquad 2.2.12$$

At times larger than σ^2/D, this equation reduces to the well-known diffusion rate constant, k_{dif}

$$k_{\mathrm{dif}} = 4\pi\sigma D \qquad 2.2.13$$

which in principle can only be applied under the conditions for which Smoluchowski derived it – substantially larger (compared to the solvent molecules) and spherical

reactant particles, pseudo-first order conditions, and much faster reaction rate constant compared to the diffusion rate constant. We can also utilize the Stokes-Einstein equation for diffusion coefficient D obtaining

$$k_{\mathrm{dif}} = \frac{2k_{\mathrm{B}}T}{3\eta} \qquad 2.2.14$$

Almost one century after the publication of his work, his solution is still considered as exact for the target problem, under the above referred conditions. Generalizing, for bimolecular reaction that fulfils above assumptions and where diffusion is limiting stage of the process, the maximal value of rate constant depends on the reaction medium viscosity.

2.3 Kinetic scheme for bimolecular quenching reactions

Quenching of excited states in bimolecular reactions is a complex matter [28] but for the purpose of this dissertation we will limit it to two general pathways - energy and electron transfer. Quenching by electron transfer is a one electron reaction in which an electron jumps from an occupied orbital of one reactant to an unoccupied orbital of the other. The electron can be transferred as either oxidative hole transfer or reductive electron transfer [29]. In either case, quenching by electron transfer between uncharged species leads to a radical ion pair or a charge-transfer complex. Quenching by energy transfer can occur according to two fundamentally different mechanisms. In the electron-exchange (also called the Dexter) mechanism, two single independent electron are transferred, one in each direction resulting in the formation of the sensitizer's ground state and quencher's excited state. The second one is called the Forster or the Coulombic energy transfer. In this case energy is transferred by the oscillating electrons within an excited-state of the donor coupled with those of the acceptor by a dipole-dipole interaction. Since both, electron transfer and energy transfer processes are governed by electron exchange requiring a close approach for effective orbital overlap, a similar kinetic formalism may be used in both cases [22]. The effective range of the Dexter mechanism is limited to distances of less than 10 Å. In contrast, the Coulombic energy transfer does not involve orbital overlap and can be effective up to separation distances as large as 100 Å and cannot be described by the same mechanism as the Dexter energy

transfer or electron transfer.This section is intended to describe such processes as the Dexter energy transfer or electron transfer in terms of reaction rates and concentrations as well as to provide equations that link theoretically assumed reaction scheme with experimentally obtained rate constant, k_q. In the case of energy transfer, kinetic scheme can be written as

$$\begin{array}{ccccccc} *D + A & \underset{k_{-dif}}{\overset{k_{dif}}{\rightleftharpoons}} & [*D...A] & \underset{k_b}{\overset{k_f}{\rightleftharpoons}} & [D...*A] & \xrightarrow{k_{-dif}} & D + *A \\ \downarrow 1/\tau_D & & & & & & \downarrow 1/\tau_A \\ D & & & & & & A \end{array} \qquad 2.3.1$$

where k_f and k_b are intrinsic energy transfer rates constants in the encounter complex. The scheme includes the diffusion of reactants to form encounter complex with diffusion rate constant k_{dif} and the reverse process with a rate constant k_{-dif}. Kinetic scheme can be described by a set of differential equations:

$$\begin{cases} \dfrac{d[*D]}{dt} = -[*D](k_{dif}[A] + \dfrac{1}{\tau_D}) + k_{-dif}[*D...A] \\ \dfrac{d[*D...A]}{dt} = k_{dif}[*D][A] + k_b[D...*A] - k_{-dif}[*D...A] - k_f[*D...A] \\ \dfrac{d[D...*A]}{dt} = -k_b[D...*A] - k_{-dif}[D...*A] + k_f[*D...A] \\ \dfrac{d[*A]}{dt} = -\dfrac{1}{\tau_A}[*A] + k_{-dif}[D...*A] \end{cases} \qquad 2.3.2$$

The intermediate species ([D*…A] and [D…*A]) are constants according to a steady-state approximation

$$\begin{cases} \dfrac{d[*D]}{dt} = -[*D](k_{dif}[A] + \dfrac{1}{\tau_D}) + k_{-dif}[*D...A] \\ \dfrac{d[*D..A]}{dt} = k_{dif}[*D][A] + k_b[D...*A] - k_{-dif}[*D..A] - k_f[*D...A] = 0 \\ \dfrac{d[D..*A]}{dt} = -k_b[D...*A] - k_{-dif}[D...*A] + k_f[*D...A] = 0 \\ \dfrac{d[*A]}{dt} = -\dfrac{1}{\tau_A}[*A] + k_{-dif}[D...*A] \end{cases} \qquad 2.3.3$$

Then the second and third equation from the equations 2.3.3 set can be transformed into

$$[*\mathrm{D}...\mathrm{A}](k_{-\mathrm{dif}} + k_{\mathrm{f}}) = k_{\mathrm{dif}}[*\mathrm{D}][\mathrm{A}] + k_{\mathrm{b}}[\mathrm{D}...*\mathrm{A}] \qquad 2.3.4$$

$$[\mathrm{D}...*\mathrm{A}](k_{-\mathrm{diff}} + k_{\mathrm{b}}) = k_{\mathrm{f}}[*\mathrm{D}...\mathrm{A}] \qquad 2.3.5$$

Then substituting 2.3.5 into 2.3.4 yields

$$k_{\mathrm{dif}}[*\mathrm{D}][\mathrm{A}] - k_{-\mathrm{dif}}[*\mathrm{D}...\mathrm{A}] - k_{\mathrm{f}}[*\mathrm{D}...\mathrm{A}] + k_{\mathrm{b}}\frac{k_{\mathrm{f}}}{(k_{-\mathrm{dif}} + k_{\mathrm{b}})}[*\mathrm{D}...\mathrm{A}] = 0 \qquad 2.3.6$$

$$k_{\mathrm{dif}}[*\mathrm{D}][\mathrm{A}] - [*\mathrm{D}...\mathrm{A}]\left[k_{-\mathrm{dif}} - k_{\mathrm{f}} + k_{\mathrm{b}}\frac{k_{\mathrm{f}}}{(k_{-\mathrm{dif}} + k_{\mathrm{b}})}\right] = 0 \qquad 2.3.7$$

$$[*\mathrm{D}...\mathrm{A}] = [*\mathrm{D}][\mathrm{A}]k_{\mathrm{dif}}\frac{1 + k_b / k_{-\mathrm{dif}}}{k_{\mathrm{b}} + k_{-\mathrm{dif}} + k_{\mathrm{f}}} \qquad 2.3.8$$

Substituting expression 2.3.8 into the first differential equation from 2.3.2 set yields

$$\frac{d[*\mathrm{D}]}{dt} = -k_{\mathrm{dif}}[*\mathrm{D}][\mathrm{A}] + \frac{1}{\tau_{\mathrm{D}}}[*\mathrm{D}] + k_{\mathrm{dif}}[*\mathrm{D}][\mathrm{A}]\frac{k_{\mathrm{b}} + k_{-\mathrm{dif}}}{k_{\mathrm{b}} + k_{-\mathrm{dif}} + k_{\mathrm{f}}} \qquad 2.3.9$$

The expression 2.3.9 can now be compared with the depopulation of excited state of the donor with overall quenching rate k_{q}

$$-\frac{d[*\mathrm{D}]}{dt} = k_{\mathrm{q}}[*\mathrm{D}][\mathrm{A}] + \frac{1}{\tau_{\mathrm{D}}}[*\mathrm{D}] \qquad 2.3.10$$

Finally comparing expression 2.3.9 with 2.3.10 one obtains

$$k_{\mathrm{q}} = k_{\mathrm{dif}}\frac{k_{\mathrm{b}} + k_{-\mathrm{dif}} + k_{\mathrm{f}} - k_{\mathrm{b}} - k_{-\mathrm{dif}}}{k_{\mathrm{b}} + k_{-\mathrm{dif}} + k_{\mathrm{f}}} \qquad 2.3.11$$

that after simplification leads to the final expression linking the theoretically assumed reaction rates with experimentally obtained depopulation of excited state of the donor

$$k_{\mathrm{q}} = \frac{k_{\mathrm{dif}}}{1 + k_{-\mathrm{dif}} / k_{\mathrm{f}} + k_{\mathrm{b}} / k_{\mathrm{f}}} \qquad 2.3.12$$

If one assume Boltzmann equilibrium

$$\frac{k_{\mathrm{f}}}{k_{\mathrm{b}}} = \exp\left[\frac{\Delta G_{\mathrm{EN}}}{RT}\right] \qquad 2.3.13$$

then substitution to equation 2.3.13 yields expression for observable rate k_{q} in a form

$$k_{\mathrm{q}} = \frac{k_{\mathrm{dif}}}{1+\exp(\Delta G_{\mathrm{EN}} / RT) + k_{-\mathrm{dif}} / k_{\mathrm{f}}} \qquad 2.3.14$$

This result is useful in discussion of thermodynamics aspects of energy transfer process as it connects the observable rate k_{q} with the reaction exothermicity ΔG_{EN}. In the case of electron the frames for discussion of factors that influence ET process is provided by kinetic equations. In particular case of reductive electron transfer, the reaction scheme postulated by Rehm and Weller [30] can be summarized as follow

$$\begin{array}{ccccccc} {}^{*}\mathrm{D}+\mathrm{A} & \underset{k_{-\mathrm{dif}}}{\overset{k_{\mathrm{dif}}}{\rightleftharpoons}} & {}^{*}[\mathrm{D}...\mathrm{A}] & \underset{k_{-\mathrm{ET}}}{\overset{k_{\mathrm{ET}}}{\rightleftharpoons}} & [\mathrm{D}^{-}...\mathrm{A}^{+}] & \underset{k_{-\mathrm{s}}}{\overset{k_{\mathrm{s}}}{\rightleftharpoons}} & \mathrm{D}^{-}+\mathrm{A}^{+} \\ \downarrow 1/\tau_{\mathrm{D}} & & & & \downarrow k_{\mathrm{fg}} & & \\ \mathrm{D} & & & & [\mathrm{D}...\mathrm{A}] & \underset{k_{\mathrm{dif}}}{\overset{k_{-\mathrm{dif}}}{\rightleftharpoons}} & \mathrm{D}+\mathrm{A} \end{array} \qquad 2.3.15$$

The intermediates in the above scheme are an encounter complex [*D...A], charged ion pair [D⁻…A⁺] and ions [D⁻] and [A⁺] as well as solvent separated donor and acceptor [D…A]. Mechanism include diffusion reactants to form encounter complex with diffusion rate constant k_{dif}, natural decay of the donor excited state $1/\tau_{\mathrm{D}}$, reversible transfer of electron within encounter pair with forward k_{ET} and backward $k_{-\mathrm{ET}}$ rates, and the reversible dissociation/association into/form a bulk solution described by k_{s} and $k_{-\mathrm{s}}$ rates. Additional electron transfer process occurring within the encounter pair [D⁻…A⁺] with the rate k_{fg} leads to generation of solvent separated ground-state products. Now to test it against experimentally obtained rate constant k_{q} one must compare the depopulation of the experimentally obtained excited state (which is assumed to follow scheme)

$$\begin{array}{ccc} [*D]+[A] & \xrightarrow{k_q} & [D]+[A] \\ \downarrow 1/\tau_D & & \\ [D] & & \end{array} \qquad 2.3.16$$

with depopulation obtained from theoretical scheme. In case of scheme 2.3.15 the resulting the overall quenching rate constant k_q is given by equation

$$k_q = \frac{k_{dif}}{1 + k_{-dif}/k_{ET} + k_{-dif}k_{-ET}/k_{ET}(k_{fg} + k_s)} \qquad 2.3.17$$

The derivation of equation 2.3.17 can be found in [30]. One must keep in mind that presented scheme is one of the simplest and models present in the literature can take into account additional factors as well as additional reactions [31] which can lead to a more complicated expressions. Each of them has different solution but rules of constructing them are the same. The determination of the rate limiting step in case of the electron transfer processes is a challenging task. Key role for this reaction, independently of assumed scheme, plays dependence of k_{ET} on a driving force of the reaction. A detailed analysis of thermodynamic aspects of electron transfer rate k_{ET} is given in subsequent chapter. It is important, however, to stress that the obtained expression 2.3.17 can be now tested against experimental results which can prove or disprove assumed kinetic scheme.

2.4 Basic concepts of energy transfer phenomenon

2.4.1 Energy transfer from the quantum point of view

Considering that only two electrons are involved in a transition, one on donor molecule D and one on acceptor molecule A, and an anti-symmetrized wave-functions for the initial excited state Ψ_i (D is excited and A not) and the final excited state Ψ_f (A is excited and not D) can be written as

$$\Psi_i = N\left[\Psi_{D^*}(1)\Psi_A(2) - \Psi_{D^*}(2)\Psi_A(1)\right] \qquad 2.4.1$$

$$\Psi_f = N\left[\Psi_D(1)\Psi_{A^*}(2) - \Psi_D(2)\Psi_{A^*}(1)\right] \qquad 2.4.2$$

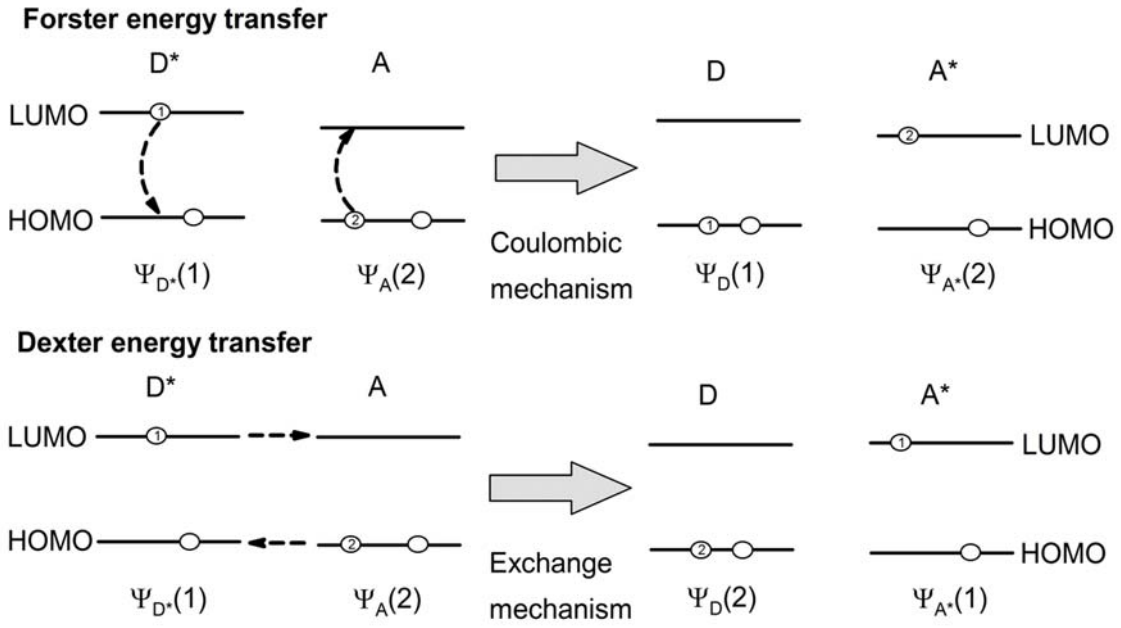

Figure 2.4.1 Schematic representation of the Coulombic and exchange mechanisms of excitation energy transfer.

where N is a normalization factor, Ψ_D and Ψ_A are wave-functions of donor and acceptor molecules and numbers 1 and 2 refer to the two electrons involved. The coupling between the initial and final states is given by integral

$$U = \left\langle \Psi_i \middle| V \middle| \Psi_f \right\rangle \qquad 2.4.3$$

where V can be treated as perturbation to total Hamiltonian of form $\hat{H} = \hat{H}_D + \hat{H}_A + V$. Substituting 2.4.1 and 2.4.2 to equation 2.4.3 yields equation for interaction energy between a donor molecule and an acceptor molecule.

$$U = \left\langle \Psi_{D^*}(1)\Psi_A(2) \middle| V \middle| \Psi_D(1)\Psi_{A^*}(2) \right\rangle - \left\langle \Psi_{D^*}(1)\Psi_A(2) \middle| V \middle| \Psi_D(2)\Psi_{A^*}(1) \right\rangle \qquad 2.4.4$$

The two terms in the equation correspond to two different mechanisms of energy transfer. In the first term, U_C, usually called the Coulombic term, the initially excited electron on donor returns to the ground state orbital while an electron on acceptor is simultaneously promoted to the excited state. In the second term, called the exchange or the Dexter term, U_{ex}, the excited electron is transferred to the acceptor's excited state while electron from

the acceptors ground state is transferred to the donor ground state. The exchange interaction is a quantum mechanical effect arising from the symmetry properties of the wave-functions with respect to the exchange of spin and space coordinates of two electrons. Whereas for the excited singlet state both mechanisms can be operative, energy transfer between triplet states can principally occur according to the Dexter mechanism.

2.4.2 Resonance energy transfer

In a qualitative manner resonance energy transfer is similar to the behavior of two coupled oscillating dipoles. Upon this assumption Forster [6] developed a model describing conditions required for the Coulombic energy transfer to take place and the dependence of rate of energy transfer rate on the distance. The expression describing this can be derived by multipole expansion [32] of the Coulombic term into a sum of terms (multipole-multipole series). The most important term representing the dipole-dipole interaction between the transition dipole moments of the donor and acceptor can be used to approximate the Coulombic term U_c

$$U_c = \frac{1}{4\pi\varepsilon_0}\frac{|M_D||M_A|}{r^3}(\cos(\theta_{DA}) - 3\cos(\theta_A)\cos(\theta_D)) \qquad 2.4.5$$

where M_D and M_A are the transition dipole moments of the transitions D → *D and A → *A, r is the donor-acceptor separation distance and θ_{DA}, θ_A, θ_D are the angle between the two transition moments and the angles between each transition moment and the vector connecting them, respectively. For the expression for transfer rate constant a similar equations have been derived from classical and quantum mechanical considerations. On the quantum-mechanical grounds the Fermi Golden Rule [33] allows to obtain energy transfer rate k_C

$$k_C = \frac{2\pi}{\hbar}U_c^2\rho \qquad 2.4.6$$

where ρ is a measure of the density of the interacting initial and final states, as determined by the Franck-Condon factors [33], and is related to the overlap integral between the emission spectrum of the donor and the absorption spectrum of the acceptor.

In the classical analog (dipole oscillators) the energy of interaction of the two dipoles is inversely proportional to the third power of the distance separating the dipoles (r^{-3}) and directly proportional to the oscillator strength. Using this classical analog Forster has been able to develop a quantitative expression for the rate of energy transfer due to dipole-dipole interaction in terms of experimental parameters.

$$k_C = \frac{9000\ln(10)\kappa^2\Phi_D^0}{128\pi^5 N_A n^4 \tau_D r^6}\int_0^\infty I_D(\lambda)\varepsilon_A(\lambda)\lambda^4 d\lambda \qquad 2.4.7$$

where κ^2 is the orientation factor, τ_D is its lifetime of the donor in the absence of quenching, Φ_D^0 is the fluorescence quantum yield of the donor in the absence of energy transfer, n is the average refractive index of the medium in the wavelength range where spectral overlap is significant, $I_D(\lambda)$ is the normalized fluorescence spectrum of the donor and $\varepsilon_A(\lambda)$ is the molar absorption coefficient of the acceptor. The orientation factor κ^2, is given by

$$\kappa^2 = \cos(\theta_{DA}) - 3\cos(\theta_A)\cos(\theta_D) \qquad 2.4.8$$

and for a random distribution is equal to ⅔. The equation 2.4.7 can be written in the form similar to equation 2.4.6

$$k_C = \frac{1}{\tau_D}\left[\frac{R_0}{r}\right]^6 \qquad 2.4.9$$

where R_0 is a is the critical distance or the Forster radius that is the distance at which energy transfer and spontaneous decay of the excited donor are equally probable. The R_0 distance, which can be determined from spectroscopic data, is given by

$$R_0^6 = \frac{9000\ln(10)\kappa^2\Phi_D^0}{128\pi^5 N_A n^4}\int_0^\infty I_D(\lambda)\varepsilon_A(\lambda)\lambda^4 d\lambda \qquad 2.4.10$$

It is important to note that the squares of the transition dipole moments are proportional to the oscillator strengths of A → *A and D → *D transitions which can be estimated experimentally. In some cases one may exclude resonance energy transfer process, *i.e.* when there is a lack of allowed absorption transitions for the quencher in the emission wavelength range of the donor.

2.4.3 Exchange energy transfer

The second term in equation 2.4.4 is responsible for short-range interaction called exchange mechanism which is a purely quantum mechanical phenomenon and does not depend on the oscillator strengths of the transitions involved. As derived by Dexter [7] the exchange interaction for two electrons separated by a distance r_{12}, can be written as

$$U_{EX} = \left\langle \Phi_{D^*}(1)\Phi_A(2)\left|\frac{e^2}{r_{12}}\right|\Phi_D(2)\Phi_{A^*}(1)\right\rangle \qquad 2.4.11$$

where Φ_D, Φ_{D^*}, Φ_A, and Φ_{A^*} represent contributions of the spatial wave-function to the total wave-function that include spin. Expression has non zero elements only if there is a spatial overlap between orbital of initial and final state. Therefore it's called the overlap or collision mechanism as it requires formation of an encounter complex (*D...A) to appear. The range of exchange interaction decreases exponentially with the donor-acceptor separation distance. Rate constant for the Dexter exchange energy transfer k_{EX}, is obtained substituting equation 2.4.11 into the Fermi Golden Rule formula

$$k_{EX} = \frac{2\pi}{\hbar} U_{EX}^2 \rho \qquad 2.4.12$$

which yields to final expression for the Dexter-type energy transfer rate constant

$$k_{EX} = \frac{2\pi}{h} K \exp(-\frac{2r}{L}) \int_0^\infty I_D(\lambda)\varepsilon_A(\lambda)d\lambda \qquad 2.4.13$$

where *K* is a constant with the dimension of energy and *L* is so-called the effective Bohr radius, which measures the spatial extent of the donor and acceptor wave functions. $I_D(\lambda)$ and $\varepsilon_A(\lambda)$ are the normalized donor emission and acceptor absorption spectra, respectively. The integral of the products of these two functions fulfill condition

$$\int_0^\infty I_D(\lambda)d\lambda = \int_0^\infty \varepsilon_A(\lambda)d\lambda = 1 \qquad 2.4.14$$

as it is the mathematical expression for the energy conservation constraint. It is important to mention that equation 2.4.13 is applicable only in environments with fixed distances between species involved in the energy transfer process such as crystals. For bimolecular

reactions in liquid media, diffusion is important part of the process which affects most of the parameters present in equation 2.4.13. One of the controversies is caused by integral of normalized donor emission and acceptor absorption spectra. For the triplet-triplet energy transfer this integral is usually equal to zero (due to absence of singlet-triplet absorption mainly) while energy can be transferred efficiently. Mentioned integral can also be zero in case of singlet-singlet energy transfer. If the donor emission is sufficiently higher in energy than acceptors absorption spectra will not overlap but transfer will be still possible.

Attempts to directly link the Dexter theory (equation 2.4.13) with simple kinetic model, like the Perrin [34] model, are present in the literature [12] but quality of the extracted date raise doubts about the correctness of whole approach. The next section is devoted to models in which diffusion plays a key role in determining net result of energy transfer reactions. The reactions obey selection rules for the Dexter-type energy transfer but in fact that is main connection with model presented above. The allowed transitions (selection rules) for exchange mechanism are

$$^{1}*D + {}^{1}A \leftrightarrow {}^{1}D + {}^{1}*A \qquad \text{singlet-singlet energy transfer}$$

and

$$^{3}*D + {}^{1}A \leftrightarrow {}^{1}D + {}^{3}*A \qquad \text{triplet-triplet energy transfer}$$

Leaving aside mechanistic consideration, next section concerns kinetic models in liquid solutions. Chemical kinetics is concerned with the rates of chemical reactions, that is, with the quantitative description of how fast chemical reactions occur, and of the factors affecting these rates. Main goal of below presented models is to provide expression that explains the experimentally obtained bimolecular rates for energy transfer process in terms of kinetic scheme and rate constants. Dependence of the rate constants on physical parameters of the involved species (like energy of the excited state, molecular volume, dipole moment or redox potential, etc.) or properties of the solvent (like density, dielectric constant, viscosity, etc.) is often used to test validity of the model. All presented models (including further described electron transfer) share common assumption that the molecules in order to transfer energy must be in contact and (at least in the first

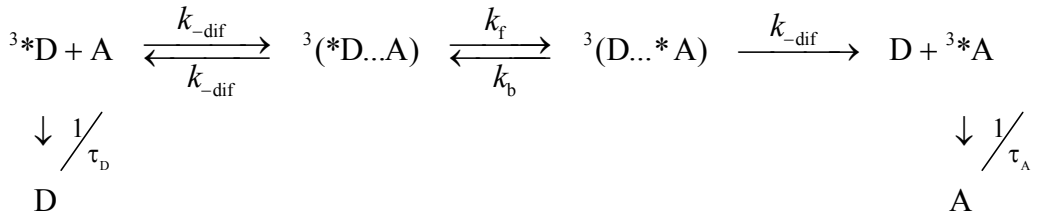

Figure 2.4.2. Scheme of the bimolecular energy transfer for the Sandros model within ^{3}*D...A and D...^{3}*A pairs. The forward and backward (reverse) energy transfers rate constant fulfill the Bolzmann condition $k_f / k_b = \exp(-\Delta G_{EN} / RT)$ and the value of k_{dif} is given by the Smoluchowski equation. The τ_D and τ_A are the natural lifetime of the donor and acceptor, respectively.

approximation) no noticeable distance dependence of the rate constant is present. Further assumptions, that there is no bond breaking or forming during the reaction and that energy transfer occurs, according to the Kasha rule [35], from vibrationally relaxed states are also worth mentioning.

2.4.4 Kinetic limitations – Sandros model for energy transfer processes.

First kinetic approach was elaborated by Sandros in early sixties. He summarized work on energy transfer done so far by Porter [36], Ermolaev [37, 38] and himself [39-43]. He's objective was to explain and eventually predict, experimentally obtained energy transfer rates from quenching experiments. He assumed that the kinetic scheme must go beyond simple *D +A ↔ D + *A reaction and include formation of an activated complex. That means molecules of donor and acceptor (^{3}*D...A and D...^{3}*A) are trapped in a "solvent cage" (Figure 2.4.2). The Sandros's scheme does not include excitation of the donor to its singlet state, the vibrational relaxation of the donor in its singlet state and intersystem crossing to triplet state as mentioned processes occurs in much shorter time scale. He also assumed that, due to an extremely fast intrinsic energy transfer step, a full equilibration between ^{3}*D...A and D...^{3}*A forms of an activated encounter complex must be reached. Consequently, the ratio of probabilities of the separation of the reacting species to form free ^{3}*D + A and D + ^{3}*A pairs, should obey the Boltzmann distribution law being equal to $\exp(-\Delta G_{EN} / RT)$ where ΔG_{EN} is a difference between energy level of donor and acceptor ($\Delta G_{EN} = E_D - E_A$).

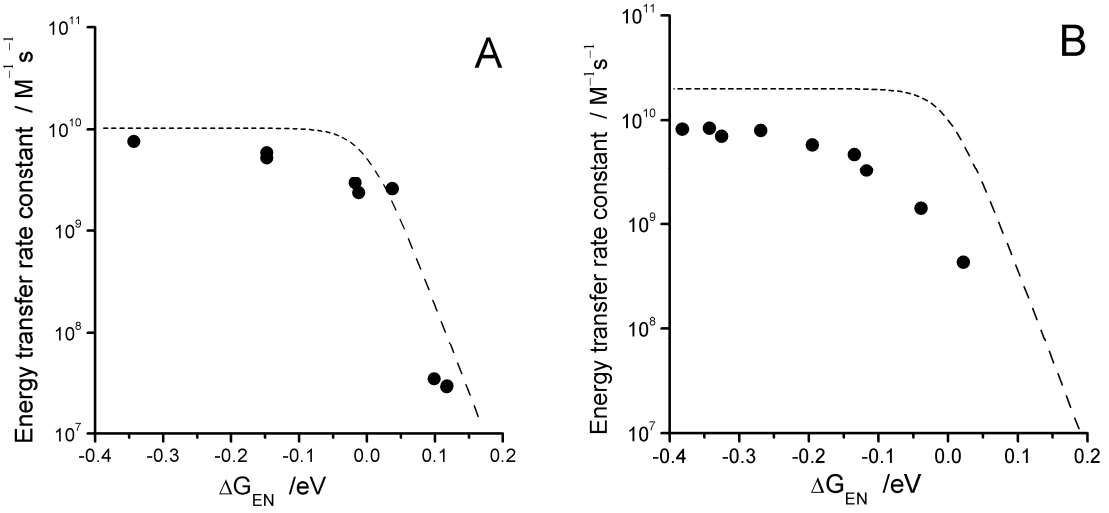

Figure 2.4.3. Dependency of the overall energy transfer rate constants k_{EN} on the reaction exergonicity ΔG_{EN}. Chart A - energy transfer rates from ^{3}*biacetyl to different acceptors in benzene solutions (data from ref. [40]). Chart B - energy transfer rates from ^{3}*Ru(bpy)$_3^{2+}$ to a different acceptors in acetonitrile solutions (data from ref [43]). Dotted lines correspond to the theoretical predictions calculated according to the Sandros model.

This clearly shows that the rate of energy transfer process should be mainly dependent on the energy difference ΔG_{EN}. Expecting also that formation and dissociation of an activated encounter complex are governed by diffusion, one can obtain the following relationships describing the dependence of the rate constants in a bimolecular process on the energy difference ΔG_{EN}

$$k_q = \frac{k_{dif}}{1+\exp(\Delta G_{EN}/RT)} \qquad 2.4.15$$

where k_{dif} is the diffusion rate constant at infinite time taken from the Einstein-Smoluchowski equation [26]. The same result is predicted by equation 2.3.11 with assumption that intrinsic energy transfer rate, k_f is much faster than k_{dif}. The Sandros model predicts that for all ΔG_{EN} values the reaction is diffusion controlled and for enough negative ΔG_{EN} values process should occur with a rate constant equal to k_{dif}, whereas for $\Delta G_{EN} = 0$ energy transfer process should be exactly two times slower. Also the experimentally observed values of the energy transfer rate constants should be inversely proportional to viscosity in the same manner as k_{dif} in the whole range of ΔG_{EN} values. Moreover, at the ΔG_{EN} values near zero, a linear relationship between $\ln(k_{EN})$ and $\Delta G_{EN}/RT$ with slope equal unity, should be observed. At the time the proposed model

seems to be able to reproduce existing experimental data (Figure 2.4.3 chart A). However subsequent experimental works on the topic (different solvents and much more experimental points) revealed a major deviation from theoretical model (Figure 2.4.3 chart B). A detailed analysis of the Sandros model and possible reasons for fact that agreement between theory and experiments cannot be regarded as satisfactory are presented in subsequent chapters.

2.4.5 Kinetic limitations – Balzani model for energy transfer processes

Due to the doubts about correctness of Sandros model, in the year 1980 Vincenzo Balzani presented a different theoretical approach. According to the Balzani model [22, 45] the intrinsic energy transfer step exhibits features similar to non-adiabatic electron transfer as both reactions may be governed by the similar mechanisms. Using the same kinetic scheme as for the quenching via electron transfer by a collisional mechanism (Figure 2.4.4), he proposed an approach similar to the Marcus theory [46] to express the dependence of k_f and k_b rate constants for both, the forward and the reverse energy transfer within the activated encounter ^{3}*D...A and D...^{3}*A complexes, respectively.

Balzani also assumed that the deactivation of excited acceptor state with is much slower than diffusion process and this channel of reaction can be omitted. Also the energy transfer rate constants follow the Bolzmann distribution

$$\frac{k_f}{k_b} = \exp\left[\frac{\Delta G_{EN}}{RT}\right] \qquad 2.4.16$$

and can be expressed independently of direction (forward or backward) by the transition state theory.

$$k_{EN} = A_{EN} \exp(-\Delta G_{EN}^{\#} / RT) \qquad 2.4.17$$

The term $\Delta G_{EN}^{\#}$ stands for activation energy (free enthalpy of activation) and originates directly from the Marcus theory. For electron transfer there at least are several ways to express this quantity but for energy transfer, Balzani claimed that $\Delta G_{EN}^{\#}$ is related to the distortion between ground and excited states determining the intrinsic barrier to energy transfer. The free enthalpy of activation $\Delta G_{EN}^{\#}$ receives contributions from changes in the inner nuclear coordinates of the molecule ("inner-sphere'' reorganization energy, $\Delta G_i^{\#}$**)**

and from changes in the solvent arrangement around the molecule ("outer-sphere" reorganization energy, $\Delta G_{\mathrm{o}}^{\#}$) [47].

$$\Delta G_{\mathrm{EN}}^{\#} = \Delta G_{\mathrm{i}}^{\#} + \Delta G_{\mathrm{o}}^{\#} \qquad 2.4.18$$

Contrary to that what happens in the electron-transfer processes, $\Delta G_{\mathrm{o}}^{\#}$ is usually very small because in the energy-transfer processes the electric charges of the reactants remain unchanged. At most, there are changes in dipole moments and polarizabilities, which usually do not cause a drastic rearrangement of the solvation sphere. For quantitative description of $\Delta G_{\mathrm{EN}}^{\#}$ values, Balzani proposed the Agmon and Levine [48, 49] model with assumption that $\Delta G_{\mathrm{EN}}^{\#}$ is negligible.

$$\Delta G_{\mathrm{EN}}^{\#} = \Delta G_{\mathrm{EN}} + \frac{\Delta G_{\mathrm{EN}}^{\#}(0)}{\ln 2} \ln\left[1 + \exp\left[-\frac{\Delta G_{\mathrm{EN}} \ln 2}{\Delta G_{\mathrm{EN}}^{\#}(0)}\right]\right] \qquad 2.4.19$$

where $\Delta G_{\mathrm{EN}}^{\#}(0)$ is $\Delta G_{\mathrm{EN}}^{\#}$ for the case where ΔG_{EN} is equal zero. It is worth mentioning that, as it stems from the Balzani's consideration, $\Delta G_{\mathrm{EN}}^{\#}$ and related to its $\Delta G_{\mathrm{EN}}^{\#}(0)$ values are not directly related to any measurable quantity. The second important part of the equation 2.4.17, a pre-exponential factor, A_{EN} has been explained on the basis of transition state theory [50].

$$A_{\mathrm{EN}} = \kappa_{\mathrm{tr}} \frac{k_{\mathrm{B}} T}{h} \qquad 2.4.20$$

where $k_{\mathrm{B}}T/h$ is a frequency factor and κ_{tr} is so-called transmission coefficient [51] which is a composition of partition functions for all compounds featuring in the reaction.

$$\begin{array}{ccccccc} {}^3\mathrm{*D} + \mathrm{A} & \underset{k_{-\mathrm{dif}}}{\overset{k_{\mathrm{dif}}}{\rightleftharpoons}} & {}^3(\mathrm{*D..A}) & \underset{k_{\mathrm{b}}}{\overset{k_{\mathrm{f}}}{\rightleftharpoons}} & {}^3(\mathrm{D..*A}) & \underset{k_{\mathrm{dif}}}{\overset{k_{-\mathrm{dif}}}{\rightleftharpoons}} & \mathrm{D} + {}^3\mathrm{*A} \\ \downarrow 1/\tau_{\mathrm{D}} & & & & & & \\ \mathrm{D} & & & & & & \end{array}$$

Figure 2.4.4. Scheme of the bimolecular energy transfer for the Balzani model within ^{3}*D...A and D...^{3}*A pairs. The intrinsic energy transfers rate constant in the activated complex is given by $k_{\mathrm{f}} = A_{\mathrm{EN}} \exp(-\Delta G_{\mathrm{EN}}^{\neq} / RT)$ and the values of k_{dif} and $k_{-\mathrm{dif}}$ are given by the Einstein-Smoluchowski equation. The τ_{D} is the natural lifetime of the excited donor.

Now after having considered the meaning of intrinsic energy transfer rates, k_f and k_b, Balzani applied them to a general reaction scheme for energy transfer (Figure 2.4.4). The solution for this scheme under a steady-state approximation has been discussed in chapter 2.3 and the expression for k_q is given by equation 2.3.15. Combing Balzani's theoretical approach with solution of energy transfer kinetic scheme (equation 2.3.14) one obtains

$$k_q = \frac{k_{dif}}{1+\exp\left[\frac{\Delta G_{EN}}{RT}\right]+\frac{k_{dif}}{A_{EN}}\exp\left[\frac{\Delta G_{EN}}{RT}+\frac{\Delta G^{\#}_{EN}(0)}{RT\ln 2}\ln\left[1+\exp\left(-\frac{\Delta G_{EN}\ln 2}{\Delta G^{\#}_{EN}(0)}\right)\right]\right]}$$

2.4.21

Above expression should describe quenching rate constant in any particular solvent so one should consider influence of solvent properties on both pre-exponential factor, A_{EN} and free enthalpy of activation, $\Delta G^{\#}_{EN}$. As mentioned above $\Delta G^{\#}_{EN}$ value depends mainly on the inner reorganization energy $\Delta G^{\#}_{i}$ of the reactants. The corresponding contribution from the outer reorganization energy $\Delta G^{\#}_{o}$ should be negligible because no charged species are formed or destroyed in the energy transfer processes. Thus the magnitude of the $\Delta G^{\#}_{EN}$ parameter, being an intrinsic property of the donor and acceptor molecules, can be considered for the given A + D systems as constant over the whole range of the investigated solvents. Similarly, the transmission coefficient A_{EN} responsible for the pre-exponential factors should depend only on the nature of the reacting donor and acceptor molecules, remaining, at least in first approximation, solvent independent. This leads to conclusion that the same intrinsic energy transfer rate constants k_f and k_b can be used to fit to the experimental data for the same compounds in different solvents. This is especially important clue for conducting systematic solvent studies of energy transfer processes as presented in this dissertation. Using k_f terms (formally bimolecular rate constants) as fitting parameters one can find that the Balzani model is quite well able to reproduce experimental quenching rate values. Deeper insight into the details of the model leads, however, to some questions that are very difficult to answer. Whole discussion about correctness of the Balzani model on the basis of obtained results during the course of this work is presented in subsequent chapters.

2.5 Electron transfer reactions

Electron transfer (ET) reactions in solution have been summarized and reviewed by many authors in works concerning different aspects of the theory as well as experimental results [52-63]. Thus, in this chapter the relevant ideas and equations are only briefly summarized to present basics concepts underlying electron transfer phenomenon. Electron transfer is one of the most important chemical processes in nature and it plays a central role in many aspects of biology and biochemistry. Of special interest in the view of this dissertation are photo-induced electron transfer and its comparison with energy transfer.

In case of photo-induced electron transfer, in bimolecular systems, process can be categorized as either oxidative or reductive electron transfer (Figure 2.5.1). Interestingly, that if both of these processes occur simultaneously, the final result will be exactly the same as in case of the Dexter type energy transfer. This may be the reason why electron transfer and the Dexter type of energy transfer require similar condition to occur. Both processes are contact reactions (due to requirement of spatial overlap between their orbitals) and no bonds are breaking or forming during the reaction. Thus some features of the electron transfer phenomena should be also observed in the energy transfer

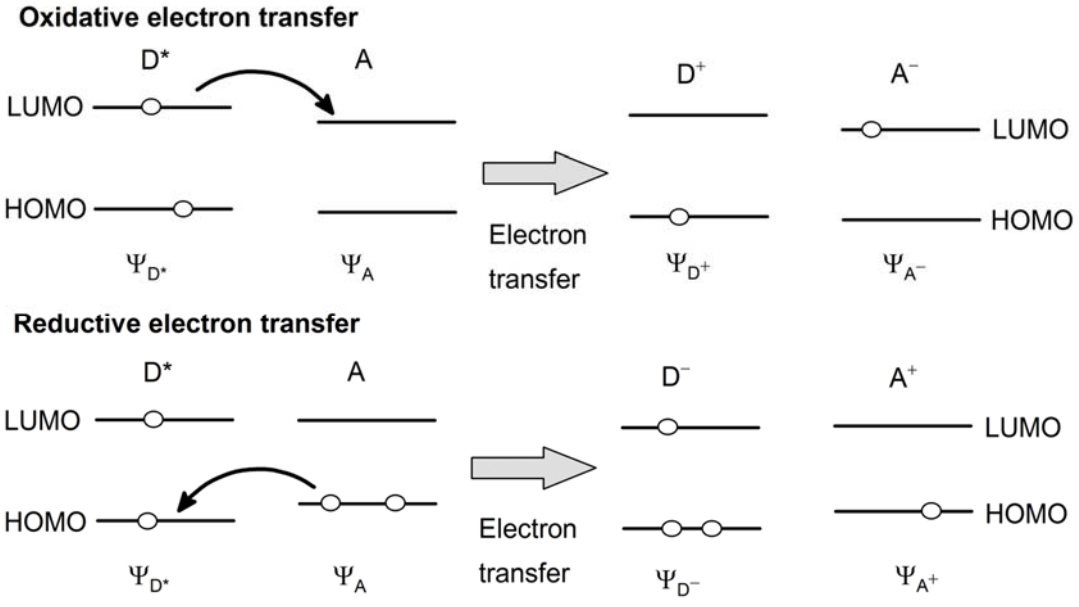

Figure 2.5.1. Illustration of the photo-induced electron transfer for oxidative and reductive mechanisms.

processes. As an example, the dependence of rate of energy transfer process on driving force of reaction looks similar to the Rehm-Weller plot for electron transfer.

The present electron transfer theory covers all kinds of possible environments and nuclear arrangements during the process, but Marcus developed his theory [46] for outer sphere electron transfer reactions, that is for the casa with a redox process in which no bonds are created or formed, and process is not assisted by any kind of transient bond. The potential energy of both product and substrate is a function of the translational, rotational and vibrational coordinates of the reacting species and of the molecules of the surrounding medium. The system moves from substrates to products along the reaction coordinate, *q*, which include all that factors. Marcus assumed that potential energy of reacting species can be approximated by a parabolic curve and this assumption provided framework for discussion of the dependence of activation energy for electron transfer process. In this picture the energy is just dependent on the square of the distance from the equilibrium according to the Hook's law.

To calculate activation energy let's assume that substrates parabola has origin at point (0, 0) and its equation is $y_s(x) = x^2$. The origin of products parabola is at (*a*, *b*) therefore its equation is $y_p(x) - b = (x-a)^2$. On the intersection of two parabolas when $y_s(x) - y_p(x) = 0$ we have

$$x^2 = x^2 - 2ax + a^2 + b \qquad 2.5.1$$

$$x = \frac{a^2 + b}{2a} \qquad 2.5.2$$

The value of function *y*(*x*) at intersection of two parabolas is equal to activation energy $\Delta G_{ET}^{\#}$ of the process

$$\Delta G_{ET}^{\#} = \left[\frac{a^2 + b}{2a}\right]^2 \qquad 2.5.3$$

We can identify parameter *b* as ΔG_{ET} difference between energy of initial and final state. The second parameter, a^2, is the distance along reaction coordinate and according to Hook's law it has dimension of energy. Marcus identified this parameter as

reorganization energy, λ. It is the amount of energy required to distort the nuclear configuration of the reactants into the nuclear configuration of the products without electron transfer occurring (Figure 2.5.2). So that the expression for activation energy in case of electron transfer is given by

$$\Delta G_{\mathrm{ET}}^{\#} = \frac{(\lambda + \Delta G_{\mathrm{ET}})^2}{4\lambda} \qquad 2.5.4$$

Magnitude of ΔG_{ET} can be straightforwardly calculated from values of the redox potentials of reduction E_{red} and oxidation E_{ox} of the reactant species with appropriate corrections for work terms corresponding to the electrostatic repulsion or attraction forces between the electron transfer reactants w_{R} and products w_{P}

$$\Delta G_{\mathrm{ET}} = F(E_{\mathrm{red}} - E_{\mathrm{ox}}) - w_{\mathrm{R}} + w_{\mathrm{P}} \qquad 2.5.5$$

where F denotes the Faraday constants.

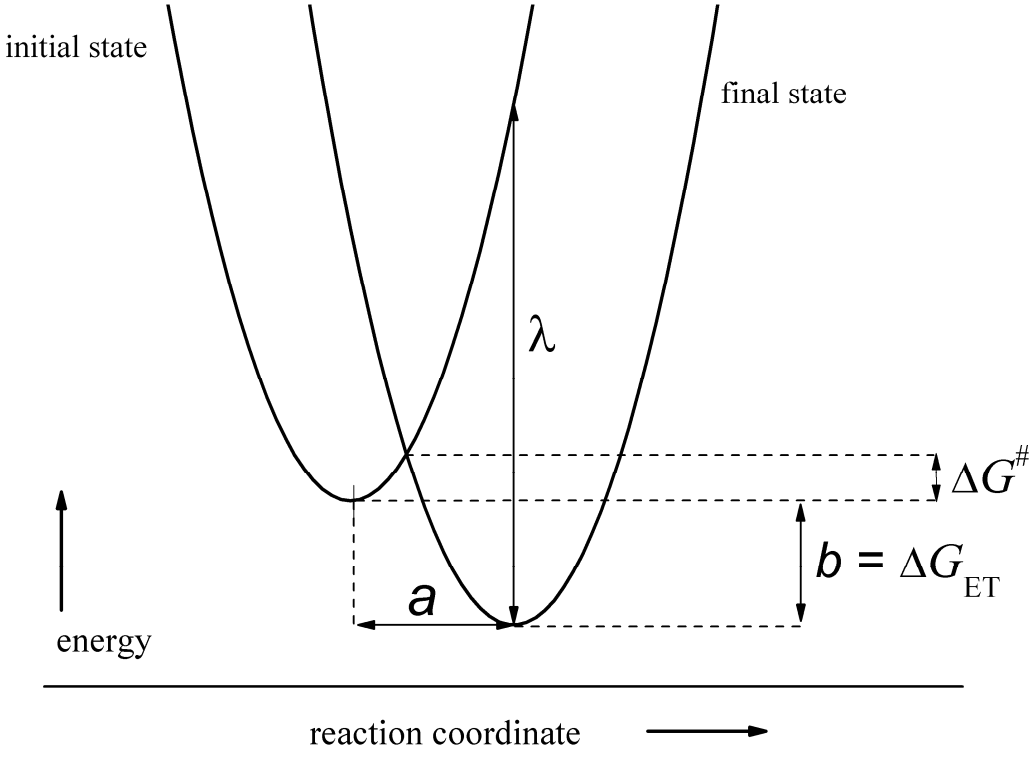

Figure 2.5.2. The scheme of approximated potential energy parabolas for substrates and products of energy transfer reaction in the function of reaction coordinate. The indicated values of activation energy $\Delta G_{\mathrm{ET}}^{\#}$, difference between energy of initial and final state ΔG_{ET} and reorganization energy λ.

The energy w_R corresponds to the interaction between reactants and is the energy required to bring the reactants together to the most probable separation distance *d* at which the electron transfer takes place. Analogously, w_P is the energy required to bring the products into the activated complex. The reorganization energy is a sum of two contributions: λ_i – the inner, required for bond length and angle changes, and λ_o – the outer, necessary for reorganization of the solvent. The standard estimation for outer reorganization energy was obtained by using a model in which reactants and products were modeled as spheres and the solvent as a dielectric continuum. On the basis of the Born solvation theory, λ_o is given by

$$\lambda_o = \frac{e_0^2}{4\pi\varepsilon_0}\left[\frac{1}{2r_A}+\frac{1}{2r_D}-\frac{1}{d}\right]\left[\frac{1}{n^2}-\frac{1}{\varepsilon}\right] \qquad 2.5.6$$

where *n* and ε are the refractive index and the dielectric constant of the reaction medium, ε_0 is vacuum dielectric permittivity, whereas r_A and r_D are the effective radii of the redox centers involved in the electron transfer reaction, with the center-to-center separation distance *d* [64-65].

The energy λ_i required to reorganize the intramolecular bonds can be calculated by using a harmonic oscillator approximation. The energy needed to change the atomic distances from their equilibrium values in the initial state to those appropriate to the final state can be calculated by taking into account the force constants in the reactant and product (f_i and f_f, respectively) and the changes in equilibrium values of all affected bonds (Δq_{if}):

$$\lambda_i = \sum \frac{f_i f_f}{f_i + f_f}\left(\Delta q_{if}\right)^2 \qquad 2.5.7$$

The values of f_i and f_f can be obtained from the infrared spectroscopy and from crystallography (Δq_{if}) if appropriate data are known for both redox forms involved in the electron transfer process [66]. An alternative method for λ_i estimation is based on semi-empirical quantum-chemical calculations [67].

The final expression for electron transfer rate constant k_{ET} is derived on the basis of transition state theory (TST)

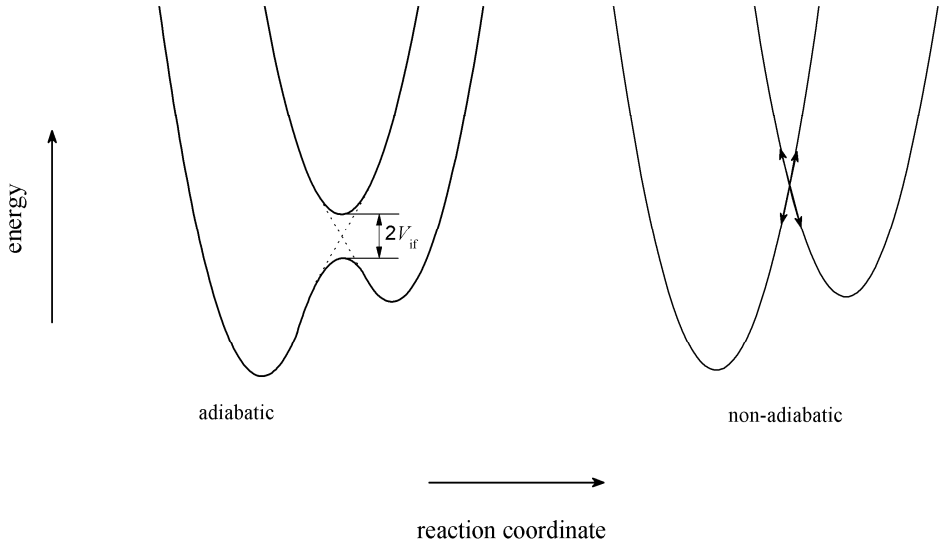

Figure 2.5.3 Scheme for adiabatic and diabatic (or non-adiabatic) potential energy curves for an electron transfer reaction.

$$k_{ET} = A\exp\left[\frac{(\lambda + \Delta G_{ET})^2}{4\lambda RT}\right] \qquad 2.5.8$$

The pre-exponential factor A in case of electron transfer is equal to the magnitude of electron hopping frequency ν_{ET} describing the probability of the intrinsic electron transfer act. The important part of this factor is the coupling element V_{if}, related to the exchange between quantum states for substrates and products. This is essential parameter for the electron transfer reactions as its magnitude divides reaction into two regimes: adiabatic (when the two energy curves are well separated, isolated from each other, by a large coupling) and diabatic (when crossing to the upper surface is still possible). In the first case the system will always remain on the lowest surface as it moves from left to right in Figure 2.5.3. This causes that the activation energy of the process is reduced by a factor V_{if}. On the other hand, if the splitting is negligible, a system initially on the surface of the substrates will tend to remain on it as it passes to the right across the intersection and this can eventually open an additional reaction path. This leads to a different expression for rate constant for relatively small (non-adiabatic limit) or large (adiabatic limit) values of V_{if}.

According to the Landau-Zener theory the pre-exponential factor ν_{ET} for relatively small values of V_{if} is equal to

$$\nu_{ET} = \frac{4\pi^2}{h} V_{if}^2 \sqrt{\frac{1}{4\pi\lambda RT}} \qquad 2.5.9$$

while for large values of V_{if}

$$\nu_{ET} = \frac{1}{\tau_L} \sqrt{\frac{\lambda_o}{16\pi RT}} \qquad 2.5.10$$

where τ_L is longitudinal relaxation time $\tau_L = \tau_D \varepsilon_\infty / \varepsilon$ is related to the Debye relaxation time τ_D and the dielectric permittivities of the given solvent, static ε and high frequency ε_∞ values, respectively. The final expression for electron transfer rate k_{ET} are

$$k_{ET} = \frac{4\pi^2}{h} V_{if}^2 \sqrt{\frac{1}{4\pi\lambda RT}} \exp\left[\frac{-(\lambda + \Delta G_{ET})^2}{4\lambda RT}\right] \qquad 2.5.11$$

for relatively small (non-adiabatic limit) values of V_{if} and

$$k_{ET} = \frac{1}{\tau_L} \sqrt{\frac{\lambda_o}{16\pi RT}} \exp\left[\frac{-(\lambda + \Delta G_{ET})^2}{4\lambda RT}\right] \qquad 2.5.12$$

for enough large (adiabatic limit) values of V_{if}.

The last interesting issue is unexpected consequence of presented theory. In general, one expects that the rate *k* of any chemical reaction is the faster the greater is the release of the Gibbs energy that drives the reaction. In case of electron transfer as described by the Marcus theory we can distinguish three particular cases. For a given λ value, activation energy depends on the electron transfer exothermicity ΔG_{ET}. For moderately exergonic reaction with $\lambda + \Delta G_{ET} > 0$ rate constant k_{ET}, increase with decreasing reaction exothermicity (normal region). When $\lambda + \Delta G_{ET} = 0$ reaction rate is maximized and the process is barrierless. The most interesting however, is the case when $\lambda + \Delta G_{ET} < 0$. In this region, contrary to all intuition, a further increase in the exergonicity causes a decrease in the reaction rate. Such behavior is a consequence of the parabolic shapes of the potential energy curves.

For the bimolecular electron transfer reactions the theoretical prediction has been confirmed in the normal region but not in the inverted region. The classical Rehm and Weller experiments clearly showed that for bimolecular reactions in the inverted region

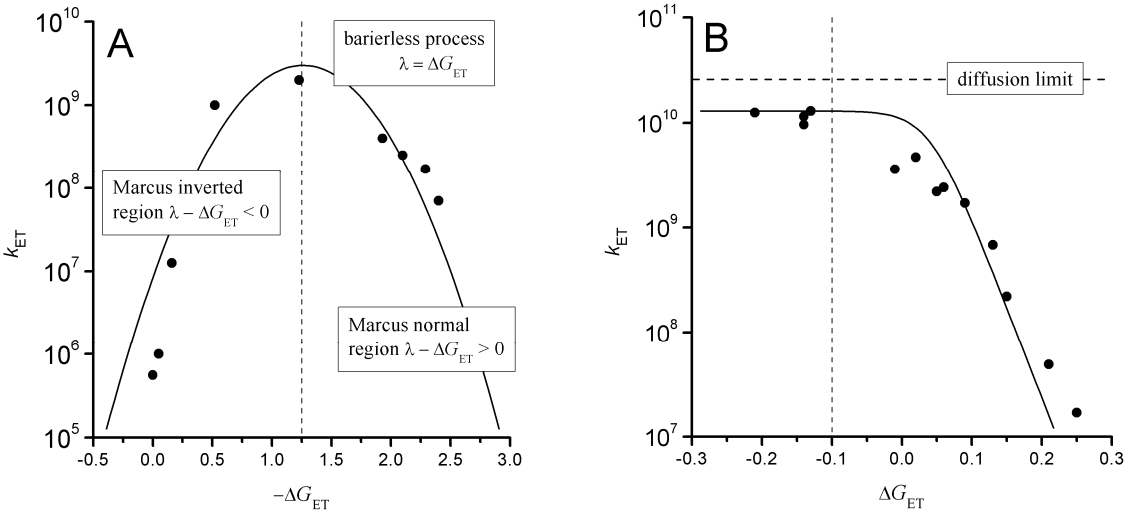

Figure 2.5.4. The experimental data [68] for intramolecular electron transfer reaction with theoretically predicted curve by the Marcus theory (A) and the Rehm-Weller curve for bimolecular electron transfer along with experimental data [69] (B).

the rate constant of the process approaches the diffusion-controlled rate k_{dif} (Figure 2.5.4). Nevertheless, the inverse region is observed in the particular case where the electron donor and the electron acceptor are linked by a molecular bridge.

3. Object of investigations

The general aim of this dissertation is to contribute to understanding of factors that govern efficiency of the Dexter-type energy transfer in the liquid media, and the influence of the diffusion on the elementary energy transfer reaction step. The starting point for investigations was the difference between electron and energy transfer quenching rates plotted against driving force of the reaction. The rate constant of fluorescence quenching by bimolecular electron transfer has a well-established energy dependence following the well-known Rehm-Weller relationship with a maximum rate constant approaching the diffusional limit at sufficiently high reaction exergonicity. Considering that both, electron and energy transfer processes, can be described using a common formalism [70] one should expect that the bimolecular energy transfer reactions rate constants will follow the Rehm-Weller like relationship too [71]. However, there are clear evidences [14, 15] that bimolecular energy transfer reactions do not reach the diffusion limited rate constant even for strongly exothermic reactions. The discrepancy is especially large in low-viscosity solvents in which the rate constants for exothermic energy transfer are *ca*. three times smaller than expected from diffusional limitation. The origin of this phenomenon, known for many years, [72] still remains unresolved.

In a similar way, the relationship between free energies ΔG_{EN} (defined as the difference between the excited energy level of donor, ^{3}*D and acceptor, ^{3}*A) and bimolecular rate constants k_{EN} of energy transfer processes, remains an open question at least in my opinion. Mainly two kinetic models have been applied in order to describe the k_{EN} rate constants as function of ΔG_{EN}. The first one was proposed by Sandros who considered that the energy transfer rate constant is equal to the rate constant of encounters formation between excited donor and acceptor molecules, being solely influenced by the energy difference between those. However, the experimental systems depart from this description in both ΔG_{EN} regions ($\Delta G_{EN} << 0$ and $\Delta G_{EN} \sim 0$) and this model does not fit the experimental results properly. The second model, inspired by the Marcus theory of electron transfer processes has been elaborated by Balzani. The model introduces reactants reorganization dependent energy transfer rate constant between geminate pairs

as an independent fitting parameter, though in the case of energy transfer processes the solvent reorganization energy should be considered as negligible. According to this model the solvent and/or solute reorganization energies may cause the lower than diffusion rate constant in the exothermic region of ΔG_{EN}. The resulting description of the experimental data is better than in the case of the Sandros model, but unexpectedly large values of reorganization energies and/or small values of pre-exponential factors are required to reproduce k_{EN} *vs.* ΔG_{EN} relationship.

A next issue of interest is the dependence of the bimolecular energy transfer rate constants on solvent properties and/or possible solvent/solute specific interactions. Theoretical predictions indicate that in the region of very negative ΔG_{EN} the viscosity of reaction medium should be the main factor influencing the energy transfer rate constant, whereas, as mentioned above, experimental data show that other kinetic limitations seem to be present. These limitations should still be more important in the case of moderately exergonic or iso-energetic energy transfer processes where viscosity effects causing diffusional limitation are expected to play a much less pronounced role. Thus, kinetic data for bimolecular energy transfer processes occurring at $\Delta G_{EN} \sim 0$ may bring new insight about the nature of additional kinetic limitations that play a role in these processes. Especially, kinetic data for $\Delta G_{EN} \sim 0$ in different solvents should reveal the influence and importance of these factors leading to a reasonable explanation why bimolecular energy transfer processes involving the excited triplet states are slower than expected.

Upon checking the available literature for the bimolecular ^{3}*D + A $\rightarrow$ D + ^{3}*A processes occurring at $\Delta G_{EN} \sim 0$ a conclusion may be drawn that the existing data are scarce and mostly not accurate enough for a more advanced discussion. Undoubtedly, scarcity of such data for "pure" organic systems arises from difficulties in transient absorption measurements usually used in such studies due to the non-luminescent character of the excited triplet states of organic molecules. In the case of luminescent transition metal chelates, kinetic data were usually obtained using the ordinary Stern-Volmer procedure [73] what is only correct assuming that the reverse energy transfer ^{3}*D + A $\leftarrow$ D + ^{3}*A takes place with negligible yield. Usually this is not the case for reactions with ΔG_{EN} around zero because the yield of the back energy transfer is substantial and usually cannot be omitted. Therefore ordinary Stern-Volmer procedure

results in under-estimation of k_{EN} rate constants for processes occurring at $\Delta G_{EN} \sim 0$. Thus luminescence studies performed with the Stern-Volmer procedure can be accurate only for systems with fairly negative ΔG_{EN} values and more advanced time-resolved luminescence measurements are necessary for the correct kinetic analysis of iso-energetic or nearly iso-energetic energy transfer processes [19].

To overcome that problem the new methodology was developed for accurate extraction of kinetic parameter of the energy transfer process at $\Delta G_{EN} \sim 0$. Method is based on application of the Birks [74] solution of the differential equations describing reversible energy transfer (REN) scheme and application it to luminescence decays of the donor. Of course, emission based techniques can be only applied when at least one emitter is involved in the investigated REN process.

The main part of presented dissertation are results from the kinetic measurements of bimolecular energy transfer processes involving different metallorganic complexes and organic quenchers in several common organic solvents of various properties. The measurements have been performed for ^{3}*D + A → D + ^{3}*A processes occurring in two energetic regimes, for $\Delta G_{EN} << 0$ and $\Delta G_{EN} \sim 0$, respectively. The obtained data are discussed within both kinetic models already present in the literature. Due to the failure of these models, a new model has been proposed which takes into account the quantum magnetic number conservation rule (known also as the Winans selection rule [20]).The proposed approach allows for kinetic description of the energy transfer quenching data obtained during the course of this thesis as well as the already available literature data.

Like every newly developed approach, the proposed model needs further experimental verifications. One of possible opportunity for that may be given by combined solvent and temperature effects studies on kinetic of bimolecular energy transfer processes within systems involving excited ^{3}*MLCT (metal-to-ligand-charge-transfer) states and organic quencher. Two ^{3}*D/A systems, namely $Ir(ppy)_3$ – chrysene and $Ru(bpy)_3^{2+}$ – pyrene pairs have been investigated in several organic solvents at different temperatures. The obtained kinetic data provides additional arguments for validation of models used in description of the Dexter type electronic energy transfer in the liquid media.

4. Experimental

4.1 Materials

4.1.1 Solvents

For all experiments, solvents of spectroscopic purity or HPLC grade were purchased from commercially available sources and used as received. In Table 4.1.1 a list of the most important properties of the solvents used in this work is given along with abbreviations. Most of the data are available at 20°C, the arbitrary temperature chosen in this work. The three macroscopic solvent properties of main interest in the presented studies were the viscosity, η, the refractive index, n, and the dielectric constant, ε [75].

Table 4.1.1. Selected properties of used solvents that are relevant concerning this Dissertation.

Solvent		ε	η /cP	n	MP /K	d /gcm^{-3}	k_{dif} /10^{9}M^{-1}s^{-1}
acetonitrile	ACN	35.9	0.341	1.341	229	0.436	19.2
dimethylsulfoxide	DMSO	46.5	1.991	1.477	291	0.513	3.3
propylene carbonate	PC	64.9	2.530	1.419	118	0.550	2.6
toluene	TOL	2.38	0.553	1.494	178	0.568	11.8
tetrahydrofuran	THF	7.58	0.462	1.404	165	0.504	14.2
1,4-dioxane	DX	2.2	1.194	1.477	285	0.524	5.5
N,N-dimethylformamide	DMF	36.7	0.802	1.428	212	0.521	8.2
sulfolane	TMS	43.3	10.286	1.481	302		0.6
ethanol	EtOH	24.6	1.083	1.359	159	0.469	6.0
n-octanol	OcOH	10.3	7.363	1.427	258	0.685	0.9
methanol	MeOH	32.7	0.551	1.326	175	0.408	11.9
di-n-butyl ether	DBE	3.1	0.645	1.396	178	0.669	10.1
ethanol-d_1	EtOD	24.6	1.083	1.359	143	0.469	6.0
anisole	ANS	4.3	0.984	1.514	235	0.584	6.7
acetone	AC	20.6	0.303	1.356	179	0.482	21.6

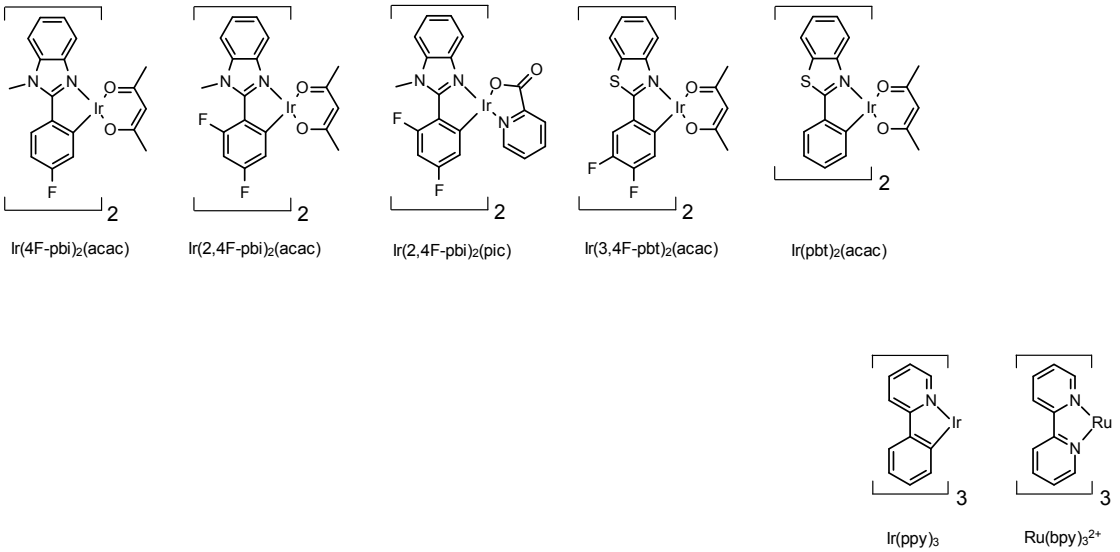

Figure 4.1.2. Structural formulas of the studied energy donors – iridium(III) and ruthenium(II) complexes.

4.1.2 Energy donors

The investigated iridium(III) complexes were synthesized and purified as described in [76-78]. Luminescent transition metal complexes exhibiting long-lived (μs) emission from the excited metal-to-ligand-charge-transfer (^{3}*MLCT triplet with emission allowed by spin-orbit coupling) can be considered as a perfect fluorophores for quenching

Table 4.1.3. The relevant photophysical and electrochemical properties of used energy donors. Position of 0-0 transitions in room temperature emission spectra E_{00}, emission quantum yields ϕ_{em} and lifetimes τ_D values in ACN solutions. Electrochemical oxidation E_{ox} and reduction E_{red} potentials (values *vs*. ferrocene/ferrocene$^+$ internal reference redox system) Electrochemical data for 0.1 M $TBAPF_6$ ACN/DX 1:1 solutions taken form ref [76-78].

Donor	E_{00} / eV	ϕ_{em}	τ_D / 10^{-6}	E_{ox} / V	E_{red} / V
Ir(2,4F_2-bpi)$_2$(pic)	2.60	0.51	1.87	0.75	–2.42
Ir(2,4F_2-bpi)$_2$(acac)	2.54	0.46	0.90	0.59	*
Ir(3,4F_2-bpt)$_2$(acac)	2.52	0.31	0.87	0.72	–2.16
Ir(4F-bpi)$_2$(acac)	2.51	0.27	0.81	0.70	*
Ir(pbt)$_2$(acac)	2.16	0.44	1.74	0.57	–2.30
Ru(bpy)$_3$	2.12	0.052	0.84	0.88	–1.73
Ir(ppy)$_3$	2.50	0.86	1.84	0.31	–2.70

* - irreversible electrochemical reduction

studies. Their emission wavelength can be tuned by functionalizing the ligands with electron donating or electron withdrawing substituents. Moreover, the redox potentials of transition metal chelates can be also tuned by appropriate metal/ligand(s) combination that enables excluding the possibility of electron transfer quenching. The effect of the electron donating and/or withdrawing groups has been systematically studied [79, 80].

4.1.3 Energy acceptors

The acceptors used for this work were chosen for various reasons. Firstly the redox potentials chosen to exclude the possibility of electron transfer quenching, secondly energy of the triplet states must been well defined in solution. The values of triplet energy

Table. 4.1.4 The relevant photophysical and electrochemical properties of used energy acceptors. Energies of the lowest excited singlet E_S and triplet states E_T. Electrochemical oxidation E_{ox} and reduction E_{red} potentials (values *vs*. ferrocene/ferrocene$^+$ internal reference redox system). Data for acetonitrile solutions taken from ref [81].

Acceptor	E_S / eV	E_T / eV	E_{ox} / V	E_{red} / V
acenaphthene	3.88	2.56	0.81	–2.95
anthracence	3.30	1.85	0.69	–1.95
benzanthracene	3.22	2.05	0.78	–2.43
chrysene	3.43	2.48	0.95	–2.71
fluoranthene	3.06	2.29	1.05	–2.14
naphthalene	3.99	2.63	1.14	–2.87
pyrene	3.34	2.10	0.85	–2.40

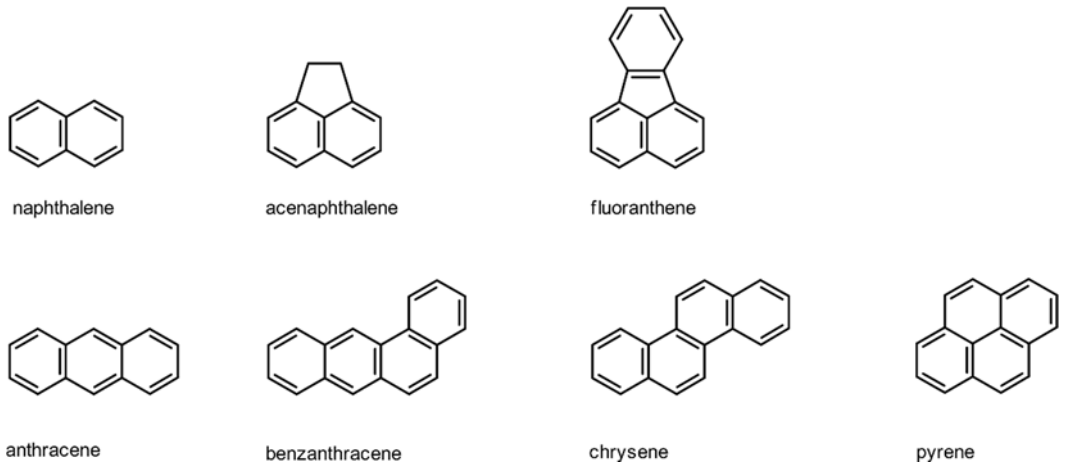

Figure 4.1.5. Organic energy acceptors used in this work.

levels extracted from low temperature phosphorescence spectra differ from those at ambient temperature by a magnitude of entropic contribution. According to [82] this contribution is nearly negligible in rigid chromophores like naphthalene and similar molecules with no intramolecular rotational degrees of freedom.

4.2 Instruments

UV-Vis absorption and luminescence spectra were recorded using a Shimadzu UV2401 spectrophotometer and a Varian Cary Eclipse fluorimeter or Edinburgh Instruments FS900 steady-state fluorometer. Time-resolved measurements were done using a home-built setup with a pulsed PBBO dye laser used as excitation source (emission tunable from 395-415 nm with energy of 5-6 μJ) pumped by a pulsed nitrogen laser (337 nm. 5 Hz repetition rate 0.27 mJ) or the Lambda Physik Lextra XeCl excimer laser (308 nm. adjustable repetition rate 160 mJ). A liquid nitrogen cooled LN/CCD detector (Princeton Instruments) was used for collecting spectra from 300 nm to 800nm. The 2.5 GHz TDS3032 digital oscilloscope (Tektronix) was used for recording time-resolved signals. *i.e.*, the light emitted by the investigated samples passed through

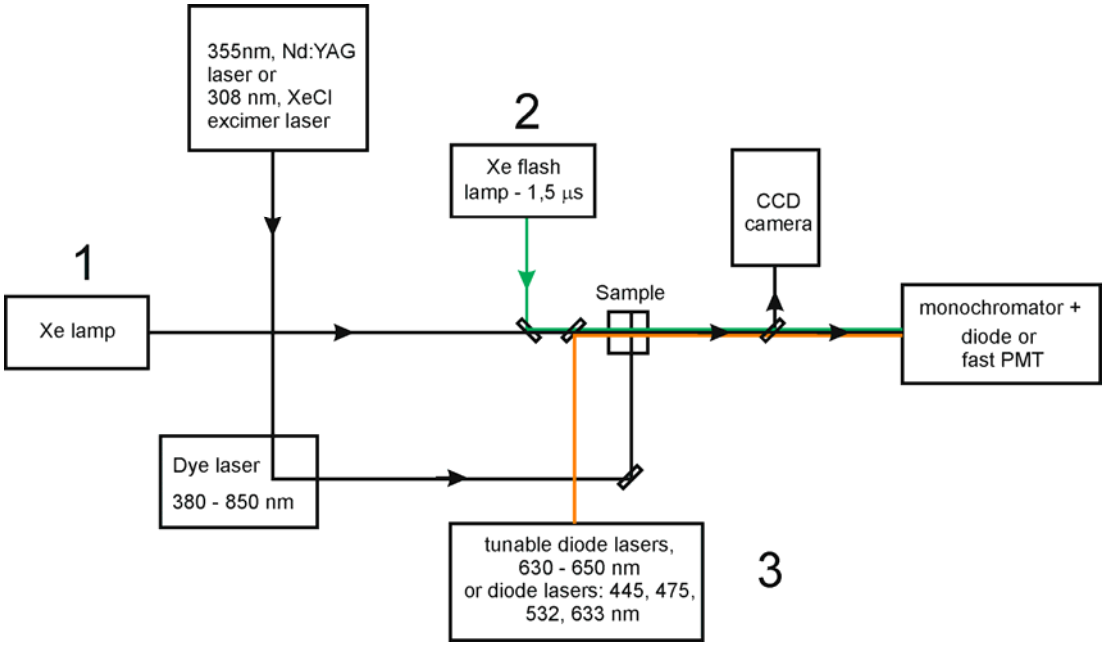

Figure 4.2.1. The home-built transient absorption setup. Branches 1 and 3 are used for kinetic measurements from several ns to ms, branch 2 – for time-resolved transient absorption spectra from 1 μs to seconds delay.

a monochromator and detected by a Hamamatsu H6780-20 photomultiplier. For transient absorption the slightly modified setup was used with continuous light of laser-driven Xe lamp (Energetiq EQ-99-Plus-EU) and pump pulses of Xe flash lamp (PerkinElmer 1100 Series) for probing samples and the Lambda Physik Lextra XeCl excimer laser (308 nm, adjustable repetition rate, 160 mJ energy) for together with set of dye lasers for pumping. The setup is equipped with the two-channel CCD spectrometer (Avantes AvaSpec-ULS2048-2-USB2) for spectral measurements and allows registration of time-resolved spectra within time range from 1 μs to 10 ms.

4.3 Sample Preparation

In a system consisting of any combination of the iridium(III) or ruthenium(II) complexes and organic acceptor here discussed only the organometallic complex can be photo-excited by 395 nm radiation (none of the organic acceptors used absorbs at this wavelength). Therefore, it was possible to ascribe unambiguously the role of the energy donor and the energy acceptor to the organometallic complex and organic co-reactant, respectively. The investigated solutions were deoxygenated by saturation with purified and dried argon. If not stated otherwise experiments were performed at room temperature (20 °C). The usual concentration range for donors was 1×10^{-5} to 5×10^{-3} M whereas acceptor concentrations were varied typically from 1×10^{-5} to 5×10^{-2} M.

4.4 Data processing

As usual the measured signal has been regarded as a convolution of the instrument response function and the decay of the excited state of emissive species. The instrument response function of the setup can be reasonably well reproduced by a Gaussian function. The convolution of an exponential decay with a Gaussian function can be performed analytically [83] according to Eq. 4.3.1.

$$F(t) = y_0 + \sum_{i=1}^{n} \frac{A_i}{2} \exp\left[-(t-t_0)/\tau_i\right] \times \exp\left[\Delta^2/4\tau_i^2\right] \times \left[1+erf\left((t-t_0-\Delta^2/2\tau_i)/\Delta\right)\right] \quad 4.3.1$$

where the parameters stand for: y_0 the background signal, A_i the normalized amplitudes, t_0 a delay time between the excitation impulse and the recorded decay, τ_i the emission lifetimes and Δ the width of the instrument response function. The difference between the square of this test function with two exponential components and the experimental decay was minimized using a Levenberg-Marquardt Matlab based routine with gaussian weight.

4.4.1 Irreversible quenching – the Stern-Volmer method

The most widely used and popular method of extracting quenching rate constant from donor luminescence intensity or donor life time is the Stern-Volmer formalism [11]. It assumes irreversible quenching of the fluorophore by quencher accompanied by the fluorophore natural decay. In general, this process can be represented by a simple scheme

$$\begin{array}{ccc} {}^*\mathrm{D} + \mathrm{Q} & \xrightarrow{k_q} & \mathrm{D} + {}^*\mathrm{Q} \\ \downarrow\ 1/\tau_D & & \\ \mathrm{D} & & \end{array} \qquad 4.3.2$$

Solution to the differential equations describing this scheme is time evolution of the donor excited state [*D] and may be depicted by equation

$$[{}^*\mathrm{D}] = [{}^*\mathrm{D}]_0 \exp\left[(-1/\tau_D - k_q[\mathrm{A}])t\right] \qquad 4.3.3$$

with initial concentration of excited state equal to $[{}^*D]_0$. Equation 4.3.3 is used to derive final expression for the Stern-Volmer method by comparing the amounts of light emitted (which is directly proportional to concentration of the excited state) in the absence (*i.e.*, $k_q = 0$) and presence of a quencher (*i.e.*, $k_q > 0$). The final form is given by equation

$$\frac{I_0}{I} = 1 + k_q \tau_D [Q] \qquad 4.3.4$$

where I_0, I are intensity of fluorescence without and with the quencher respective, k_q is quenching rate, τ_D lifetime of the donor. This equation is used to extract quenching rate constant k_q. The method is also valid if in the right hand side of equation 4.3.3, instead of intensity of fluorescence I_0 / I, one substitute lifetimes of the donor excited state with and without (τ_D) presence of the quencher, τ and τ_D, respectively.

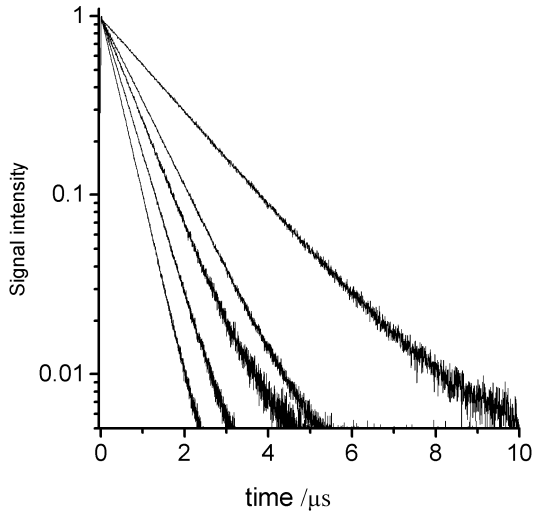

Figure 4.3.1. Typical examples of luminescence decays as recorded for the studied donor/acceptor systems with the exergonic irreversible energy transfer.

$$\frac{\tau_D}{\tau} = 1 + k_q \tau_D [Q] \qquad 4.3.5$$

To isolate the effects of quenching, fluorescence lifetime measurements are carried out over a range of quenching agent concentrations The plot of I_0 / I or τ_D / τ versus [Q] is usually called the Stern-Volmer plot and in the case of purely collisional quenching should yield a straight line with a slope equal $k_q \tau_D$ and intercept equal to one.

4.4.2 Irreversible quenching and the transient absorption

The irreversible quenching rate constant k_q, may be obtained also form analysis of time evolution of acceptor. In order to do that we must consider extended scheme for irreversible quenching that includes temporal evolution of excited state of acceptor.

$$\begin{array}{ccc} {}^*D + A & \xrightarrow{k_q} & D + {}^*A \\ \downarrow 1/\tau_D & & \downarrow 1/\tau_A \\ D & & A \end{array} \qquad 4.36$$

Above kinetic scheme can be described by set of differential equation with solution describing time profile of concentrations [*D] and [*A]. The time evolution of the donor is identical with the one from equation 4.3.3 as the kinetic scheme from the donor point

of view remain unchanged. The time evolution of acceptor excited state [*A] is described by the equation

$$[^*\mathrm{A}] = C \times \left[\exp\left[(-t/\tau_\mathrm{D} - k_\mathrm{q}[\mathrm{A}])t \right] - \exp(t/\tau_\mathrm{A}) \right] \qquad 4.3.7$$

where C is amplitude of transient absorption signal. Such temporal profile of acceptor excited state (Figure 4.3.2) may be measured by transient absorption. Applying the above equation one may extract not only quenching rate constant k_q, but also the natural lifetime of the acceptor τ_A.

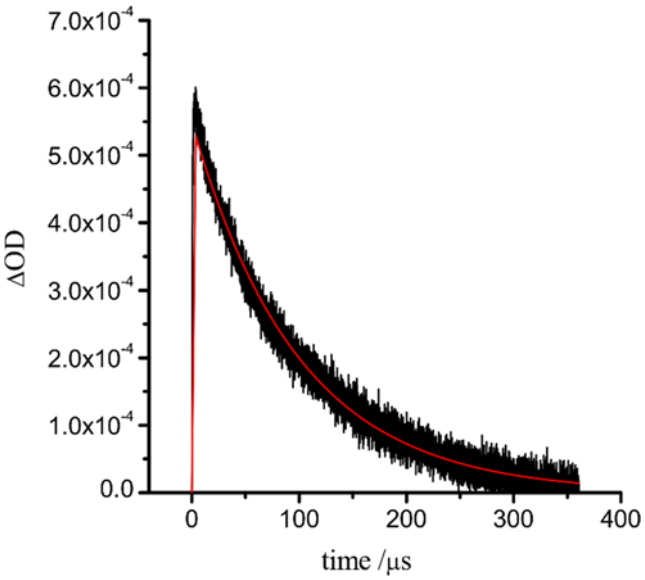

Figure. 4.3.2. Typical example of transient absorption decays as recorded for the studied donor/acceptor systems with the exergonic irreversible energy transfer. Red line represents best fit with equation $f(t) = C \times [\exp(-\lambda_1 t) - \exp(-\lambda_2 t)]$.

4.4.3 Reversible quenching – the Birks method

For reversible quenching process extraction of reaction rates is more complicated as the overall quenching rate is affected by the rate constant of the back process as well as by the lifetime of the acceptor and concentrations of both reactants. One must keep in mind that a certain conditions must be fulfilled to observe re-population of the donor excited state. In particular the energy gap between donor and the quencher must be reasonably small and back energy transfer rate must be faster or at least comparable to deactivation rate of the excited acceptor state which allows re-population

of the donor excited state. The kinetic scheme presented bellow takes into account all above mentioned processes.

$$\begin{array}{ccc} {}^*\mathrm{D} + \mathrm{A} & \underset{k_b}{\overset{k_f}{\rightleftharpoons}} & \mathrm{D} + {}^*\mathrm{A} \\ \downarrow 1/\tau_D & & \downarrow 1/\tau_A \\ \mathrm{D} & & \mathrm{A} \end{array} \qquad 4.3.8$$

Scheme can be described by set of differential equations

$$\begin{cases} \dfrac{d}{dt}[\mathrm{D}^*] = -(1/\tau_D + k_f[\mathrm{A}])[\mathrm{D}^*] + k_b[\mathrm{A}^*][\mathrm{D}] \\ \dfrac{d}{dt}[\mathrm{A}^*] = -(1/\tau_A + k_b[\mathrm{D}])[\mathrm{A}^*] + k_f[\mathrm{D}^*][\mathrm{A}] \end{cases} \qquad 4.3.9$$

which has been solved by Birks leading to the well-known solution for the donor [D*] decay after pulsed excitation

$$[\mathrm{D}^*] = \frac{[\mathrm{D}^*]_0}{\lambda_2 - \lambda_1} \times \left[(\lambda_2 - k_X)\exp(-\lambda_1 t) + (k_X - \lambda_1)\exp(-\lambda_2 t)\right] \qquad 4.3.10$$

and for the acceptor [A*] temporal profile

$$[A^*] = \frac{k_f[D^*]_0}{\lambda_2 - \lambda_1} \times \left[\exp(-\lambda_1 t) - \exp(-\lambda_2 t)\right] \qquad 4.3.11$$

where

$$k_Y = 1/\tau_A + k_b \times [\mathrm{D}] \qquad 4.3.12$$

$$k_X = 1/\tau_D + k_f \times [\mathrm{A}] \qquad 4.3.13$$

and

$$\lambda_{1,2} = \frac{1}{2}\left(k_Y + k_X \mp \sqrt{(k_Y - k_X)^2 + 4 \times (k_Y - 1/\tau_A)(k_X - 1/\tau_D)}\right) \qquad 4.3.14$$

The solution obtained by Birks for time-resolved emission of the donor can be adopted to obtain kinetic parameters k_f, k_b, τ_D, and τ_A. The time resolved profile of the donor [D*] excited state of is clearly bi-exponential as presented in equation 4.3.7.

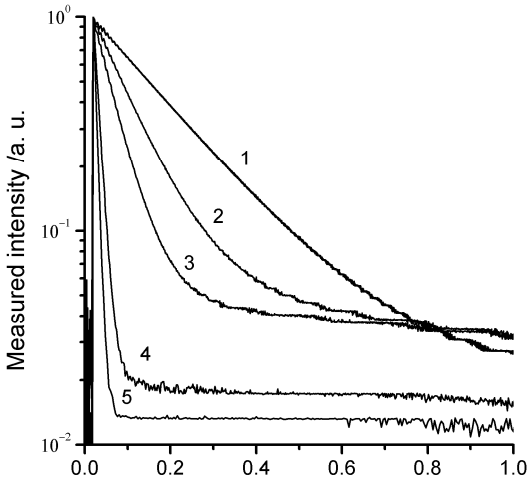

Figure 4.3.3. Typical examples of luminescence decays as recorded for the studied donor/acceptor systems with the iso-energetic reversible energy transfer.

Both overall k_f and k_b rates can be extracted from the bi-exponential decay of emission of excited state of the donor [D*]. The measured emission decays are characterized by two normalized amplitudes (A_1, A_2 with $A_1 + A_2 = 1$) and two decay times (τ_1, τ_2). The extracted decay parameters permit the estimation of the both k_f and k_b rates according to the following relationships

$$\frac{A_1}{\tau_1} + \frac{A_2}{\tau_2} = \frac{1}{\tau_D} + k_f[\mathrm{A}] \quad \text{and} \quad \frac{A_2}{\tau_1} + \frac{A_1}{\tau_2} = \frac{1}{\tau_A} + k_b[\mathrm{D}] \qquad 4.3.15$$

Taking into account the values of all four parameters describing the measured bi-exponential decays the rate constants k_f and k_b have been determined from linear plots of $A_1/\tau_1 + A_2/\tau_2$ *vs.* [A] and $A_2/\tau_1 + A_1/\tau_2$ *vs.* [D] using data from the decay measurement performed for several sets of [A] and [D] concentrations, respectively.

Usually, for the donor/acceptor systems under study the ΔG_{EN} energies were found to be somewhat different (up to ±0.02 eV) from $\Delta G_{EN} = 0$ as required for the exactly iso-energetic energy transfer processes. It is experimentally rather difficult to find systems with exact zero energy difference between ^{3}*D and ^{3}*A states, but, taking into account that for ΔG_{EN} around zero a linear relationship (in semi-logarithmic scale) between ΔG_{EN} and k_f or k_b rate constants holds, one can interpolate the measured k_f or

k_b values to obtain those characterizing the iso-energetic case. Either k_f or k_b rate constants can be related to ΔG_{EN} value according the following equations

$$k_f = k_f(\Delta G_{EN} = 0) \times \exp(-\alpha \Delta G_{EN}) \quad 4.3.16$$

$$k_b = k_b(\Delta G_{EN} = 0) \times \exp(\alpha \Delta G_{EN}) \quad 4.3.17$$

where α coefficient determines slope in the linear relationship between $\ln(k_f)$ or $\ln(k_b)$ *vs*. ΔG_{EN}. Thus (because $k_{EN}(0) = k_f = k_b$ for $\Delta G_{EN} = 0$) one can simply estimate the energy transfer rate $k_{EN}(0)$ describing the iso-energetic case from the experimentally measured forward and backward rates as follows

$$k_f k_b = k_f(\Delta G_{EN} = 0) \times \exp(-\alpha \Delta G_{EN}) \times k_b(\Delta G_{EN} = 0) \times \exp(\alpha \Delta G_{EN}) \quad 4.3.18$$

$$k_f k_b = k_f(\Delta G_{EN} = 0) \times k_b(\Delta G_{EN} = 0) = k_{EN}(0)^2 \quad 4.3.19$$

$k_{EN}(0)$ values, interpolated as described above, are used in this work to discuss solvent effect in the studied nearly iso-energetic energy transfer processes.

5. Results and discussion

5.1 k_{EN} *vs.* ΔG_{EN} relationship

5.1.1 Introductory remarks

Mentioned in the previous chapter three problems with proper theoretical description of energy transfer phenomenon may steam from the fact that the existing experimental data are scarce and mostly not accurate enough for a more advanced discussion. Observation of bi-exponential decays of luminescence from the donor in bimolecular energy transfer proved that accuracy of experimental data is especially problematic in the region of iso-energetic energy transfer. The bi-exponential decays of donor excited state is a direct proof that the yield of the back energy transfer is substantial and cannot be omitted. Therefore ordinary Stern-Volmer procedure results in under-estimation of energy transfer rate constants for processes occurring at $\Delta G_{EN} \sim 0$. Unfortunately most of literature available experimental data in this region were obtained using this method [14, 15, 21-25, 39-44, 85-88]. In order gain more accurate insight into the observed reversible energy transfer process (REN) processes, direct access to the forward and backward rates is desirable, as has been tempted via transient absorption measurements of the reactants and/or products [89-91]. Unfortunately, often the transient absorption spectra are difficult to fully characterize which may hinder a quantitative determination of the rate constants [91-92]. Time-resolved emission spectroscopy, despite some limitations, usually offers higher sensitivity and may allow better separation of the signals from different contributions, as in the case of reversible charge transfer [92]. Of course, emission based techniques can be only applied when at least one emitter is involved in the investigated REN process. As predicted, and experimentally confirmed, the kinetics of the donor – the triplet transition metal complex – may be bi-exponential in the long time scale, and is easily accessible using digital oscilloscopes. Under proper conditions measurements provide both the forward and backward reaction rate constants of the reversible reaction and, by making use of the Gibbs law, the free enthalpy of the REN reaction and finally the energy of ^{3*}A. However above statements has not been systematically studied and experimentally confirmed.

In this chapter a group of iridium(III) complexes and organic acceptors of well-known characteristics are employed to test the discussed approach. The measured bi-exponential decays of luminescence over different ranges of donor and acceptor concentrations are discussed in terms of Birks formalism in order to test the accuracy of the proposed method.

5.1.2 Separation of forward and backward energy transfer processes

In the range of donor and acceptor concentrations used for a given driving force of the energy transfer reaction around zero, the ^{3*}MLCT emission of the donor should be, and indeed is, clearly bi-exponential. The driving force ΔG_{EN} of the reaction has been calculated (as it was first proposed by Sandros from the known triplet energy levels of both donor $E_T(D)$ and acceptor $E_T(A)$ for each A and D pair (*cf.* Table 5.1.2) according to

$$\Delta G_{EN} = E_T(A) - E_T(D) \qquad 5.1.1$$

for the reaction scheme in Figure 5.1.1.

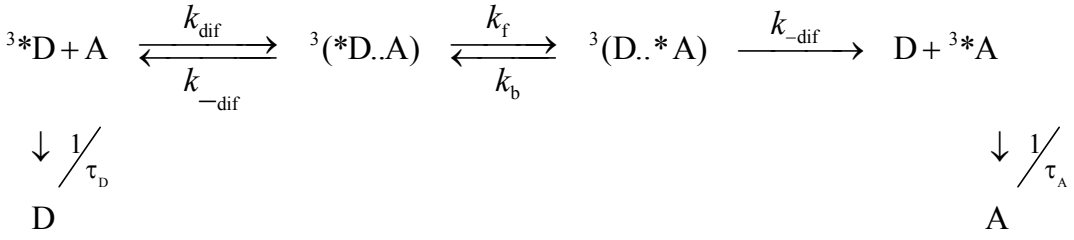

Figure 5.1.1. Kinetic scheme of the reversible energy transfer between the primary excited donor ^{3*}D and the excitation energy acceptor A.

In this scheme we have omitted the cage complex formation and dissociation as the reaction in the studied range of energies is kinetically (not diffusionally) controlled. Note that in the case here described, no charged molecules are present nor are charge transferred; hence no work correction (Coulombic attraction or repulsion) terms are needed. The fact that excited state energies can be used for the calculation of a Gibbs free energy has been discussed in the past very clearly, [93] and in the present case none of the restrictions to the use of Eq. 5.1.1 apply since no large entropic contributions are

expected nor are there large molecular deformations respect to the ground state. Note, that there are deviations from Eq. 5.1.1 in some cases of ultra-fast energy transfer reactions, [94] though it is not the case here. The reaction is spin allowed following the Wigner-Witmer selection rules [95]. It has also to be remarked that in the present case electron transfer reactions are prevented by too large values of ΔG_{ET} (*cf*. Table 5.1.2) as calculated from the redox potentials of the reactants with the Weller equation [96]. It has

Table 5.1.2. The forward k_f and backward k_b energy transfer rate constants, lifetimes of donors and acceptors and calculated and measured ΔG_{EN} values for the investigated donor-acceptor systems, as well as the electron transfer energies ΔG_{ET}. (data for acetonitrile solutions).

System (donor & acceptor)	k_f	k_b	τ_D	τ_A	ΔG_{EN} (1)	ΔG_{EN} (2)	ΔG_{ET} (3)	ΔG_{ET} (4)
Ir(2,4F$_2$-bpi)$_2$(acac) naphthalene	0.39 ± 0.02	4.89 ± 0.55	0.85 ± 0.04	35.4 ± 53.5	0.105	0.065	1.04	*
Ir(2,4F$_2$-bpi)$_2$(pic) naphthalene	1.26 ± 0.05	2.31 ± 0.11	1.77 ± 0.09	73.9 ± 16.4	0.037	0.015	1.07	0.99
Ir(F-bpi)$_2$(acac) naphthalene	0.36 ± 0.03	4.11 ± 0.23	0.74 ± 0.04	54.6 ± 19.2	0.111	0.062	0.79	*
Ir(2,4F$_2$-bpi)$_2$(acac) acenaphthene	1.35 ± 0.10	2.30 ± 0.20	0.79 ± 0.04	38.9 ± 10.8	0.041	0.014	1.16	*
Ir(2,4F$_2$-bpi)$_2$(pic) acenaphthene	2.20 ± 0.16	0.58 ± 0.05	1.62 ± 0.12	43.6 ± 6.28	–0.027	–0.034	1.25	0.66
Ir(F-bpi)$_2$(acac) acenaphthene	2.01 ± 0.17	2.49 ± 0.01	1.06 ± 0.14	26.6 ± 9.13	0.047	0.006	0.97	*

Lifetimes of the excited ^{3*}MLCT states of iridium complexes (measured directly): Ir(2,4F$_2$-bpi)$_2$(acac) = 0.88 μs, Ir(2,4F$_2$-bpi)$_2$(pic) = 1.87 μs, Ir(F-bpi)$_2$(acac) = 0.81 μs [77,78]. Lifetime of naphthalene excited triplet state = 38 μs from ref. [97]. ΔG_{EN} (1) is the energy of the reaction as calculated from Eq. 2, while $\Delta G_{EN\,N}$ (2) is obtained from the rates in the first two columns and Eq. 10. ΔG_{ET} values correspond to both possible ionization processes $^{3*}D + A \rightleftarrows D^+ + A^-$ (3) and $^{3*}D + A \rightarrow D^- + A^+$ (4) calculated according to the Weller equation using redox potentials values from Refs. [77, 78, 98] *All complexes containing acac$^-$ anion do not possess a reversible reduction wave, so the second set of ΔG_{ET} values could not be accurately estimated. Because irreversible electrochemical reduction of IrL$_2$(acac) complexes occurs at only somewhat more positive potentials than characteristic for their IrL$_2$(pic) counterpart, the appropriate ΔG_{ET} values must be comparable to those calculated for IrL$_2$(pic) – naphthalene or IrL$_2$(pic) – acenaphthene pairs.

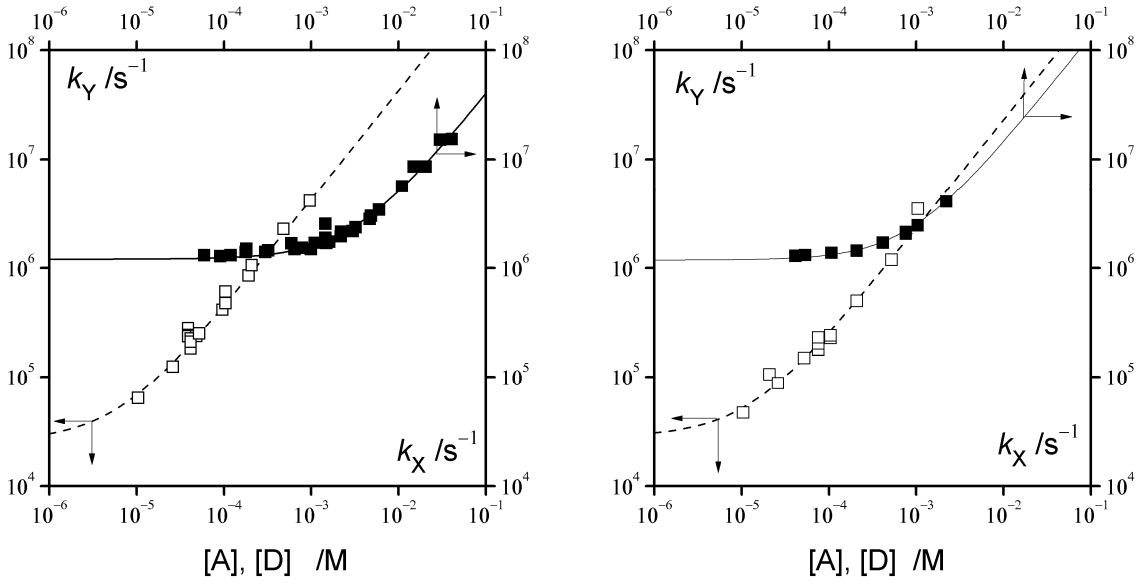

Figure 5.1.3. Birks model rates (Eqs. 5.1.2 and 5.1.3) as a function of donor and acceptor concentrations. k_x *vs*. [A] (*open squares*) and k_y *vs*. [D] (*filled squares*) for two system investigated. The dashed line and the solid lines represent the best fit of k_Y and k_X quantities, respectively. In both cases the slopes are k_f and k_b, respectively and ordinates at the origin of abscissa $1/\tau_D$ and $1/\tau_A$, respectively. Data in acetonitrile solutions for Ir(2,4F$_2$-bpi)$_2$(acac) – acenaphthene (*left chart*) and Ir(2,4F$_2$-bpi)$_2$(acac) – naphthalene (*right chart*) systems.

finally to be borne in mind that the dipole-dipole or the Förster energy transfer mechanism are hardly possible because of the very small (if not nil) transition dipole moment for $S_0 \rightarrow T_1$ transitions within the organic acceptors employed.

In absence of energy acceptor, the iridium complexes exhibit mono-exponential decays of phosphorescence independent of their concentration in the range studied. In the presence of energy acceptor, however, the systems exhibit bi-exponential decays characterized by two normalized amplitudes (A_1 and A_2 with $A_1 + A_2 = 1$) and two decay times (τ_1, τ_2) (*cf*. Figure 4.3.3). As it has been explained in chapter 4, the observed decay of the donor luminescence should be described by equation 4.3.10. It is convenient to rewrite the equations in the following way to link the Birks' parameters and the extracted amplitudes and decay times from the experiment:

$$k_X = A_1 / \tau_1 + A_2 / \tau_2 = 1/\tau_D + k_f[A] \qquad 5.1.2$$

and

$$k_Y = A_2 / \tau_1 + A_1 / \tau_2 = 1/\tau_A + k_b[D] \qquad 5.1.3$$

In this form there is a clear link between experimentally obtained parameters (amplitudes A_1, A_2 and decay times τ_1, τ_2) and theoretically assumed (k_f, k_b, τ_D, τ_A). Thus, the plots of the k_X *vs*. [A] should be linear with origin coordinates $1/\tau_D$ and slope k_f. Correspondingly, the plots of the k_Y *vs*. [D] should be linear as well allowing estimation of $1/\tau_A$ and k_b. Examples fulfilling this expectation are shown for our experiments in Figure 5.1.3 where presentations in doubly logarithmic scale were used for more clarity.

5.1.3 "Kinetic" and "photo-physical" ΔG_{EN} values

In this manner, for the six systems studied we could obtain not only the rate constants for the forward and backward processes but also the lifetimes of the donor and acceptor triplet excited states. All obtained data are compiled in Table 5.1.3. In order to check the accuracy of the kinetically obtained ΔG_{EN} were calculated using the Gibbs equation:

$$\Delta G_{EN} = -RT \ln\left[\frac{k_f}{k_b}\right] \qquad 5.1.4$$

The obtained "kinetic" ΔG_{EN} values can be compared to the "spectroscopic" value obtained with Eq. 5.1.1. The estimated ΔG_{EN} values have been found to be somewhat different from those calculated taking into account the differences between energies of ^{3}*D and ^{3}*A states assessed from the 0-0 transition observed in ^{3}*D room-temperature luminescence and ^{3}*A 77K phosphorescence spectra. Most probably the observed differences in "kinetic" and "photophysical" ΔG_{EN} values arise from the different condition applied for ^{3}*D and ^{3}*A emission measurements.

Noteworthy, the agreement between "kinetic" and "photo-physical" ΔG_{EN} values is much better when the 0-0 transition data from published observations of the room-temperature phosphorescence of aromatic hydrocarbons are taken for estimating the ^{3}*A energies [99, 100]. The former leads us to conclude that the experimentally available "kinetic" as well as the calculated "photophysical" ΔG_{EN} values are quite reasonable and operational in further discussion of k_f and k_b data. As one can see from Table 5.1.2, both values do not deviate by more than 0.06 eV (about 500 cm^{-1}) which is

indeed a very nice agreement and shows a quite high precision of the measured rate constants.

Other check quantities of this methodology are the recovered lifetimes of donor and acceptor excited triplet states. Also from Table 5.1.2 it can be read that they are in good correspondence with the independently measured values for the investigated iridium complexes. For the organic acceptors we only consider the naphthalene value, which is neither far from the one recovered by this methodology (55 μs in average as compared to literature value 38 μs [97]). This larger deviation can be understood in view of the limited accessible range of concentrations of donor and acceptor in which well resolved bi-exponential decays with a decent signal to noise ratio and low fitting uncertainty can be obtained. In fact, it is rather difficult to measure such decays at very low reactants concentrations with the small rate constants we are dealing with, concomitant to the small driving force range we are working in. One can expect, however, that application of single photon timing technique may lead to distinct improvement in accuracy of the measurements, especially at extremely low concentration of the investigated donor and acceptor pair. It should be also noted that errors in τ_A estimations only marginally affect the extracted k_f and k_b values. An additional concern is the possible triplet-triplet annihilation either of the donor or the acceptor. Measured lifetime of the donor at several concentrations shows no deviations from the low concentration lifetime. The annihilation of the organic acceptor triplet can be ruled out by considering the fact that no systematic deviations of its extracted lifetime or of the rate constants, has been found with the change of iridium(III) complex concentration. Neither emission from the acceptor singlet could be observed. All the former is reasonable taking into account the relatively small extinction coefficient of the Iridium complexes (6×10^4 $M^{-1}s^{-1}$ at most at 395 nm) and the relatively low irradiances used in our experiments.

Summing facts up, as it has been demonstrated, the analysis of observed bi-exponential decays (performed using the Birks' formalism) enables the accurate determination of the kinetic parameters characterizing the investigated forward and backward REN processes. Moreover by use of the Gibbs law one is able to determine the triplet energies of the acceptors as well as their lifetimes. To some extend method could be useful for the triplet energy determination of transition metal complexes with non-

structured emission. Finally, it is instructive to represent the rate constants obtained as functions of the ΔG_{EN} of the forward and backward processes. It is shown in Figure 5.1.4 together with data for the energy transfer quenching of the ^{3*}MLCT emission of $^{3*}Ru(bipy)_3^{2+}$ complex by several organic acceptors reported by de Carvalho and Gehlen, [44] who studied the reaction by means of steady-state quenching experiments and 2-nitrothiophene triplet quenching by Martins and Kemp [87] studied by the means of transient absorption.

The comparison with experimental points from steady-state quenching (Figure 5.1.4 – chart A) is accurate only for $\Delta G_{EN} < -0.2$ eV where the measured k_q values are mostly governed by the forward energy transfer process occurring with a rate constant equal to k_f. This is, however, not the case at $\Delta G_{EN} > -0.2$ eV because the overall quenching rate is affected by the rate constant of the back energy transfer as well as by the lifetime of the acceptor and the donor concentration. This results in underestimation of experimental k_q values obtained by the steady-state quenching method. In the case of 2-nitrothiophene triplet quenching data (Figure 5.1.4 – chart B), measured by the means of transient absorption the experimental points are too scattered for a good quantitative comparison. This, however, is most probably due to inaccuracy of the method not the

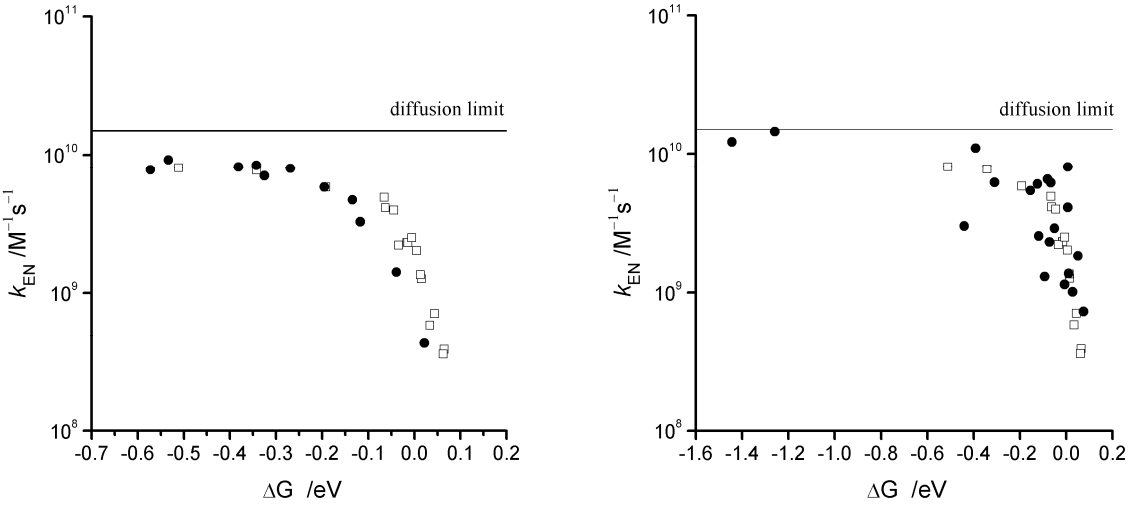

Figure 5.1.4. Dependency of k_{EN} rate constants on ΔG_{EN}. Plot (A) quenching rates obtained by steady-state luminescence quenching measurements (*filled circles*) from reference [43] and time-resolved measurements results of the present work (*open squares*), plot (B) quenching rates obtained by transient absorption (*filled circles*) from reference [85] and time-resolved measurements results of the present work (*open squares*).

quality of experiments. It may serve as good examples that accuracy of the emission based techniques are, to some extend superior to transient absorption measurements.

Having a reliable tool for studying energy transfer process in whole range of ΔG_{EN} one may start investigating process itself and factors that influence this phenomenon.

5.2 Solvent effect studies

5.2.1 Introductory remarks

Upon checking available literature data it is seen that the ΔG_{EN} dependence of energy transfer reactions do not reach a maximum value identical to the estimated diffusion limited rate constant for bimolecular reactions even for strongly exothermic reactions. This sub-diffusional plateau appears for reactions with exothermicity a least $\Delta G_{EN} < -0.2$ eV and concerns not only energy transfer from organometallic complex to organic acceptor as investigated in the course of this thesis but also energy transfer between "pure" organic molecules. Also this phenomenon seems to be independent of the used solvent as sub-diffusional plateau can be observed in almost all reported experimental data. It may indicate that additional factors, like the spin moment in the triplet manifold, may play an important role and keep the reaction kinetically controlled over the whole ΔG_{EN} range. This conclusion raises another question, if the same kinetic control is present in the whole ΔG_{EN} range or if iso-energetic reactions are influenced by the different factors. Those questions still waits for a convincing explanation.

In this chapter the kinetic measurements of bimolecular energy transfer processes involving excited cyclometalated iridium(III) complexes and organic quenchers (structures depicted in Figures 4.1.2 and 4.1.5) are reported in several common organic solvents of various properties. The measurements have been performed for ^{3}*D + A → D + ^{3}*A processes occurring in two energetic regimes, for $\Delta G_{EN} << 0$ and $\Delta G_{EN} \sim 0$, respectively. Analysis of the obtained kinetic data have been performed in the framework available in the literature models (Sandros and Balzani) with the main conclusion that both of the models are inadequate for proper kinetic description of the investigated ^{3*}D + A → D + ^{3}*A processes, especially in relation to the energy transfer

energetic and solvent viscosity effects. Due to the failure of these models, we invoke a new model including the quantum magnetic number conservation rule (known also as the Winans selection rule) [20]. The proposed approach allows for kinetic description of the energy transfer quenching data obtained of the here reported investigations as well of the already available literature data. To our best knowledge, the Winans selection rule has not been applied yet in the kinetic description of bimolecular energy transfer reactions, despite that the magnetic number should be conserved in such processes [101], as it can be evidenced by direct observation of the electron spin polarization transfer in the triplet-triplet energy transfer in fluid solution [102-106].

5.2.2 Iso-energetic and strongly exergonic energy transfer systems

Similarly as for the energy transfer systems described in the previous chapter, all possible processes that could interfere with energy transfer processes can be straightforwardly excluded. All the luminophore-quencher systems described in this sub-chapter undergo Dexter type energy transfer (electron exchange) quenching. The other two conceivable reactions can be safely excluded. The Förster or dipole-dipole type energy transfer is not likely because of the lack of allowed absorption transitions for the quenchers in the emission wavelength range of the organometallic luminophores studied. Besides, electron transfer processes are neither affordable for these systems as none of them have enough negative free energy for this process, at least in aprotic media. Some doubts about this can occur for the alcoholic solvents where redox potential values either for energy donors or the energy acceptors studied are not available. However, data from transient absorption studies performed in both classes of the investigated solvents show no traces of absorption signals attributable to the ionic forms of the studied energy donors or acceptors.

In all the cases the excitation is restricted to the luminophore. The observed emission comes solely from its excited ^{3}*MLCT (*metal-to-ligand-charge-transfer*) triplet state. The only possible processes in presence of the used organic singlet quenchers are the non-radiative and radiative deactivation of the triplet luminophore ^{3}*D recovering its ground singlet state D, or the population of the triplet excited state of the quencher ^{3}*A according to the Wigner-Witmer selection rule applied to electron exchange reactions. In

Table 5.2.1. Interpolated values of the energy transfer rate constants $k_{EN}(0)$ for the iso-energetic ^{3}*D + A → D + ^{3}*A processes ($\Delta G_{EN} = 0$ case). Diffusion rate constants k_{dif} as calculated from the Einstein–Smoluchowski equation. Data for $(2,4F_2\text{-pbi})_2$Ir(pic) – naphthalene (A), $(2,4F_2\text{-pbi})_2$Ir(acac) – naphthalene (B), $(pbt)_2$Ir(acac) – fluoranthene (C), $(3,4F_2\text{-pbt})_2$(acac) – fluoranthene (D), $(4F\text{-pbi})_2$Ir(acac) – naphthalene (E), and $(4F\text{-pbi})_2$Ir(acac) – acenaphthene (F) systems.

Solvent	k_{dif} /10^{-9}M^{-1}s^{-1}	$k_{EN}(0)$ / 10^{-9}M^{-1}s^{-1}					
		A	B	C	D	E	F
ACN	19.3	1.70	1.40	1.70		1.20	2.20
THF	14.2	1.10	0.83	1.16			
TOL	11.9	1.70		1.90		0.79	
MeOH	11.9			4.10			
DBE	10.2			2.30			
DMF	8.20	0.38		0.65	0.73		
EtOH	6.08			1.70			
EtOD	6.08			2.20			
DX	5.51	0.60	0.56	0.93			
DMSO	3.30	0.58		0.64	0.42	0.49	
PC	2.60	0.52	0.32	0.46			
OcOH	0.89			0.22			
TMS	0.64		0.23			0.13	

all experiments there were no observation of any traces of the spin-forbidden phosphorescence from ^{3}*A or fluorescence from ^{1}*A despite the fact that, due to the acceptors triplet-triplet annihilation ^{3}*A + ^{3}*A → ^{1}*A + A, the latter is principally possible. Lack of emission from ^{1}*A can be attributed to the rather low concentration of the produced acceptor triplets, as it can be deduced taking into account light intensity of the applied excitation sources.

As it was already pointed above, the energy transfer rate constants were determined in two energetic regimes. In the region of very small reaction driving forces

Table 5.2.2. Experimental values of the energy transfer rate constants k_{EN} for the exergonic $^3*D + A \rightarrow D + {}^3*A$ processes $\Delta G_{EN} << 0$ case). Diffusion rate constants k_{dif} as calculated from the Einstein-Smoluchowski equation. Data for $(pbt)_2Ir(acac)$ – anthracene (A), $(pbt)_2Ir(acac)$ – benzanthracene (B), $(2,4F_2\text{-}pbi)_2Ir(pic)$ – pyrene (C), $(2,4F_2\text{-}pbi)_2Ir(acac)$ – pyrene (D), $Ir(2,4F_2\text{-}bpi)_2(acac)$ – benzanthracene (E), and $(pbt)Ir(acac)$ – pyrene (F) systems.

Solvent	$k_{dif}/10^{-9}M^{-1}s^{-1}$	$k_{EN}/10^{-9}M^{-1}\,s^{-1}$					
		A	B	C	D	E	F
ACN	19.3	7.70	5.80	8.00			
THF	14.2	4.80		4.50			
TOL	11.9	5.70		5.60			
MeOH	11.9	7.80					4.20
DBE	10.2	5.30					
DMF	8.20	3.00		2.10			
EtOH	6.08	5.70	4.70				
EtOD	6.08	4.20					
DX	5.51	3.70		2.80	2.50	2.10	
DMSO	3.30	1.90	1.70	1.70	1.60	1.70	
PC	2.60	2.00		1.70			
OcOH	0.89	1.10	0.92				0.95
TMS	0.64	0.44			0.62		

$(|\Delta G_{EN}| < 0.2\text{ eV})$, the recorded luminescence decays were bi-exponential as expected for reversible excited state kinetics. The two lifetimes and amplitudes extracted from these decays were analyzed as described in the Experimental section leading to the forward k_f and the backward k_b reaction rate constants. The observed rate constants for the forward and backward processes were further used for estimating the iso-energetic energy transfer rate by interpolating as described above. The interpolated $k_{EN}(0)$ values are collected in the Table 5.2.1.

On the other hand, in the region of very negative driving forces $(\Delta G_{EN} < -0.2\text{ eV})$ the observed decays of $^3*D$ were found to be mono-exponential in all

of the investigated cases. Emission life-times τ_{em} have been found to be dependent on concentration of the applied organic quencher in the expected way. Thence, the classical Stern-Volmer analysis of the extracted decay times provides the quenching rate constant k_{EN} values. The obtained data are collected in the Table 5.2.2. In a given solvent the k_{EN} values were found to be nearly independent of the energy donor and energy acceptor combinations, indicating the presence of a plateau region for sufficiently exergonic systems (*cf*. Figure 5.2.3).

As it could be expected in the view of previously published works, the experimental points, *i.e*. k_f and k_b values (plotted *vs*. ΔG_{EN} for k_f and *vs*. $-\Delta G_{EN}$ for k_b) form curves similar to the famous Rehm-Weller plot for the bimolecular electron transfer reactions. In a given solvent the relation between the energy transfer rate and reaction exothermicity seems to be uniform without expressing any significant dependence on the nature of donor or acceptor pair as it is shown in Figure 5.2.1. Similarly as it was reported in previous chapter to construct the k_f *vs*. ΔG_{EN} and k_b *vs*. $-\Delta G_{EN}$ plots, the values of ΔG_{EN} has been extracted from equation

$$\Delta G_{EN} = -RT \ln\left[\frac{k_f}{k_b}\right] \qquad 5.2.1$$

instead of using those calculated taking into account the differences between energies of ^{3}*D and ^{3}*A states assessed from the 0-0 transition observed in ^{3}*D room-temperature luminescence and ^{3}*A 77K phosphorescence spectra. This was only a minor correction as both values differs by 600 cm^{-1} in the worst case.

Typical dependencies of the energy transfer rate constants on ΔG_{EN} for two solvents, acetonitrile and 1,2-dioxane are presented in Figure 5.2.3. Noteworthy, in both solvents the plateau observed at sufficiently negative energies, lays well below the expected value ($k_{dif} = 8000RT/\eta$) as calculated from the Einstein-Smoluchowski equation for the diffusion-controlled processes in liquid media with viscosity η. Similar behavior has been found in the most of the investigated solvents; only in extremely viscous *n*-octanol or sulfolane the measured energy transfer rate constants are approaching values expected from the diffusional limitation. In solvents with lower viscosity, the maximal energy transfer rate constants are smaller than k_{dif} with the observed deviations especially large in the low viscosity solvents like acetonitrile or

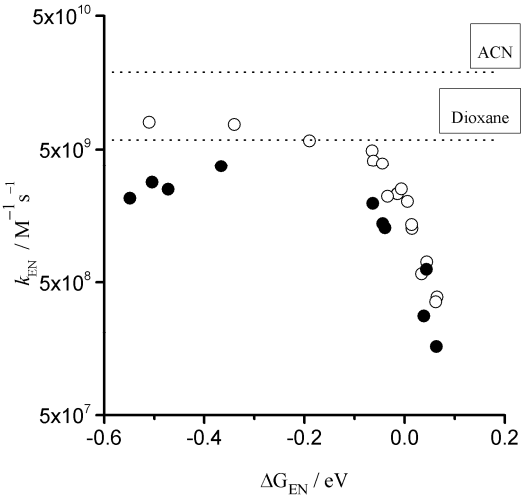

Figure 5.2.3. Dependency of the overall energy transfer rates constants k_f and k_b on the reaction exergonicity ΔG_{EN} in acetonitrile (*open circles*) and dioxane solutions (*filled circles*). Dotted lines correspond to the diffusional limits as calculated from the Einstein-Smoluchowski equation.

tetrahydrofuran. Similar effects have been already reported for the energy transfer systems involving "pure" organic substrates [14, 15], what drives concluding that the observation is a general behavior in the bimolecular energy transfer processes involving the excited triplet state.

The rate constants of the iso-energetic bimolecular processes (expressed in terms of the $k_{EN}(0)$ values interpolated to $\Delta G_{EN} = 0$) are smaller than the $k_{EN}(0)$ found for $\Delta G_{EN} << 0$ what suggests that in this case the diffusional limitation should play less pronounced role. Somewhat unexpectedly, however, the $k_{EN}(0)$ values seem to be also correlated with solvent viscosity in a way similar to that found for the strongly exergonic energy transfer processes. To the best of our knowledge such finding has not been reported in the literature and needs more attention because serves as an additional test for any kinetic model describing the energy transfer processes, especially in terms of $k_{EN}(0)$ *vs*. ΔG_{EN} relationships.

In order to investigate the dependence of the energy transfer rates on the environment we performed quenching experiments in both regions of ΔG_{EN} in twelve different solvents. Solvents were chosen to cover a wide range of most common physical parameters like viscosity, refractive index, dielectric constant, *etc*. Among all

physicochemical properties of the solvents studied, the rate constants of the energy transfer processes seem to depend only on solvent viscosity η. Changing the reaction medium viscosity causes proportionally a change in the rate constant in both energetic regimes of $\Delta G_{EN} \approx 0$ as well as $\Delta G_{EN} << 0$. In all the solvents investigated the energy transfer rate constant $k_{EN}(0)$ values interpolated for the region $\Delta G_{EN} \approx 0$ are roughly 2-4 times smaller than the corresponding maximum k_{EN} value in the sub-diffusional plateau. It suggests that the same or at least similar, kinetic limitations influence in the investigated energy transfer processes over the whole range of its exergonicity. So at least one important question stated in the introduction part found an experimental answer. In subsequent part of this chapter a discussion about the nature of these kinetic limitations will lead to the proposition of a new model describing energy transfer reactions in solutions.

5.2.3 Transient absorption studies

A separate part of discussion must be devoted to energy transfer in alcohols. Since electrochemical potentials (E_{ox} and E_{red} values) in protic solvents are unknown for the investigated energy donors and energy acceptors supplementary verification of assumed reaction mechanism is necessary to exclude any additional quenching reaction channel. The possible additional quenching path may be electron transfer reaction between ^{3}*D and A reactants involved in the investigated energy transfer processes or between the excited ^{3}*D or ^{3}*A species and alcohol molecules. The imaginable additional reaction channel may be also connected with direct deactivation of excited encounter complex ^{3}(*D…A) with hydrogen generation as iridium complexes are widely used as catalyst for this kind of reactions [107-110]. All these additional reactions might distort the correct determination of relevant kinetic parameters in alcoholic solutions that would lead to false interpretation of the measured quantities.

To exclude a possibility of an additional quenching reaction channel due to electron transfer or the photochemical reaction in excited state involving molecules of solvent additional transient absorption measurements have been performed for selected donor/acceptor/solvent systems. Those kinds of measurements allow confirming the assumed reaction mechanism by monitoring excited acceptor state time evolution and are

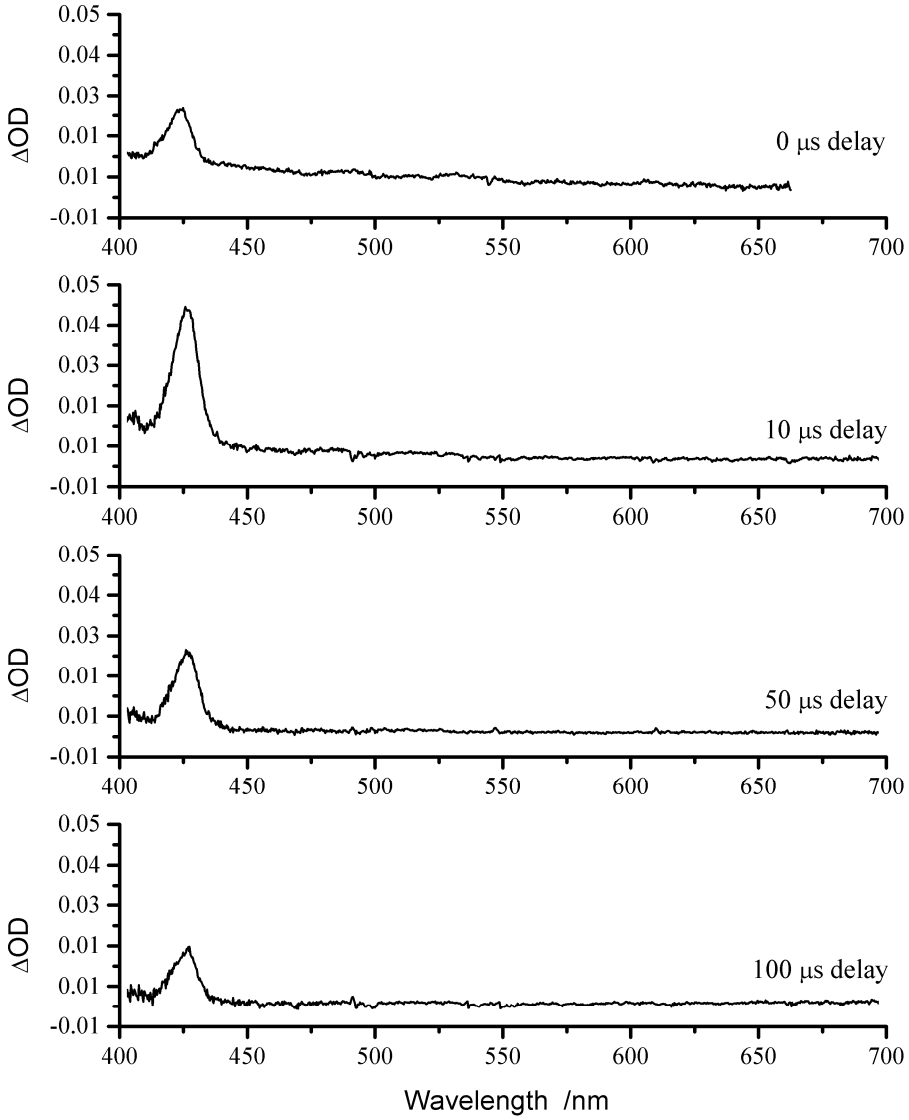

Figure 5.2.4. The transient absorption spectra of $Ir(pbt)_2(acac)$ – anthracene system, measured in ethanol solutions with different delay after excitation pulse.

complementary to emission data form emission measurements. It may be also able to indicate additional reaction paths.To check the issue the transient absorption measurements were performed on one system of donor namely $Ir(pbt)_2(acac)$ with anthracene as an acceptor. Kinetic of excited state of the acceptor were recorded monitoring time evolution of transient absorption signal at wavelength 413 nm. Additionally a number of transient absorption spectra were recorded with delay from excitation pulse varying between 0 and 150 μs. The time evolution (exponential growth and decay) was fitted to according to equation 4.3.7.

Table 5.2.5. Experimental values of the energy transfer rate constants for $Ir(pbt)_2(acac)$ – anthracene system. The rates $k_{EN}(1)$ and lifetimes τ_D obtained by time resolved emission and the rates $k_{EN}(2)$ and lifetimes τ_A obtained by transient absorption measurements.

Solvent	Viscosity η / cp	τ_D / μs	τ_A / μs	k_{dif} $/10^{-9}M^{-1}s^{-1}$	$k_{EN}(1)$ $/10^{-9}M^{-1}s^{-1}$	$k_{EN}(2)$ $/10^{-9}\ M^{-1}s^{-1}$
ACN	0.341	1.94	71.9	19	7.6	8.5
EtOH	1.083	1,68	34.2	6.3	5.7	5.7
EtOD	1.083	1.61	23.7	6.3	4.2	2.3

Transient absorption spectrum (Figure 5.2.4) shows no signs of additional bands in whole time range of measurements. All former observations leas to conclusion that energy transfer process in alcohols is not affected either by neither electron transfer nor photochemical reaction involving excited acceptor species. The quenching rate constant extracted from transient absorption are approximately the same as one measured by the means of time resolved emission technique (*cf*. data in Table 5.2.5) which indicates that there seems to be no subsequent photochemical reactions from excited triplet state of the acceptor. Also electron transfer can be excluded. The product of such reaction would be anthracene ion with very intense and characteristic transient absorption bands in red part of the spectra [106,107]. Additionally transient absorption measurement in ACN solutions provide important conclusion that in all of the investigated cases energy transfer reactions are not affected by any side reaction.

5.2.4 Model discussion

The next section is devoted to analysis of gathered experimental data performed in the framework of different kinetic models. The results for each model are represented by a plot of theoretically predicted $k_{EN}(\text{calc})$ values versus the experimentally obtained $k_{EN}(\text{exp})$ rate constants. Of course the ideal case is when $k_{EN}(\text{exp}) = k_{EN}(\text{calc})$ and the slope of the plot is equal to one (marked by a straight line in each plot). The parameter which can estimate how predicted values of energy transfer rate constant match experimentally obtained ones can be obtained by averaging expression $k_{EN}(\text{exp}) / k_{EN}(\text{calc})$ over the whole dataset. For the perfect agreement between

theoretical prediction and experiment this coefficient takes the value of one. Values departing from one indicate less accurate agreement. This coefficient however can serve as very rough estimation of accuracy of the model and depend strongly on the assumptions underlying the construction of the model.

5.2.4.1 Model 1

First a simple model describing the relationship between k_{EN} and ΔG_{EN} was elaborated by Sandros. His idea is based on the assumption that, due to an extremely fast intrinsic energy transfer step, a full equilibration between ^{3}*D…A and D…^{3}*A forms of an activated encounter complex must be reached. Consequently, the ratio of probabilities of the separation of the reacting species to form free ^{3}*A + D and D + ^{3}*A pairs, should obey the Boltzmann distribution law being equal to $\exp(-\Delta G_{EN} / RT)$. Assuming also that formation and dissociation of an activated encounter complex are governed by diffusion, one can obtain the following relationships describing the dependence of the rate constants in a bimolecular process with the energy difference ΔG_{EN}

$$k_f = \frac{k_{dif}}{1+\exp(\Delta G_{EN} / RT)} \quad \text{and} \quad k_b = \frac{k_{dif}}{1+\exp(-\Delta G_{EN} / RT)} \qquad 5.2.2$$

where k_{dif} is the diffusion rate constant at infinite time taken from the Einstein-Smoluchowski equation. The Sandros model predicts that for all ΔG_{EN} values the reaction is diffusion controlled and for enough negative ΔG_{EN} values it should occurs with a rate constant equal to k_{dif}, whereas for $\Delta G_{EN} = 0$ it should be exactly two times slower. Also the experimentally observed values of the energy transfer rate constants should be inversely proportional to viscosity in the same manner as k_{dif} in the whole range of ΔG_{EN} values. Moreover, at the ΔG_{EN} values near zero, a linear relationship between $\ln(k_{EN})$ and $\Delta G_{EN} / RT$ with slope equal unity, should be observed.

For the investigated donor/acceptor systems, the relationship between the rate constants predicted by the Sandros model and the experimentally found k_{EN} values is presented in Figure 5.2.6 where the calculated k_{EN} and $k_{EN}(0)$ are equal to k_{dif} and $k_{EN} = ½ k_{dif}$ for the exergonic ($\Delta G_{EN} << 0$) and the iso-energetic ($\Delta G_{EN} = 0$) regions, respectively. The value of average of the $k_{EN}(\text{exp}) / k_{EN}(\text{calc})$ expression is equal to 0.45. The agreement between theory and experiments cannot be regarded as satisfactory.

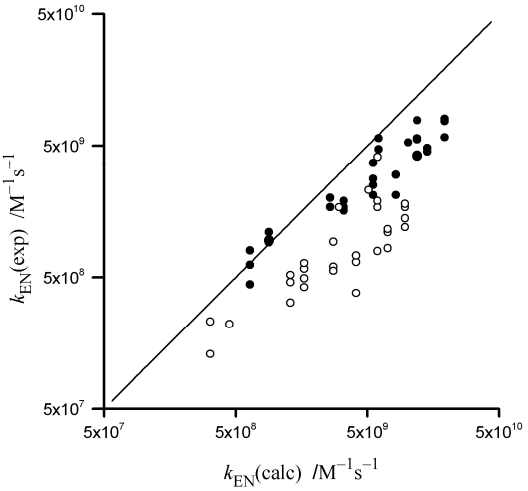

Figure 5.2.6. Comparison between the theoretically predicted $k_{EN}(\text{calc})$ values (calculated according to the Sandros model) and the experimentally obtained $k_{EN}(\text{exp})$ rate constants. Kinetic data (all studied solvents) for the investigated donor/acceptor systems within the iso-energetic $\Delta G_{EN} = 0$ (*open circles*) and the exergonic $\Delta G_{EN} << 0$ (*filled circles*) regions.

A possible explanation for the fact that in the particular case of triplet energy transfer processes, the diffusion rate constants are smaller than predicted by the Einstein-Smoluchowski equation cannot be *a priori* excluded from consideration but this option seems to be unlikely taking into account that in many other bimolecular processes (*e.g.* electron transfer quenching of the excited singlet states) the maximal observed rate constants are really close to that predicted theoretically. Moreover, in a given solvent different k_{dif} rate constants should be applied for the proper reproduction of the k_{EN} values in the exothermic $\Delta G_{EN} << 0$ and in the iso-energetic $\Delta G_{EN} = 0$ regimes, what seems to be still more doubtful. Another possible explanation may be given assuming that the intrinsic energy transfer step is slower than diffusion as it was proposed by Balzani. This option is discussed in the following subsection.

5.2.4.2 Model 2

According to the Balzani model the intrinsic energy transfer step exhibits features similar to non-adiabatic electron transfer as both reactions may be governed by the similar mechanisms. Upon this assumption Balzani has used an approach similar to the Marcus theory to express the dependence of k_f' and k_b'rate constants for both, the forward and the reverse energy transfer within the activated encounter ^{3}*D...A and

D…^{3}*A complexes, respectively. For given k_f' and k_b' values the overall rates of the forward and reverse energy transfer can be expressed by

$$k_f = \frac{k_{dif}}{1+\exp(\Delta G_{EN}/RT)+k_{-dif}/k_f'} \quad \text{and} \quad k_b = \frac{k_{dif}}{1+\exp(-\Delta G_{EN}/RT)+k_{-dif}/k_b'} \qquad 5.2.3$$

where both k_f' and k_b' rate constants depend on the reaction exothermicity according to the Marcus theory. Thus for both particular cases of $\Delta G_{EN} = 0$ and $\Delta G_{EN} << 0$ the observed k_{EN} rate constants can be simply related to the k_{dif}, k_f', and k_b' values. Taking into account that $k_f' = k_b'$ for $\Delta G_{EN} = 0$ and that $k_f' >> k_b'$ for $\Delta G_{EN} << 0$ one can simply derive expressions for the observed rate constants in both regimes

$$k_{EN}(0) = \frac{k_{dif}}{2+k_{-dif}/k_f'} \qquad 5.2.4$$

$$k_{EN} = \frac{k_{dif}}{1+k_{-dif}/k_f'} \qquad 5.2.5$$

In the case of the energy transfer reactions unlike in that of electron transfer, the overall reorganization energy λ determining the activation energy $\Delta G_{EN}^{\#}$ depends mainly on the inner reorganization energy λ_i of the reactants. The corresponding contribution from the outer reorganization energy λ_o should be negligible because no charged species are formed or destroyed in the energy transfer processes. Thus the magnitude of the λ parameter, being an intrinsic property of the donor and acceptor molecules, can be considered as constant over the whole range of the investigated solvents. Similarly, the electron coupling elements responsible for the pre-exponential factors A_{EN}' determining k_f' rate constants according to $k_f' = A_{EN}'\exp(-\Delta G_{EN}^{\#}/RT)$ should depend only on the nature of the reacting donor and acceptor molecules, remaining, at least in first approximation, solvent independent. Main controversy concerning both reorganization energy, as well as coupling elements is that they are not straightly connected to any experimental quantity and in fact can be chosen arbitrary for each different system of donor and acceptor. Consequently, the same k_f' rate constant can be used to fit to the experimental $k_{EN}(0)$ data for the iso-energetic systems under study. The same assumption about constant k_f' rate can be also applied in the cases of strongly exergonic energy

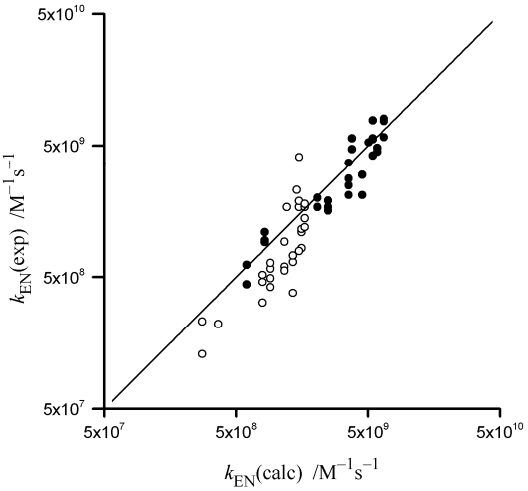

Figure 5.2.7. Comparison between the theoretically predicted $k_{EN}(calc)$ values (calculated according to the Balzani model) and the experimentally obtained $k_{EN}(exp)$ rates. Kinetic data (all studied solvents) for the investigated donor/acceptor systems within the iso-energetic $\Delta G_{EN} = 0$ (*open circles*) and the exergonic $\Delta G_{EN} << 0$ (*filled circles*) regions.

transfer processes because the observed $k_{EN}(0)$ values are found to be independent of ΔG_{EN} although the only justification for this choice is that it produces a good agreement between model and experiment. Using $(k_{dif} / k_{-dif})k_f'$ terms (formally bimolecular rate constants) as fitting parameters one can find that the Balzani model is quite well able to reproduce experimental values of $k_{EN}(0)$ values for the systems with $\Delta G_{EN} = 0$ as well as for those with $\Delta G_{EN} << 0$ (*cf.* Figure 5.2.7). In the first case a $k_f'k_{dif} / k_{-dif} \sim 2\times10^9$ $M^{-1}s^{-1}$ is required to properly reproduce the experimental $k_{EN}(0)$, whereas in the second one $k_f'k_{dif} / k_{-dif} \sim 1\times10^{10}$ $M^{-1}s^{-1}$ is necessary. The average of $k_{EN}(exp) / k_{EN}(calc)$ equals to 0.86 which also indicate good agreement between model and experiment. Considering the agreement between the experimental and the fitted k_{EN} values one can conclude that the Balzani model works quite well in the studied cases. Deeper insight into both $k_f'k_{dif} / k_{-dif}$ $\sim 2\times10^9$ $M^{-1}s^{-1}$ (for $\Delta G_{EN} = 0$) and $k_f'k_{dif} / k_{-dif} \sim 1\times10^{10}$ $M^{-1}s^{-1}$ ($\Delta G_{EN} << 0$) values leads, however, to some questions that are very difficult to answer. Comparing both values one can conclude that the energy activation $\Delta G_{EN}^{\neq}$ characteristic for the iso-energetic energy transfer processes must be very small (according to the Marcus theory $\Delta G_{EN}^{\neq} = (\lambda_o + \lambda_i) / 4$ at $\Delta G_{EN} = 0$) in agreement with the expected small values of the inner reorganization energies λ_i (as it can be deducted from ^{3}*D and ^{3}*A emission profiles [111]) and negligible values of the outer reorganization energies λ_o.

Correspondingly, the value of the pre-exponential factor A_{EN}' must be relatively small to lead to the observed k_f' values, what remains in serious conflict with typical values of the electronic coupling elements V characteristic for the bimolecular electron transfer reactions involving molecules with extended π-electronic character [65]. Taking into account possible V values one can conclude that the pre-exponential factor A_{EN}' should be quite large considering particularly that energy transfer (contrary to electron transfer) is expected not to be suppressed by dielectric relaxation of the reaction medium. In the view of the anticipated large value of the pre-exponential factor and small value of the activation energy it is very difficult to rationalize small values of k_f' rate constants with any convincing clarification. The simplest explanation that the energy transfer takes place at larger distances leads immediately to question why in fluid media the reacting molecules do not prefer shorter contact distance that would allow them react much faster.

5.2.4.3 Model 3

Taking into account the problems encountered by both of the previous models, it may be concluded that there is something missing in the description of the energy transfer reaction. An issue that may control the energy transfer and is not included in any of the former models, is that during the bimolecular energy transfer the total angular momentum J of reacting molecules should be conserved ($\Delta J = 0$) [98]. The value of J is the vector sum of the component of electronic orbital angular momentum L, the component of spin angular momentum S and the angular momentum of the nuclei. This fact was established by Winans [20] and it is known as the Winans selection rule. Therefore, this additional rule may seriously impact on kinetics of bimolecular processes involving the excited triplet state because ^{3}*A as well as ^{3}*D species which, independently of the L number, have three available sub-states with different J number. Then the excited triplet state ^{3}*D can transfer energy to one excited state sublevel of ^{3}*A conserving J number or to two excited state sublevels of ^{3}*A with a change in J number. Taking into account three initial states and three final states we can consider nine independent reaction channels. If we assume that three of them (occurring with k_f' and k_b' rates) are distinctly faster than the remaining six (occurring with k_f'' and k_b'' rates) then the overall energy transfer k_f and k_b rates may be expressed as the sum of two components, correspondingly for “allowed” and for “forbidden” transitions:

$$k_{\mathrm{f}} = \frac{1}{3} \times \frac{k_{\mathrm{dif}}}{1 + \exp(\Delta G_{\mathrm{EN}} / RT) + k_{-\mathrm{dif}} / k_{\mathrm{f}}'} + \frac{2}{3} \times \frac{k_{\mathrm{dif}}}{1 + \exp(\Delta G_{\mathrm{EN}} / RT) + k_{-\mathrm{dif}} / k_{\mathrm{f}}''}$$

5.2.6

$$k_{\mathrm{b}} = \frac{1}{3} \times \frac{k_{\mathrm{dif}}}{1 + \exp(-\Delta G_{\mathrm{EN}} / RT) + k_{-\mathrm{dif}} / k_{\mathrm{b}}'} + \frac{2}{3} \times \frac{k_{\mathrm{dif}}}{1 + \exp(-\Delta G_{\mathrm{EN}} / RT) + k_{-\mathrm{dif}} / k_{\mathrm{b}}''}$$

5.2.7

Assuming next that the "allowed" transitions occur with rate constants much faster than diffusion and that the "forbidden" transitions occur with rate constants slower than diffusion one can further simplify the above equations to:

$$k_{\mathrm{f}} = \frac{1}{3} \times \frac{k_{\mathrm{dif}}}{1 + \exp(\Delta G_{\mathrm{EN}} / RT)} + \frac{2}{3} \times \frac{k_{\mathrm{dif}}}{1 + \exp(\Delta G_{\mathrm{EN}} / RT) + k_{-\mathrm{dif}} / k_{\mathrm{f}}''} \qquad 5.2.8$$

$$k_{\mathrm{b}} = \frac{1}{3} \times \frac{k_{\mathrm{dif}}}{1 + \exp(-\Delta G_{\mathrm{EN}} / RT)} + \frac{2}{3} \times \frac{k_{\mathrm{dif}}}{1 + \exp(-\Delta G_{\mathrm{EN}} / RT) + k_{-\mathrm{dif}} / k_{\mathrm{b}}''} \qquad 5.2.9$$

Now one may reconsider two regions of ΔG_{EN}, one where $\Delta G_{\mathrm{EN}} << 0$ and other where $\Delta G_{\mathrm{EN}} = 0$, with the resulting final expressions as follow:

$$k_{\mathrm{EN}} = \frac{k_{\mathrm{diff}}}{3} + \frac{2}{3} \times \frac{k_{\mathrm{diff}}}{(1 + k_{-\mathrm{diff}} / k_{\mathrm{f}}'')} \quad \text{and} \quad k_{\mathrm{EN}}(0) = \frac{k_{\mathrm{diff}}}{6} + \frac{2}{3} \times \frac{k_{\mathrm{diff}}}{(2 + k_{-\mathrm{diff}} / k_{\mathrm{f}}'')}$$

5.2.10

Then for each case we can ascribe two boundary conditions, $k_{\mathrm{f}}'' << k_{\mathrm{dif}}$ and $k_{\mathrm{f}}'' >> k_{\mathrm{dif}}$. The first limit gives $k_{\mathrm{EN}} = \frac{1}{3} k_{\mathrm{dif}}$ for $\Delta G_{\mathrm{EN}} << 0$ and $k_{\mathrm{EN}} = \frac{1}{6} k_{\mathrm{dif}}$ for $\Delta G_{\mathrm{EN}} = 0$. At the second extreme limit $k_{\mathrm{EN}} = k_{\mathrm{dif}}$ for $\Delta G_{\mathrm{EN}} << 0$ and $k_{\mathrm{EN}} = \frac{1}{2} k_{\mathrm{dif}}$ for $\Delta G_{\mathrm{EN}} \approx 0$. The above presented approach explains the sub-diffusional plateau in the k_{EN} *vs.* ΔG_{EN} plots for the strongly exergonic energy transfer reactions with a maximal k_{EN} rate constant *ca.* three times smaller than k_{dif}, as it is indeed observed in the low-viscosity solvents like acetonitrile or tetrahydrofuran. In the more viscous media, when the term $k_{\mathrm{f}}''/k_{-\mathrm{diff}}$ becomes larger and more important, one can expect $k_{\mathrm{EN}} \approx k_{\mathrm{dif}}$. It is also observed for the donor/acceptor systems investigated in this work as well as for literature data. Moreover, the proposed approach rationalizes the relatively small differences between the experimentally found k_{EN} values in the iso-energetic and strongly exergonic regimes.

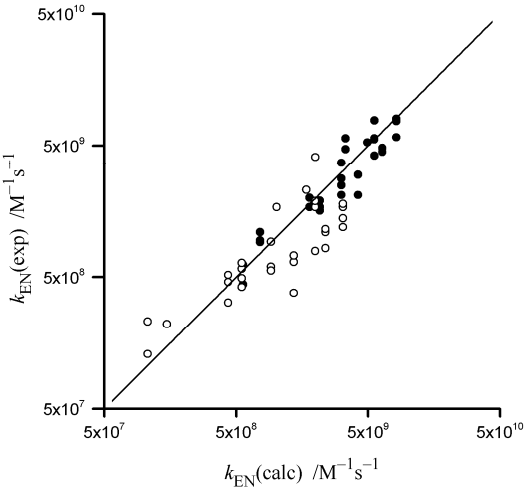

Figure 5.2.8. Comparison between the theoretically predicted $k_{EN}(\text{calc})$ values (calculated according to the model proposed in this work) and the experimentally obtained $k_{EN}(\text{exp})$ rates. Kinetic data (all studied solvents) for the investigated donor/acceptor systems within the iso-energetic $\Delta G_{EN} = 0$ (*open circles*) and the exergonic $\Delta G_{EN} << 0$ (*filled circles*) regions.

Depending on the $k_f"$ values, the ratio of the k_{EN} rate constants in both energetic regimes can only vary within a rather small range from 2 to 6, what remains in nice agreement with the experimental results. A so small variation, even in the case of extremely different $k_f"$ values in both $\Delta G_{EN} = 0$ and $\Delta G_{EN} << 0$ regimes, arises simply from the diffusional limitation in a way similar to that of the Sandros model. Finally, it should be noted that the proposed model predicts (at ΔG_{EN} around zero) that the slopes in the linear relationship between $\ln(k_f)$ or $\ln(k_b)$ *vs.* $\Delta G_{EN} / RT$ should be close to unity what remains (in contrary to prediction from the Balzani model) in agreement with experimental results. The average of $k_{EN}(\text{exp}) / k_{EN}(\text{calc})$ equals to 0.92 which also indicate very good agreement between model and experiment.

Using the $k_f" k_{dif} / k_{-dif}$ terms as fitting parameters one can find that the discussed model is quite well able to reproduce the experimental values of k_{EN} for the systems with $\Delta G_{EN} = 0$ as well as for those with $\Delta G_{EN} << 0$ (*cf.* Figure 5.2.8). The model correctly reproduces the experimental k_{EN} values for negative ΔG_{EN} with a fitted $k_f" k_{dif} / k_{-dif}$ value ~ 3×10^9 $M^{-1}s^{-1}$ whereas for the systems with $\Delta G_{EN} = 0$ the contribution involving the "forbidden" transitions can be neglected, *i.e.*, $k_f" \sim 0$ and $k_{EN} \sim \frac{1}{6} k_{dif}$, correspondingly. The fact that the "forbidden" transitions are only operative when there is a large excess of transferred energy and are vanishing for processes with

$\Delta G_{EN} \approx 0$ seems to be reasonable. An excess of the transferred energy is required to break the selection rule for the "forbidden" transitions. In contrary to that, the "allowed" transitions, occurring with k_f' rate constant, are much faster than that characteristic for the diffusion. As compared to the "allowed" transitions the "forbidden" transitions are suppressed at least by a factor 10^2. Most probably, however, differences between k_f' and k_f'' values (and correspondingly between k_b' and k_b'' values) are still larger. In the case of the strongly exergonic energy transfer processes their k_f' rates may be as fast as the characteristic for the frequencies of the intramolecular vibration within the reacting D and A molecules. Thus the suppression factor between the rates of the "allowed" and the "forbidden" channels may be as high as 10^4.

Using the model discussed above one may also try to describe data existing in the literature. In Figure 5.2.9 literature k_{EN} data for the region of $\Delta G_{EN} << 0$ taken from references [14, 21-25, 38-43, 83-86] are compared with the theoretical prediction according to Eq. 5.2.10 with the same $(k_{dif} / k_{-dif})k_f'' \sim 3\times10^9$ $M^{-1}s^{-1}$ value. The quite good agreement between the experimental and the calculated k_{EN} values indicates that the same k_f'' rate can be applied in the kinetic data for the energy transfer quenching of the excited ^{3}*MLCT states as well as for the organic ^{3}*D triplets with differences between the experimentally found and the theoretically predicted k_{EN} rate constants not exceeding

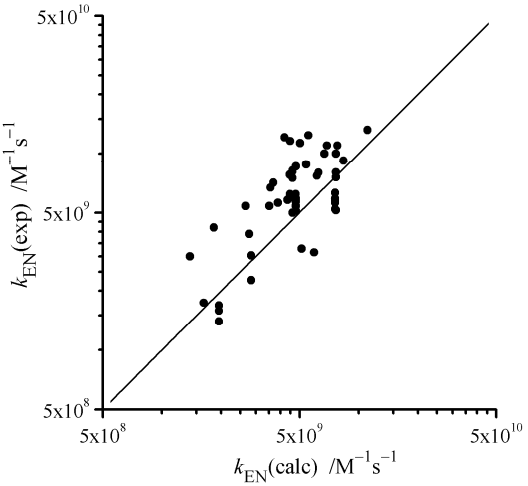

Figure 5.2.9. Comparison between the theoretically predicted $k_{EN}(\text{calc})$ values (calculated according to the model proposed in this work) and the experimentally obtained $k_{EN}(\text{exp})$ rates for "pure" organic donor/acceptor systems within $\Delta G_{EN} << 0$ 0 region. Literature data were taken from references [14, 21-25, 38-43, 83-86].

a factor of 2. Taking into account all assumed simplifications of the applied model on can emphasize that the obtained agreement can be regarded as more than satisfactory.

The main conclusion of above discussion is that the previous, Sandros and Balzani, kinetic models describing the energy transfer processes can be improved if the magnetic number conservation rule is implemented in the ^{3}*D + A → D + ^{3}*A reaction scheme. The assumption of "allowed" and "forbidden" reaction channels, leads to the proper prediction of the solvent viscosity effects in both exergonic and iso-energetic reaction regimes. The advantage of the proposed approach is that it gives a physical background for the sub-diffusional plateau in the $\Delta G_{EN} << 0$ range. The proposed model, however, needs further experimental verifications. The next chapter is entirely devoted to the temperature studies of the energy transfer process as it may provide substantial information about validity of all three models.

5.3 Temperature effect studies

5.3.1 Introductory remarks

As shown in previous chapter both kinetic models, presented by Sandros or Balzani, encounter serious difficulties to properly explain experimental results. The Sandros model seems to be too simple for description of an energy transfer process. On the other hand, according to the Balzani model, the additional kinetic limitation within an activated ^{3}*D…A and ^{3}*A…D complexes comes from the solvent and/or solute reorganization energies and may cause the lowering of the observed k_{EN} rates. However, somewhat unrealistic values of the reorganization energies λ as well as the electronic coupling elements V are required to reproduce the observed k_{EN} *vs*. ΔG_{EN} relationship. To some extent, presented model taking into account the quantum magnetic number conservation rule leads to quite proper prediction of the solvent viscosity effects in both, exergonic and iso-energetic reaction regimes for ^{3}*D + A → D + ^{3}*A and ^{3}*D + A → D + ^{3}*A processes, respectively. One of possible opportunity to confront both models is given by combined solvent and temperature effects studies performed for an iso-energetic ^{3}*D + A system. If the model with quantum magnetic number conservation rule is correct the observed changes in the $k_{EN}(0)$ values for ^{3}*D + A → D + ^{3}*A processes should

simply reflect changes in the diffusion rate k_{dif} constants with the expected $k_{EN}(0) \approx \frac{1}{6} k_{dif}$ relationship. Moreover the observed activation energies $\Delta H^{\neq}_{EN}$ for the iso-energetic energy transfer processes should be close to that characteristic for diffusion limited processes $\Delta H^{\neq}_{dif}$. On the other hand, if the Balzani model is correct then the observed changes in the $k_{EN}(0)$ values for ^{3}*D + A → D + ^{3}*A processes upon temperature change should reveal the magnitude of the reorganization energy λ which should have distinct higher value than for the diffusion limited processes. So those two models predict different behaviors with temperature changes which should be easy distinguishable upon analysis of experimental data.

In the next section the results from studies of combined solvent and temperature effects on kinetic of the bimolecular energy transfer processes within systems involving excited ^{3}*MLCT (metal-to-ligand-charge-transfer) states and organic quencher are reported. Two ^{3}*D/A systems, namely $Ir(ppy)_3$ – chrysene and $Ru(bpy)_3^{2+}$ – pyrene pairs have been investigated in several organic solvents at different temperatures. The obtained kinetic data provides additional arguments for validation of models used in description of the Dexter type electronic energy transfer in the liquid media.

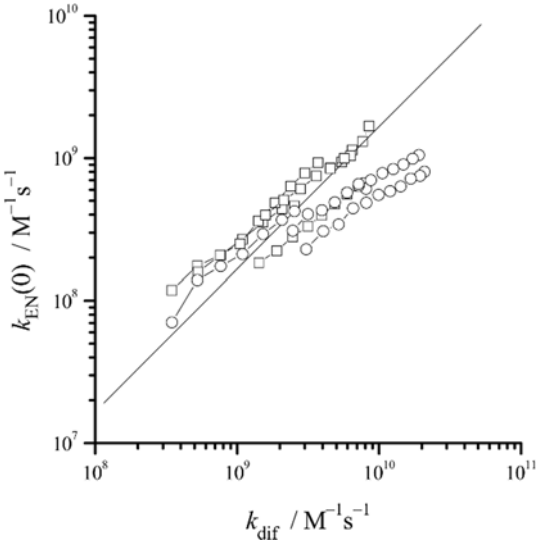

Figure 5.3.1. Plot of experimentally obtained $k_{EN}(0)$ *vs* diffusional rate constant k_{dif} in ^{3}*$Ir(ppy)_3$ – chrysene (*open squares*) and ^{3}*$Ru(bpy)_3^{2+}$ – pyrene systems (*open circles*) for all measured solvents and temperatures. Line represents $k_{EN}(0) = k_{dif} / 6$ dependence.

5.3.2 Relation between k_{EN} and k_{dif} values

Again, in both studied systems (iridium complex – chrysene and ruthenium complex – pyrene) the Dexter type energy transfer reaction is observed. Other possible processes, namely, electron transfer quenching and Forster type energy transfer can be excluded. Electron transfer reactions are prevented by too positive values of ΔG_{ET} as calculated taking into account redox potentials of D and A reactants, whereas the Forster type energy transfer processes can be straightforwardly ruled out because of the very small (if not nil) transition dipole moment for the $S_0 \rightarrow T_1$ transitions within the organic acceptors employed. In the absence of an energy acceptor, the investigated iridium and ruthenium complexes exhibit mono-exponential decays of emission independently of their concentration in the range studied and of the laser power employed. In the presence of an energy acceptor, however, bi-exponential decays (characterized by two normalized amplitudes and two decay times) have been observed, as it could be expected for the energy transfer process around $\Delta G_{EN} \sim 0$. Kinetic parameters extracted from the recorded bi-exponential decays were further analyzed as described in the Experimental (equation 4.3.15) section leading to the forward k_f and the backward k_b reaction rate constants.

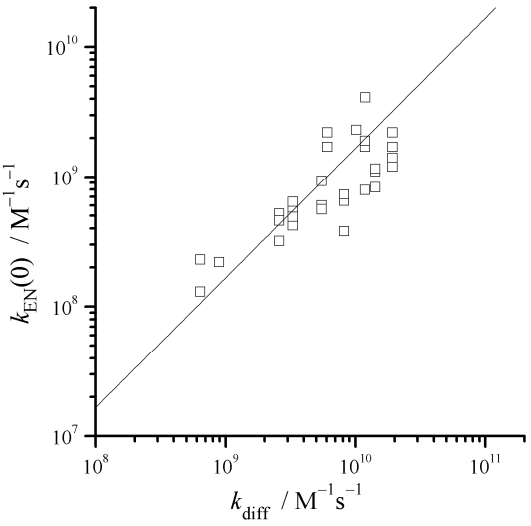

Figure 5.3.2. $k_{EN}(0)$ *vs.* k_{dif} relationship for the iso-energetic energy transfer processes involving iridium(III) chelates (energy donors) and aromatic hydrocarbons (energy acceptors) in different solvents. Room temperature data from previous chapter. Line represents $k_{EN}(0) = k_{dif} / 6$ dependence.

The observed rate constants for the forward and backward processes were further used to estimate the iso-energetic energy transfer $k_{EN}(0)$ rates by interpolation as described in the Experimental section (equation 4.3.18). In all solvents, independently of the measurements temperature, the estimated $k_{EN}(0)$ rates (*cf*. Figure 5.3.1) were found to be distinctly smaller than the diffusion rates k_{dif} calculated according to the Einstein-Smoluchowski equation

$$k_{dif} = 8000RT / 3\eta \qquad 5.3.1$$

The obtained $k_{EN}(0)$ values for the room-temperature can be compared with experimental data from previous chapter for different ^{3}*D (cyclometalated iridium(III) chelates) and A (aromatic hydrocarbons) and in the broader view seem to not exhibit any significant dependence on the nature of donor or acceptor pair (*cf*. Figure 5.3.2).

5.3.3 Energy transfer enthalpy ΔH_{EN} and entropy ΔS_{EN} values

The estimated forward k_f and backward k_b energy transfer rates were also employed to calculate the free energy changes ΔG_{EN} and estimate thermodynamic parameters (enthalpy ΔH_{EN} and entropy ΔS_{EN}) characterizing the investigated energy

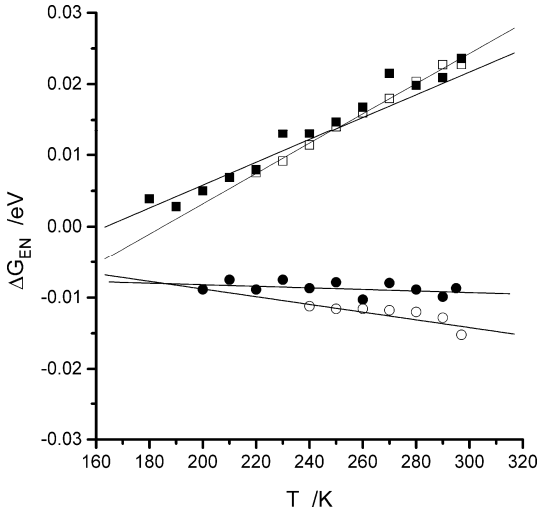

Figure. 5.3.3. Typical examples of ΔG_{EN} *vs*. *T* relationships for the investigated nearly iso-energetic energy transfer processes. Data for ^{3}*Ru(bpy)$_3^{2+}$ – pyrene in AC (open squares), ^{3}*Ru(bpy)$_3^{2+}$ – pyrene in ACN (filled squares), ^{3}*Ir(ppy)$_3$ – chrysene in DMF (filled circles), and ^{3}*Ir(ppy)$_3$ – chrysene in THF (open circles) systems.

Table 5.3.4. Summary of the thermodynamic parameters, enthalpy ΔH_{EN}, entropy ΔS_{EN}, and free energy ΔG_{EN} values (at 233 and 298 K), characterizing the investigated energy transfer ^{3}*D + A → D + ^{3}*A processes.

Solvent	Ir(ppy)$_3$ – chrysene				Ru(bpy)$_3^{2+}$ – pyrene			
	ΔH_{EN} /eV	ΔS_{EN} /meVK^{-1}	ΔG_{EN} (298 K) /eV	ΔG_{EN} (233 K) /eV	ΔH_{EN} /eV	ΔS_{EN} /meVK^{-1}	ΔG_{EN} (298 K) /eV	ΔG_{EN} (233 K) /eV
AC					–0.006	–0.017	–0.001	–0.002
ACN					0.002	0.054	–0.014	–0.011
THF	–0.026	–0.159	0.021	0.011				
DMF	–0.039	–0.211	0.024	0.010	0.016	0.057	–0.001	0.003
ANS	–0.056	–0.214	0.008	–0.006				
PC	–0.029	–0.150	0.016	–0.026	0.040	0.182	–0.014	–0.002

transfer ^{3}*A + D → A + ^{3}*D processes from the linear relationships between ΔG_{EN} *vs*. T (*cf*. Figure 5.3.3) according to

$$\Delta G_{EN} = \Delta H_{EN} - T\Delta S_{EN} \qquad 5.3.2$$

The acquired enthalpy ΔH_{EN} and entropy ΔS_{EN} parameters are summarized in the Table 5.3.4 together with ΔG_{EN} values at 298 and 233 K. The obtained ΔS_{EN} values are found to be rather small for the both investigated systems indicating that ΔG_{EN} are close to ΔH_{EN} in all of the solvent studied, although ΔS_{EN} values seems to be somewhat depend on the solvent. Nevertheless both ΔG_{EN} and ΔH_{EN} values extracted from the performed kinetic measurements remain in agreement with that expected from differences in "photophysical" energies of the excited ^{3}*D and ^{3}*A states as assessed from the 0-0 transitions observed in ^{3}*D and ^{3}*A 77K phosphorescence spectra [112]. Both, "kinetic" and "photophysical" values do not deviate by more than 0.04 eV which is indeed a very nice agreement demonstrating a quite high precision of the measured rate constants.

5.3.4 Energy transfer $\Delta H^{\#}_{EN}$ and A_{EN} activation parameters

The linear relationships between $\ln[k_{EN}(0)]$ and $1/RT$ (*cf*. Figure 5.3.5) have been found for all the investigated systems allowing estimation of A_{EN} and $\Delta H^{\neq}_{EN}$

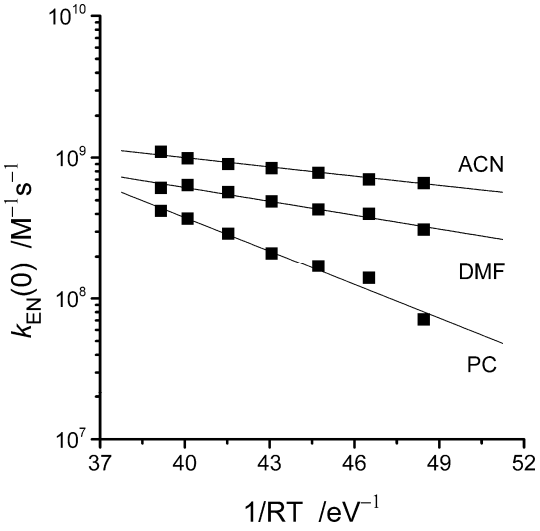

Figure 5.3.5. Typical examples of logarithm of the $k_{EN}(0)$ values plotted *vs*. 1/*RT*. Data for $Ru(bipy)_3^{2+}$ – chrysene system in acetonitrile, N,N-dimethylformamide, and propylene carbonate solutions.

parameters from the temperature dependence of $k_{EN}(0)$ rates according to the Arhenius relationship

$$k_{EN}(0) = A_{EN} \exp(-\Delta H^{\neq}_{EN} / RT) \qquad 5.3.3$$

The obtained activation energies $\Delta H^{\neq}_{EN}$ and pre-exponential factor A_{EN} values are collected in Table 5.3.6 together with $\Delta H^{\neq}_{dif}$ and A_{dif} parameters describing temperature dependence of k_{dif} rates

$$k_{dif} = A_{dif} \exp(-\Delta H^{\neq}_{dif} / RT) \qquad 5.3.4$$

Noteworthy both $\Delta H^{\neq}_{EN}$ and A_{EN} parameters have been found to be solvent dependent in way similar to that characteristic for $\Delta H^{\neq}_{dif}$ and A_{dif} (*cf*. Figures 5.3.7 and 5.3.8). Whereas $\Delta H^{\neq}_{EN}$ values in the given solvent are similar, only somewhat smaller (by 0.03-0.05 eV) than $\Delta H^{\neq}_{dif}$ values, much more distinct differences (one-two orders of magnitude) between the pre-exponential factors A_{EN} and A_{dif} can be observed. Taking into account the found relationships between $\Delta H^{\neq}_{EN}$ and $\Delta H^{\neq}_{dif}$ as well as between A_{EN} and A_{dif} one can conclude that the observed $k_{EN}(0)$ values are in any way controlled by the reaction medium viscosity despite that $k_{EN}(0)$ values are well below diffusional limitations in the

Table 5.3.6. Summary of the kinetic parameters characterizing the diffusional limitation (k_{dif} rates at 298 K, activation energies $\Delta H^{\neq}_{dif}$, pre-exponential factors A_{dif}) of the studied solvents and the investigated energy transfer ^{3}*D + A ⟶ D + ^{3}*A processes ($k_{EN}(0)$ rates at 298 K, activation energies $\Delta H^{\neq}_{EN}$, pre-exponential factors A_{EN}).

Solvent	k_{dif} /M^{-1}s^{-1}	$\Delta H^{\neq}_{dif}$ /eV	$\frac{1}{6} A_{dif}$ /M^{-1}s^{-1}	Ir(ppy)$_3$ – chrysene			Ru(bpy)$_3^{2+}$ – pyrene		
				$k_{EN}(0)$ /M^{-1}s^{-1}	$\Delta H^{\neq}_{EN}$ /eV	A_{EN} /M^{-1}s^{-1}	$k_{EN}(0)$ /M^{-1}s^{-1}	$\Delta H^{\neq}_{EN}$ /eV	A_{EN} /M^{-1}s^{-1}
AC	2.1×10^{10}	0.102	1.9×10^{10}				8.0×10^{8}	0.063	9.9×10^{9}
ACN	1.9×10^{10}	0.106	9.6×10^{10}				1.1×10^{9}	0.050	7.4×10^{9}
THF	1.4×10^{10}	0.109	1.0×10^{11}	1.7×10^{9}	0.089	5.1×10^{10}			
DMF	8.2×10^{10}	0.127	1.9×10^{11}	6.7×10^{8}	0.097	3.1×10^{10}	6.1×10^{8}	0.075	1.2×10^{10}
ANS	6.3×10^{9}	0.154	4.3×10^{11}		0.106	6.5×10^{10}			
PC	2.6×10^{9}	0.214	1.8×10^{12}	4.6×10^{8}	0.147	1.5×10^{11}	4.2×10^{8}	0.183	5.7×10^{11}

Energies of the excited ^{3*}MLCT states for Ir(ppy)$_3$ and Ru(bpy)$_3^{2+}$ chelates are 2.39 and 2.14 eV, respectively (77 K data from ref [112] and ref [113]). Energies of triplet states of the organic quenchers are 2.48 eV for chrysene and 2.09 eV for pyrene (77K data from ref [74]).

given solvent. This finding allows also to conclude that similar kinetic limitations may be present in the case of the iso-energetic ^{3}*D + A ⟶ D + ^{3}*A and (as it was described in previous chapters) in the strongly exergonic ^{3}*D + A ⟶ D + ^{3}*A energy transfer processes.

The obtained results can deliver further important arguments in discussion concerning correctness of any kinetic model describing energy transfer processes in liquid media. In the simplest case, according to the Sandros model, the observed overall energy transfer rate is related to the reaction exothermicity as follow

$$k_{EN} = \frac{k_{dif}}{1+\exp(\Delta G_{EN} / RT)} \qquad 5.3.5$$

In the studied cases with $\Delta G_{EN} = 0$ the observed $k_{EN}(0)$ rates should be equal to $\frac{1}{2} k_{dif}$. Correspondingly $\Delta H^{\neq}_{EN}$ should be close to $\Delta H^{\neq}_{dif}$ and A_{EN} close to $\frac{1}{2} A_{dif}$. Our results, being in conflict with these prediction clearly shown that the Sandros model is inadequate to proper description of the experimentally found $k_{EN}(0)$ values. Despite that the solvent

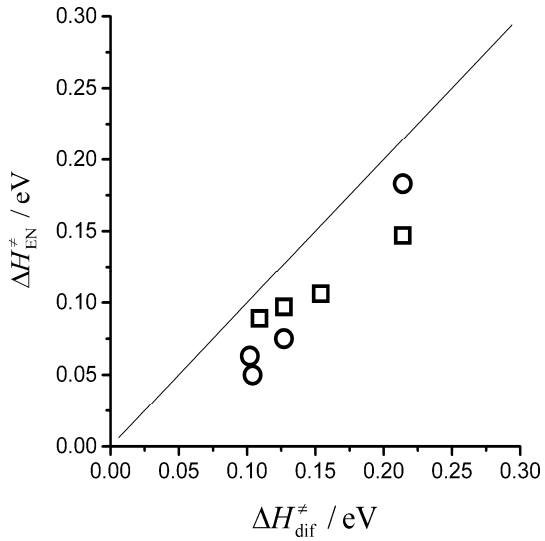

Figure 5.3.7. $\Delta H^{\neq}_{EN}$ *vs.* $\Delta H^{\neq}_{dif}$ relationship for the investigated energy transfer processes involving ^{3}*Ru(bpy)$_3^{2+}$ – pyrene (*open squares*) and ^{3}*Ir(ppy)$_3$ – chrysene (*open circles*) systems.

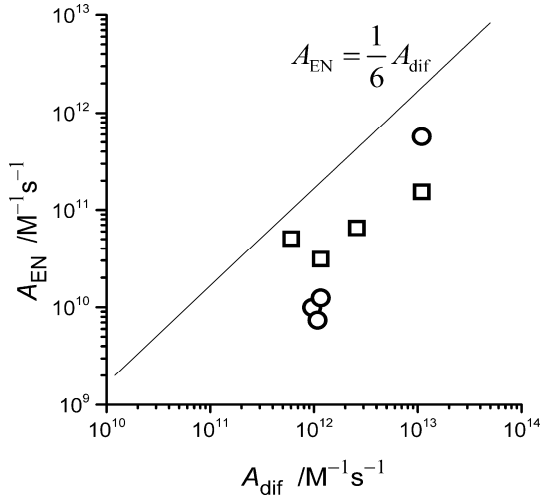

Figure 5.3.8. A_{EN} *vs.* A_{dif} relationship for the investigated energy transfer processes involving ^{3}*Ru(bpy)$_3^{2+}$ – pyrene (*filled circles*) and ^{3}*Ir(ppy)$_3$ – chrysene (*open circles*) systems.

and/or temperature induced changes of $k_{EN}(0)$ values follow the trends expected from the Sandros model, the observed rate constants are distinctly smaller than predicted.

The possible explanation of theses deviations can be discussed within the Balzani model taking into account the lowering of the reaction rate is caused by any additional kinetic limitation. According to the Balzani model the overall rate of energy transfer is given in the standard form

$$k_f = \frac{k_{dif}}{1 + \exp(\Delta G_{EN} / RT) + k_{-dif} / k_f'} \quad 5.3.6$$

$$k_b = \frac{k_{dif}}{1 + \exp(-\Delta G_{EN} / RT) + k_{-dif} / k_b'} \quad 5.3.7$$

where k_f' and k_b' are the intrinsic rate constants of energy transfer for ^{3}*D + A → D + ^{3}*A and ^{3}*A + D → A + ^{3}*D processes, respectively. In the case of studied systems with $\Delta G_{EN} = 0$ the observed $k_{EN}(0)$ rates can be analyzed simplifying equations 5.3.6 and 5.3.7 to

$$k_{EN}(0) = \frac{k_{dif}}{2 + k_{-dif} / k_f'} = \frac{k_{dif}}{2 + k_{-dif} / k_b'} \quad 5.3.8$$

Intrinsic energy transfer rates $k_f' = k_b'$ can be further discussed (according to the Balzani model) in terms of the Marcus theory

$$k_f' = k_b' = A_f \exp(-\lambda / 4RT) \quad 5.3.9$$

where pre-exponential factor A_f is, at least in first approximation, composition of the electronic transmission coefficient and the frequency factor and $¼\lambda$ is an activation energy [48] depending mainly on the inner reorganization energy λ_i of the reactants.

On the basis of the Balzani model the observed, relatively small $k_{EN}(0)$ values could be rationalized by high value of the reorganization energy λ and/or small values of the pre-exponential factor A_f. Experimental verification, however, brings down first possibility as data extracted from temperature measurements indicates activation energies in the range of 0.04-0.09 eV which is not sufficient to explain lower than expected values of $k_{EN}(0)$. As result the change in energy transfer rate constant must be attributed to alteration of pre-exponential factor A_f, although assumed model give no, even qualitative, physical explanation of the nature of changes of A_f. Interesting conclusions may be drawn upon analysis of experimental points with the same viscosity regardless of the solvent and temperature they were measured. As it turns out in all iso-viscous series the rate constants of energy transfer process are very similar to each other and can be treated as constants within the accuracy of the experimental error. This may lead to a conclusion that any kind of the reorganization energy is irrelevant for energy transfer

process and the main factor that governs rate constant of the process is viscosity of the solvent. This may be served as an argument against validity of the Balzani model.

The third considered model take into account that during the bimolecular energy transfer the total angular momentum J of reacting molecules should be conserved. The value of J is the vector sum of the component of electronic orbital angular momentum L, the component of spin angular momentum S and the angular momentum of the nuclei. Assuming that the transition with $\Delta J = 0$ are much faster than diffusion and that the transitions with $\Delta J \neq 0$ are also possible but are occurring slower than diffusion, the kinetic equations can be written as

$$k_{\mathrm{f}} = \frac{1}{3} \times \frac{k_{\mathrm{dif}}}{1 + \exp(\Delta G_{\mathrm{EN}} / RT) + k_{-\mathrm{dif}} / k_{\mathrm{f}}'} + \frac{2}{3} \times \frac{k_{\mathrm{dif}}}{1 + \exp(\Delta G_{\mathrm{EN}} / RT) + k_{-\mathrm{dif}} / k_{\mathrm{f}}''} \qquad 5.3.10$$

$$k_{\mathrm{b}} = \frac{1}{3} \times \frac{k_{\mathrm{dif}}}{1 + \exp(-\Delta G_{\mathrm{EN}} / RT) + k_{-\mathrm{dif}} / k_{\mathrm{b}}'} + \frac{2}{3} \times \frac{k_{\mathrm{dif}}}{1 + \exp(-\Delta G_{\mathrm{EN}} / RT) + k_{-\mathrm{dif}} / k_{\mathrm{b}}''} \qquad 5.3.11$$

where k_{f}'' and k_{b}'' are so called "forbidden" transition rate constant for reaction channels with $\Delta J \neq 0$ and fulfill the condition $k_{\mathrm{f}}'' < k_{\mathrm{dif}}$ and $k_{\mathrm{b}}'' < k_{\mathrm{dif}}$. For $\Delta G_{\mathrm{EN}} = 0$ the above expressions can be further simplified to

$$k_{\mathrm{EN}}(0) = k_{\mathrm{f}} = \frac{k_{\mathrm{dif}}}{6} + \frac{2}{3} \times \frac{k_{\mathrm{dif}}}{2 + k_{-\mathrm{dif}} / k_{\mathrm{f}}''} = k_{\mathrm{b}} = \frac{k_{\mathrm{dif}}}{6} + \frac{2}{3} \times \frac{k_{\mathrm{dif}}}{2 + k_{-\mathrm{dif}} / k_{\mathrm{b}}''} \approx \frac{k_{\mathrm{dif}}}{6} \qquad 5.3.12$$

Preceding equation consequents from our previous work where "forbidden" rate constant k_{b}'' was estimated to be negligible for $\Delta G_{\mathrm{EN}} = 0$ energy case. Fact that "forbidden" transitions are only operative when there is a large excess of transferred energy and vanishing when energy gap is close to zero is reproduced by fitting our present data to the equation 5.3.11.

The two reaction channels, introduced by the model, are the source of kinetic limitations that explain unusual dependence of rate of energy transfer process on viscosity. According to the model the rate of energy transfer process at $\Delta G_{\mathrm{EN}} = 0$ should

keep the ratio $k_{EN}(0) \approx \frac{1}{6} k_{dif}$ regardless of solvent. Also the temperature dependence of $k_{EN}(0)$ should reflect changes in the k_{dif} rates with the expected $k_{EN}(0) \approx \frac{1}{6} k_{dif}$ relationship and activation energy resulting solely from the temperature dependency of viscosity $(\Delta H^{\neq}_{EN} \approx \Delta H^{\neq}_{dif})$.

Application a model to experimental data yield a quite nice agreement with $k_{EN}(0) \approx \frac{1}{6} k_{dif}$ relation despite that some deviation may be noticed in low viscous solvents like ACN and AC (*cf*. Figure 5.3.1). This may be due to either experimental error or approximation in assignment of the k_{dif} values. Nevertheless dependence between energy transfer rates and medium viscosity is conserved despite shift in the $k_{EN}(0)$ values. In remaining solvents the relation much better holds (*cf*. Figure 5.3.1) over whole temperature range with k_{dif} calculated in each temperature according to the Einstein-Smoluchowski equation. Taking into account all assumed simplifications of the applied model one can emphasize that the obtained agreement strongly act in favor of the correctness of assumed model.

6. Summary and conclusions

The photo-induced energy transfer reactions have been studied extensively in the course of this thesis. At the beginning of this work the novel methodology was proposed to precisely measure the energy transfer reaction rates for iso-energetic systems of a donor and acceptor. The proposed method makes use of time-resolved emission spectroscopy quenching by organic acceptors of triplet phosphorescence from the cyclometalated iridium(III) complexes with structured emission. It has been demonstrated that the method can be used accurately to determine the triplet energies of the acceptors as well as their lifetimes. As well, it could be useful for the triplet energy determination of transition metal complexes with non-structured emission. It represents an advantage over more sophisticated methods of transient absorption and in the case of organic triplets that cannot be populated by photo-excitation or do not fully relax in low temperature matrices. The accuracy of the E_T determination is in the range of 500 cm^{-1} and the lifetimes in the range of tens of μs.

Having a reliable tool for measuring energy transfer rate constants next sections were devoted to investigation factors that influence energy transfer process and comparing results with available theoretical models. It was done by systematic solvent studies. The main conclusion of this work is that the previous, Sandros and Balzani, kinetic models describing the energy transfer processes can be improved if the magnetic number conservation rule is implemented in the $^3*D + A \rightarrow D + {}^3*A$ reaction scheme. The assumption of "allowed" and "forbidden" reaction channels, leads to the proper prediction of the solvent viscosity effects in both exergonic and iso-energetic reaction regimes. The advantage of the proposed approach is that it gives a physical background for the sub-diffusional plateau in the $\Delta G_{EN} << 0$ range. The interesting conclusion may be drawn if above reasoning is generalized to include electron transfer reactions. As mentioned, both electron and energy transfer processes are conceptually related if the latter occurs according to the Dexter mechanism. Thus, in the case of electron transfer quenching some differences can take place for processes involving the excited singlet $^1*S$ and triplet $^3*T$ states, respectively. In both cases electron transfer processes are allowed according to spin conservation rules but some differences between them should take place

if the magnetic number conservation rules will be operative as it has been above postulated for the energy transfer processes. For electron transfer quenching of the excited singlet state only one reaction channel with $\Delta J = 0$ is possible whereas in the case of the excited triplet state quenching for some reaction channels changes with $\Delta J \neq 0$ are required. Therefore the bimolecular electron transfer processes involving the excited singlet ^{1}*S precursors can reach diffusion limited rate over the whole range of solvents. For the bimolecular electron transfer processes involving the excited triplet ^{3}*T precursors, however, some kinetic limitations may be present in the low-viscosity solvents, even for the reactions with high exothermicity. Unfortunately, until now no systematic kinetic studies on the solvent effect in the photo-induced electron transfer processes were reported in the literature, most of the performed works was done in acetonitrile solutions where additional, electrochemical data usually necessary for more advanced interpretation of experimental results are easy available from literature or own measurements. Despite lack of appropriate data some remarks can be already done taking into account those already available. Usually for the strongly exergonic electron transfer of the excited singlet state the observed rate constants are close to k_{dif} value as calculated from Einstein-Smoluchowski equation. On the other hand, those results from the electron transfer quenching studies of the excited ^{3}*Ru(bipy)$_3^{2+}$ chelate in acetonitrile solutions [114, 115] suggests that both possible, the reductive and the oxidative electron transfer processes occur with measured rate constants that are smaller (even in the case of large exothermicity) than the expected from the k_{dif} value. The observed sub-diffusional plateau has been found at rate constants *ca*. 2-3 times smaller than the k_{dif} value. For the ^{3}*S + Q → S$^{-/+}$ + Q$^{+/-}$ photo-ionization processes, similarly as in the case of the energy transfer, only three from the principally possible nine reaction channels occur without changing *J* values ($\Delta J = 0$) , whereas for the remaining six changes of *J* values ($\Delta J \neq 0$) are compulsory. Of course the above presented coincidence cannot be treated as any final proof of the theory but only as a suggestion of further, more detailed studies of the solvent effects in kinetics of the photo-induced electron transfer processes involving the excited singlet and excited triplet states, both in parallel.

The proposed model, however, needs further experimental verifications. The further efforts were focused on the systematic combined solvent and temperature effects

studies for the iso-energetic ^{3}*D/^{3}*A systems with $\Delta G_{EN} = 0$. The presented results support our conclusion that description of bimolecular energy transfer process in liquids can be improved if the magnetic conservation number rule is implemented in the kinetic scheme. The temperature dependent experiments were one of the possibility to test validity of the model. Obtained results are not in contradiction with assumed model, moreover seems to fit in the frames the theory leading to proper prediction of the temperature effects. The outcome of the performed research could not be explained in the terms of remaining two models proposed by Sandros and Balzani.

7. Acknowledgements

I would like to thank prof. Andrzej Kapturkiewicz for providing topics, ideas, and a surrounding, which allowed me to grow in my scientific abilities. He was also a reliable and inexhaustible source of information, which I often used.

I want to thank Dr Gonzalo Angulo for many discussions on scientific and non-scientific subjects that have stimulated the advance of this thesis.

Dr Alexander Gorski helped me much with designing, constructing, setting and rebuilding the apparatuses used in this work. Without his technical knowledge and own developed or built set-ups it would have been hard to finish this Thesis.

I would like to thanks all colleagues in the department who was there during the course of my PhD studies for lots of laughs, interesting discussions and support in the not-so good days. Especially thanks Maja Pszona, Sylwek Gawinkowski, Michal Kijak and Michal Turowski for support and enthusiasm.

Biggest thanks to my mom for absolutely everything.

And finally to the reader for his patience and tolerance when finding mistakes (hopefully not too much) that for sure this work contains.

8. Literature

[1] A. Lavie-Cambot, C. Lincheneau, M. Cantuel, Y. Leydet, N. D. McClenagha, Reversible electronic energy transfer: a means to govern excited-state properties of supramolecular systems. *Chem. Soc. Rev*., **2010**, 39, 506.

[2] M. Mimuro, Excitation energy flow in the photosynthetic pigment systems: structure and energy transfer mechanism. *Bot. Mag. Tokyo*, **1990**, 103, 233.

[3] N. J. Farrer, L Salassa, P. J. Sadler, Photoactivated chemotherapy (PACT): the potential of excited-state d-block metals in medicine. *Dalton Trans.,* **2009**, 10690.

[4] S. Sadhu, A. Patra, A Brief Overview of Some Physical Studies on the Relaxation Dynamics and Förster Resonance Energy Transfer of Semiconductor Quantum Dots. *Chem. Phys. Chem.*, **2013**, 14, 2641.

[5] T. N. Singh-Rachford, F. N. Castellano, Photon upconversion based on sensitized triplet-triplet annihilation. *Coord. Chem. Rev.*, **2010**, 254, 2560.

[6] T. Förster, Intermolecular Energy Migration and Fluorescence. *Ann. Phys.*, **1948**, 2, 55.

[7] D. L. Dexter, A theory of sensitized luminescence in solids. *J. Chem. Phys.*, **1953**, 21, 836.

[8] T. Forster, in O. Sinanoglu (Ed), Modern Quantum Chemistry, Academic Press, New York, **1965**.

[9] B. Valeur, Molecular Fluorescence: Principles and Applications. Wiley-VCH Verlag GmbH, **2001**.

[10] D. L. Andrews, A. Demidov, (Eds) Resonance Energy Transfer. Wiley, Chichester, **1999**.

[11] J. R. Lakowicz. Principles of Fluorescence Spectroscopy, Kluwer Academic/Plenum. New York, **1999**.

[12] A. Monguzzi, R. Tubino, F. Meinardi, Upconversion-induced delayed fluorescence in multicomponent organic systems: Role of Dexter energy transfer. *Phys. Rev B.,* **2008**, 77, 155122.

[13] A. Monguzzi, R. Tubino, F. Meinardi, Diffusion Enhanced Upconversion in Organic Systems. *Int. J. Photoenergy*, **2008**, 684196.

[14] P. J. Wagner, I. Kochevar, How efficient is diffusion-controlled triplet energy transfer. *J. Am. Chem. Soc*., **1968**, 90, 2232.

[15] A. F. Vaudo, D.M. Hercules, A Study of the Viscosity Dependence of Triplet-Singlet Energy Transfer in Solution. *J. Am. Chem. Soc*, **1971**, 93, 2599.

[16] J. B. Birks, Photophysics of Aromatic Molecules. Wiley, London, **1970**.

[17] H. Yersin, A. Rausch, R. Czerwieniec, T. Hofbeck, T. Fischer, The triplet state of organo-transition metal compounds. Triplet harvesting and singlet harvesting for efficient OLEDs. *Coord. Chem. Rev*., 255, 21, 2622.

[18] J. Solarski, G. Angulo, A. Kapturkiewicz, Time-resolved luminescence investigations of the reversible energy transfer from the excited ^{3}*MLCT states to organic acceptors – An alternative method for the determination of triplet state energies and lifetimes. *J. Photochem. Photobiol*., A, **2011**, 218, 58.

[19] J. Solarski, G. Angulo, A. Kapturkiewicz, Energy transfer from the excited ^{3}*MLCT states to organic acceptors – Solvent effect studies. *J. Photochem. Photobiol*., A, **2014**, 274, 73.

[20] J. G. Winans, Partial Selection Rule for Sensitized Fluorescence. *Rev. Mod. Phys.*, **1944**, 16, 175.

[21] K. Sandros, Transfer of Triplet State Energy in Fluid Solutions. III. Reversible Energy Transfer. *Acta Chem. Scand*., **1964**, 18, 2355.

[22] V. Balzani, F. Bolletta, F. Scandola, Vertical and "Nonvertical" Energy Transfer Processes. A General Classical Treatment. *J. Am. Chem. Soc*., **1980**, 102, 2152.

[23] K. A. Connors, Chemical Kinetics: the study of reaction rates in solution, VCH Publishers, New York, **1991**.

[24] M. Rae, M. N. Berberan-Santos, A Generalized Pre-Equilibrium Approximation in Chemical and Photophysical Kinetics. *Journal of Chemical Education*, **2004**, 81, 3.

[25] B. Williamson, V. K. La-Mer, The Kinetics of Activation – Diffusion Controlled Reactions in Solution. The Temperature Dependence of the Quenching of Fluorescence. *J. Am. Chem. Soc.*, **1948**, 70, 717.

[26] M. v. Smoluchowski, Versuch einer mathematischen Theorie der Koagulationskinetik kolloider Losungen. *Z. Phys. Chem*., **1918**, 92, 129.

[27] G. Angulo, Experimental observations of non-markovian effects on diffusion-influenced photo-induced electron transfer reactions. *PhD Dissertation Thesis*, **2003**, Graz.

[28] M. R. Eftink in: J. R. Lakowicz (Ed.), Fluorescence Quenching: Theory and Applications, Topics in Fluorescence Spectroscopy, Vol. 2, Principles, Plenum Press, New York, **1991**.

[29] B. S. Brunschwig; N. Sutin, Energy surfaces, reorganization energies, and coupling elements in electron transfer. *Coord. Chem. Rev*, **1999**, 187, 233.

[30] D. Rehm, A. Weller, Kinetic and Mechanism of Electron Transfer in Fluorescence Quenching in Acetonitrile. *Ber. Bunsen. Ges*., **1969**, 73, 834.

[31] A. Kapturkiewicz, Electron transfer and spin up-conversion processes. in A. J. Bard (Ed.) Electrogenerated Chemiluminescence, Marcel Dekker, New York, **2004**.

[32] A. R. Edmonds, Angular Momentum in Quantum Mechanics, Princeton University Press, Princeton, **1996**.

[33] E. Fermi, Nuclear Physics, University of Chicago Press, **1950**.

[34] F. Perrin, Loi de decroissance du pouvoir fluorescent en fonction de la concentration. *Compt. Rend*., **1924**, 178, 1978

[35] M. Kasha, Characterization of Electronic Transitions in Complex Molecules. *Discusss. Faraday Soc*., **1950**, 914, 19.

[36] G. Porter, M. Windsor, The Triplet State in Fluid Media. *Proc. Roy. Soc*., **1958**, 245, 238.

[37] V. Ermolayev, A. J. Terenin, Energy transfer between triplet levels. *J. Chim. Phys*., **1958**, 55, 698.

[38] V. Ermolayev, K. Svitashev, Optika i Spektroskopiya, **1957**, 7, 664.

[39] H. L. J. Bäckström, K. Sandros, H. Haraldsen, A. Grönvall, B. Zaar, E. Diczfalusy, The Quenching of the Long-lived Fluorescence of Biacetyl in Solution. *Acta Chem. Scand.*, **1958**, 12, 823.

[40] H. L. J. Bäckström, K. Sandros, J.Lindgren, E. Varde, G. Westin, Transfer of Triplet State Energy in Fluid Solutions. I. Sensitized Phosphorescence and Its Application to the Determination of Triplet State Lifetimes. *Acta Chem. Scand*, **1960**, 14, 48.

[41] K. Sandros, H. L. J. Bäckström, R. Havanka, T. Briggs, G. A. D. Haslewood, Transfer of Triplet State Energy in Fluid Solutions. II. Further Studies of the Quenching of Biacetyl Phosphorescence in Solution. *Acta Chem. Scand.*, **1962**, 16, 958.

[42] K. Sandros, M. Almgren, A. Holm, P. H. Nielsen, J. Munch-Petersen, The Relative Yields of Fluorescence and Phosphorescence of Biacetyl in Fluid Solutions. *Acta Chem. Scand.*, **1963**, 17, 552.

[43] K. Sandros, F. Haglid, R. Ryhage, R. Stevens, Transfer of Triplet State Energy in Fluid Solutions. III. Reversible Energy Transfer. *Acta Chem. Scand.*, **1964**, 18, 2355.

[44] I. M. M. de Carvahlo, M. H. Gehlen, The solvent effect on electronic energy transfer between excited $[Ru(bpy)_3]^{2+}$ donor and aromatic acceptors. *J. Photochem. Photobiol., A*, **1999**, 122, 109.

[45] V. Balzani, F. Bolletta, Energy Transfer Processes Involving Distorted Excited States. *J. Am. Chem. Soc*., **1978**, 100, 7404.

[46] R. A. Marcus, On the theory of Electron-Transfer Reaction IV. Unified Treatment of Homogeneous and Electrode Reactions. *J. Chem. Phys*., **1965**, 43, 2654.

[47] W. R. Fawcett, Y. I. Kharkats, Estimation of the free energy of activation for electron transfer reactions involving dipolar reactants and products, *J. Electroanal. Chem*., **1973**, 47, 413.

[48] N. Agmon, R. D. Levine, Energy, entropy and the reaction coordinate: Thermodynamic-like relations in chemical kinetics. *Chem. Phys. Lett.*, **1977**, 52, 197.

[49] N. Agmon, Quantitative Hammond postulate. *J. Chem. Soc.***,** *Faraday Trans*., **1978**, 2, 74, 388.

[50] K. J. Laidler, Theories of Chemical Reaction Rates. McGraw-Hill, **1969**.

[51] E. V. Anslyn, D. A. Dougherty,. Transition State Theory and Related Topics.Modern Physical Organic Chemistry, University Science Books, **2006**.

[52] J. O. M. Bockris, S. U. M. Khan, Quantum Electrochemistry, Plenum: New York, **1979**.

[53] R. R. Dogonadze, A. M. Kuznetsov, T.A. Marsagishvili, The present state of the theory of charge transfer processes in condensed phase. *Electrochim. Acta,* **1980**, 25, 1.

[54] R. D. Cannon, Electron Transfer Reactions, Butterworths: London, **1980**.

[55] N. Sutin, Nuclear, electronic and frequency factors in electron-transfer reactions. *Acc. Chem. Res*., **1982**, 15, 275.

[56] L. Eberson, Electron-transfer reactions in organic chemistry. *Adv. Phys. Org.Chem*., **1982**, 18, 79.

[57] N. Sutin, Theory of electron transfer reactions: insights and hindsights. *Prog. Inorg. Chem*., **1983**, 30, 441.

[58] R. A. Marcus, N. Sutin, Electron transfer in chemistry and biology. *Biochim. Biophys. Acta,* **1985**, 811, 265.

[59] M. D. Newton, N. Sutin, Electron transfer reactions in condensed phases. *Ann. Rev. Phys. Chem*., **1984**, 35, 437.

[60] M. D. Newton, Quantum chemical probes of electron transfer kinetics: the nature of donor-acceptor interactions. *Chem. Rev*., **1991**, 91, 767.

[61] R. W. Fawcett, M. Opallo, The kinetics of heterogeneous electron transfer in polar solvents. *Angew. Chem. Int. Ed*., **1994**, 33, 2131.

[62] M. A. Fox, M. Chanon, Eds., Photoinduced Electron Transfer, Parts *A–D*, Elsevier: Amsterdam, **1998**.

[63] A. V. Barzykin,; P. A. Frantsuzov; K. Saki, A. Tachiya, Solvent effects in nonadiabatic electron-transfer reactions. Theoretical aspects. *Adv. Chem. Phys*., **2002**, 123, 511.

[64] E. D. German, A. M. Kuznetsov, Outer sphere energy of reorganization in charge transfer processes. *Electrochim. Acta,* **1981**, 26, 1595.

[65] W. R. Fawcett, Y. I. Kharkats, Estimation of the free energy of activation for electron transfer reactions involving dipolar reactants and products. *J. Electroanal. Chem*., **1973**, 47, 413.

[66] G. Grampp, W. Jaenicke, Kinetics of diabatic and adiabatic electron exchange in organic systems. Comparison of theory and experiment. *Ber. Bunsenges. Phys. Chem*., **1991**, 95, 904.

[67] G. Grampp, M. Cebe, E. Cebe, An improved bond-order/bond-length relation for the calculation of inner sphere reorganization energies of organic electron transfer reactions. *Z. Phys. Chem*. N.F. **1990**, 166, 93.

[68] J. R. Miller, L. T. Calcaterra, G. L. Gloss, Intramolecular Long-Distance Electron Transfer in Radical Anions. The Effects of Free Energy and Solvent on the Reaction Rates. *J. Am. Chem. Soc*., **1984**, 106, 3047.

[69] P. Szrebowaty, A. Kapturkiewicz, Free energy dependence on tris(2,2′-bipyridine)ruthenium(II) electrochemiluminescence efficiency. *Chem. Phys. Lett*., **2000**, 328, 160.

[70] G. L. Closs, M. D. Johnson, J. R. Miller, P. Piotrowiak, A Connection Between Intramolecular Long-Range Electron, Hole, and Triplet Energy Transfers. *J. Am. Chem. Soc*., **1989**, 111, 3751.

[71] B. Ma, P. I. Djurovich, M. E. Thompson, Excimer and electron transfer quenching studies of a cyclometalated platinum complex. *Coord. Chem. Rev*., **2005**, 249, 1501.

[72] W. G. Herkstroeter, The Triplet Energies of Azulene, β-Carotene, and Ferrocene. *J. Am. Chem. Soc*., **1975**, 97, 4161.

[73] M. Z. Hoffman, F. Bolletta, L. Moggi, G. L. Hug, Rate Constants for the Quenching of Excited States of Metal Complexes in Fluid Solution. *J. Phys. Chem. Ref. Data.,* **1989**, 18, 219.

[74] J. B. Birks, Reversible photophysical processes. *New J. Chem*., **1997**, 1, 453.

[75] Y. Marcus, The Properties of Solvents, John Wiley & Sons Ltd., Chichester, **1998**.

[76] A. Kapturkiewicz, T. Chen, I. R. Laskar, J. Nowacki, Electrochemiluminescence studies of the cyclometalated iridium(III) complexes with substituted 2-phenylbenzothiazole ligands. *Electrochem. Commun*., **2004**, 6, 827.

[77] A. Kapturkiewicz, J. Nowacki, P. Borowicz, Electrochemiluminescence studies of the cyclometalated iridium(III) L_2Ir(acetyl acetonate) complexes. *Electrochim. Acta.,* **2005**, 50, 3395.

[78] A. Kapturkiewicz, J. Nowacki, P. Borowicz, Cyclometalated Iridium(III) Complexes with 2-Phenylbenzimidazole Derivatives – Spectroscopic, Electrochemical and Electrochemiluminescence Studies. *Z. Phys. Chem*., **2006**, 220, 525.

[79] M. S. Lowry, S. Bernhard, Synthetically Tailored Excited States: Phosphorescent, Cyclometalated Iridium(III) Complexes and Their Applications. *Chem. Eur. J*., **2006**, 12, 7970.

[80] G. Zhou, C. L. Ho, W. Y. Wong, Q. Wang, D. Ma, L. Wang, Z. Lin, T. B. Marder, A. Beeby, Manipulating Charge-Transfer Character with Electron-

Withdrawing Main-Group Moieties for the Color Tuning of Iridium Electrophosphors. *Adv. Funct. Mater*., **2008**, 18, 499.

[81] E. S. Pysh, N. C. Yan, Polarographic Oxidation Potentials of Aromatic Compounds. *J. Am. Chem. Soc*., **1963**, 85 , 2124.

[82] P. B. Merkel, J. P. Dinnocenzo, Thermodynamic energies of donor and acceptor triplet states. *J. Photochem. Photobiol*. *A.*, **2008**, 193, 110.

[83] B. Lang, G. Angulo, E. Vauthey, Ultrafast solvation dynamics of coumarin 153 in imidazolium-based ionic liquids. *J. Phys. Chem. A*, **2006**, 110, 7028.

[84] A. Farmilo, F. Wilkinson, Triplet state quenching by ferrocene. *Chem. Phys. Lett*., **1975**, 34, 575.

[85] C. C. Wamser , R. T. Medary , I. E. Kochevar , N. J. Turro, P. L. Chang, Steric effects in singlet and triplet electronic energy transfer to azo compounds. *J. Am. Chem. Soc*., **1975**, 97, 4864.

[86] J. Saltiel, P.T. Shannon, O.C. Zafiriou, A.K. Uriarte, A case of fully diffusion-controlled exothermic triplet excitation transfer. *J. Am. Chem. Soc*., **1980**, 102, 6799.

[87] L. J. A. Martins, T. J. Kemp, Triplet state of 2-nitrothiophen. A laser flash-photolysis study. *J. Chem. Soc., Faraday Trans*., **1982**, 78, 519.

[88] T. Tanaka, M. Yamaji, H. Shizuka, Solvent dependence of triplet energy transfer from triplet benzophenone to naphthols and methoxynaphthalenes. *J. Chem. Soc., Faraday Trans*., **1998**, 94, 1179.

[89] A. D. Kirk, C. Namasivayam, Reversible energy transfer between chromium (III) complexes. *J. Phys. Chem*., **1989**, 93, 5488.

[90] A. Kira, J. K. Thomas, Equilibriums between triplet states of aromatic hydrocarbons. *J. Phys. Chem*., **1974**, 78, 196.

[91] M. Yamaji, K. Okada, B. Marciniak, H. Shizuka, Laser photolysis studies on triplet-equilibrium formation in a small triplet-energy gap system. *Chem. Phys. Lett*., **1997**, 277, 375.

[92] A. Demeter, T. Berces, K. A. Zachariasse, Dual fluorescence and intramolecular charge transfer with N-phenylphenanthridinones. *J. Phys. Chem. A*, **2001**, 105, 4611.

[93] Z. R. Grabowski, A. Grabowska, The Forster cycle reconsidered. *Z. Phys. Chem. NF*, **1976**, 101, 197.

[94] P. D. Laible, R. S. Knox, T. G. Owens, Detailed balance in Förster-Dexter excitation transfer and its application to photosynthesis. *J. Phys. Chem. B*, **1998**, 102, 1641.

[95] E. Wigner, E. E. Wimmer, Über die Struktur der zweiatomigen Molekelspektren nach der Quantenmechanik, *Z. Physik.*, **1928**, 51,859.

[96] A. Weller, Progress in Reactions Kinetics. Pergamon Press, London, **1961**.

[97] I. Carmichael, G. L. Hug, Triplet-triplet absorption spectra of organic molecules in condensed phases. *J. Phys. Chem. Ref. Data*, **1986**, 15, 1.

[98] S. L. Murov, I. Carmichael, G. L. Hug, Handbook of Photochemistry, 2nd ed., Marcel Dekker, New York, **1993**.

[99] A. Ghauch, J. Rima, C. Fachinger, J. Suptil, M. Martin-Bouyer, Room temperature phosphorescence analyses of polycyclic aromatic hydrocarbons using an imaging sensing system combined with a bifurcated optical fiber and a cooled charge coupled device detector. *Talanta*, **2000**, 51, 807.

[100] A. Munoz de la Peña, M. Rodríguez, G. M. Escandar, Optimization of the room-temperature phosphorescence of the 6-bromo-2-naphthol-alpha-cyclodextrin system in aqueous solution. *Talanta*, **2000,** 51, 949.

[101] M. A. El-Sayed, D. S. Tinti, E. M. Yee, Conservation of Spin Direction and Production of Spin Alignment in Triplet-Triplet Energy Transfer. *J. Chem. Phys*., **1969**, 51, 5721.

[102] J. Fujisawa, Y. Ohba, S. Yamauchi, Direct observation of electron spin polarization transfer in triplet-triplet energy transfer between porphyrins and fullerene in fluid solution. *Chem. Phys. Lett*., **1998**, 282, 181.

[103] K. Akiyama, A. Kaneko, S. Tero-Kubota, Y. Ikegami, Spin polarization conservation during triplet-triplet energy transfer in fluid solution as studied by time-resolved ESR spectroscopy. *J. Am. Chem. Soc*., **1990**, 112, 3297.

[104] S. Hoshino, K. Ishii, N. Kobayashi, M. Kimura, H. Shirai, Direct observation of electron spin polarization transfer in triplet - triplet energy transfer between porphyrins and fullerene in fluid solution. *Chem. Phys. Lett*., **2004**, 386, 149.

[105] K. Akiyama, S. Tero-Kubota, T. Ikoma, Y. Ikegami, Spin polarization conservation during intramolecular triplet-triplet energy transfer studied by time-resolved EPR spectroscopy. *J. Am. Chem. Soc*., **1994**, 116, 5324.

[106] V. P. McCaffrey, M. D. E. Forbes, Chemically induced dynamic electron spin polarization-detected energy transfer. Substrate size effects and solvent dependence. *J. Phys. Chem. A*, **2005**, 109, 4891.

[107] H. Knibbe, D. Rehm, A. Weller, Intermediates and Kinetics of Fluorescence Quenching by Electron Transfer. *Ber. Bunsenges. Phys. Chem.*, **1968**, 72, 257.

[108] T. Asahi, N. Mataga, Charge recombination process of ion pair state produced by excitation of charge-transfer complex in acetonitrile solution. Essentially different character of its energy gap dependence from that of geminate ion pair formed by encounter between fluorescer and quencher. *J. Phys. Chem*., **1989**, 93, 6575.

[109] J. I. Goldsmith , W. R. Hudson , M. S. Lowry , T. H. Anderson, Stefan Bernhard, Discovery and High-Throughput Screening of Heteroleptic Iridium Complexes for Photoinduced Hydrogen Production. *J. Am. Chem. Soc*., **2005**, 127, 7502.

[110] E. D. Cline, S. E. Adamson, S. Bernhard, Homogeneous Catalytic System for Photoinduced Hydrogen Production Utilizing Iridium and Rhodium Complexes. *Inorg. Chem*., **2008**, 47, 10378.

[111] N. D. McDaniel, F. J. Coughlin, L. L. Tinker, S. Bernhard, Cyclometalated Iridium(III) Aquo Complexes: Efficient and Tuneable Catalysts for the Homogeneous Oxidation of Water. *J. Am. Chem. Soc*., **2008**, 130, 210.

[112] C. Serpa, L. G. Arnaut, S .J. Formosinh, K. R. Naqvi, Calculation of triplet-triplet energy transfer rates from emission and absorption spectra. The quenching of hemicarcerated triplet biacetyl by aromatic hydrocarbons. *Photochem. Photobiol. Sci.*, **2003**, 2, 616.

[113] N. Kitamura, H. Kim, Y. Kawanishi, R. Obata, S. Tazuke, Time-resolved emission spectra of tris(2,2'-bipyridine)ruthenium dichloride and cis-bis(2,2'-bipyridine)dicyanoruthenium at low temperature *J. Phys. Chem.*, **1986**, 90, 1488.

[114] T. Hofbeck, H. Yersin, The Triplet State of *fac*-$Ir(ppy)_3$. *Inorg. Chem.*, **2010**, 49, 9290.

[115] N. Kitamura, H. B. Kim, S. Okano, S. Tazuke, Photoinduced electron-transfer reactions of ruthenium(II) complexes. 1. Reductive quenching of excited $Ru(bpy)_3^{2+}$ by aromatic amines. *J. Phys. Chem.*, **1989**, 93, 5750.

[116] H. B. Kim, N. Kitamura, Y. Kawanishi, S. Tazuke, Photoinduced electron-transfer reactions of ruthenium(II) complexes. 2. Oxidative quenching of excited $Ru(bpy)_3^{2+}$ by neutral organic electron acceptors. *J. Phys. Chem.*, **1989**, 93, 5757.